

# Muscle structure and water retention in fresh and cooked meat products - FINAL REPORT

---

**PROJECT CODE:** 2013-5009

---

**PREPARED BY:** Bo-Anne Rohlik, Sofia Øiseth, Tomas Bolumar Garcia, Henry Sabarez, Peter Watkins, Yalchin Oytam and Roman Buckow

---

**DATE SUBMITTED:** 14 November 2017

---

**DATE PUBLISHED:** 5 December 2017

---

**PUBLISHED BY:** AMPC

---

The Australian Meat Processor Corporation acknowledges the matching funds provided by the Australian Government to support the research and development detailed in this publication.

**Disclaimer:**

The information contained within this publication has been prepared by a third party commissioned by Australian Meat Processor Corporation Ltd (AMPC). It does not necessarily reflect the opinion or position of AMPC. Care is taken to ensure the accuracy of the information contained in this publication. However, AMPC cannot accept responsibility for the accuracy or completeness of the information or opinions contained in this publication, nor does it endorse or adopt the information contained in this report.

No part of this work may be reproduced, copied, published, communicated or adapted in any form or by any means (electronic or otherwise) without the express written permission of Australian Meat Processor Corporation Ltd. All rights are expressly reserved. Requests for further authorisation

## TABLE OF CONTENTS

1.0	EXECUTIVE SUMMARY .....	6
2.0	INTRODUCTION.....	8
3.0	PROJECT OBJECTIVES .....	9
3.1	Project background description.....	9
3.2	Ultimate pH.....	9
3.3	<i>Bos indicus</i> and <i>Bos taurus</i> .....	10
3.4	Intramuscular fat.....	10
3.5	Interventions.....	11
4.0	METHODOLOGY .....	12
4.1	Experimental design.....	12
4.1.1	Impact of cooking temperature on meat structure and tenderness including density, cook loss, and shear force .....	12
4.1.1.1	Experimental material.....	12
4.1.1.2	Method .....	13
4.1.2	Cook loss in relation to cooking temperature and ageing .....	13
4.1.2.1	Experimental material.....	13
4.1.2.2	Method .....	13
4.1.3	Cook loss in relation to ultimate pH .....	14
4.1.3.1	Experimental material.....	14
4.1.3.2	Method .....	14
4.1.4	Cook loss in relation to <i>Bos indicus</i> (BI) content .....	14
4.1.4.1	Experimental material.....	14
4.1.4.2	Method .....	15
4.1.5	Cook loss in relation to marbling.....	16
4.1.5.1	Experimental material.....	16
4.1.5.2	Method .....	17
4.1.6	Influence of interventions on the structural basis of cook loss .....	17
4.1.6.1	Pulsed electric field (PEF) - Experimental material.....	17
4.1.6.2	PEF - Method.....	18
4.1.6.3	High Pressure Thermal Processing (HPTP) - Experimental materials .....	18
4.1.6.4	HPTP - Method.....	18
4.2	Methods – cooking and processing .....	20

4.2.1	Cooking in water baths .....	20
4.2.2	Pulsed electric field processing .....	20
4.2.3	High pressure thermal processing .....	21
4.3	Characterisation methods .....	22
4.3.1	Drip loss, cook loss and weep loss .....	22
4.3.2	Dimensional changes .....	22
4.3.3	Moisture content .....	22
4.3.4	Expressible moisture.....	22
4.3.5	Colour measurement .....	23
4.3.6	pH measurements .....	23
4.3.7	Fat content.....	23
4.3.8	Mechanical measurements .....	23
4.3.9	Microstructural characterisation .....	24
4.3.9.1	Myofibril preparation.....	24
4.3.9.2	Muscle fibre fragment preparation .....	24
4.3.9.3	Endomysial ghost preparation .....	24
4.3.9.4	Epimysial fragment preparation .....	24
4.3.9.5	Endomysial fragment preparation .....	24
4.3.9.6	Structure of myofibrils by confocal laser scanning microscopy .....	25
4.3.9.7	Structure of myofibrils by optical microscopy .....	25
4.3.9.8	In-situ heating of muscle fibre fragments.....	25
4.3.9.9	Fluorescent labelling of connective tissue.....	25
4.3.9.10	Plastic embedding of muscle tissue for light microscopy .....	25
4.3.9.11	Light microscopy of embedded samples .....	26
4.3.9.12	Transmission Electron Microscopy .....	26
5.0	PROJECT OUTCOMES & DISCUSSION.....	27
5.1	Mass loss upon cooking .....	27
5.1.1	Influence of cooking time and temperature .....	28
5.1.2	Influence of ageing .....	29
5.1.3	Influence of muscle type .....	29
5.1.4	Influence of ultimate pH.....	29
5.1.4.1	Cook loss .....	29
5.1.4.2	Weep loss.....	30
5.1.4.3	Total mass loss .....	31
5.1.4.4	Moisture content. ....	31
5.1.4.5	Expressible moisture .....	31

5.1.5	Influence of <i>Bos indicus</i> content.....	31
5.1.5.1	Raw meat .....	31
5.1.5.2	Cooked meat.....	31
5.1.6	Influence of intramuscular fat .....	32
5.1.6.1	Raw meat .....	32
5.1.6.2	Cooked meat.....	33
5.1.7	Effect of interventions .....	33
5.1.7.1	Pulsed electric field treatment .....	33
5.1.7.2	High pressure thermal treatment.....	34
	Effect of salt concentration and HPTP on liquid loss .....	34
	Effect of various HPTP pressures and temperatures on mass loss.....	34
5.2	Dimensions and microstructure .....	36
5.2.1	Influence of cooking time and temperature .....	36
5.2.1.1	Cross-sectional shrinkage .....	36
5.2.1.2	Longitudinal shrinkage.....	38
5.2.1.3	Influence of muscle type.....	40
5.2.1.4	Dimensional changes of aged meat upon heating.....	41
5.2.1.5	Effect of heating on connective tissue.....	42
5.2.2	Influence of pH, <i>Bos indicus</i> content and Intramuscular fat .....	44
5.2.2.1	Ultimate pH.....	44
5.2.2.2	<i>Bos indicus</i> content .....	44
5.2.2.3	Intramuscular fat content .....	44
5.2.3	Effect of interventions .....	45
5.2.3.1	Pulsed electric field treatment .....	45
5.2.3.2	High pressure thermal processing .....	45
5.2.3.3	Stage 1 – Effect of salt type .....	45
5.3	Texture .....	47
5.3.1	Influence of cooking temperature.....	47
5.3.2	Influence of muscle type .....	48
5.3.3	Influence of ultimate pH, <i>Bos indicus</i> content and Intramuscular fat .....	49
5.3.3.1	Ultimate pH.....	49
5.3.3.2	<i>Bos indicus</i> content .....	51
5.3.3.3	Intramuscular fat (IMF).....	52
5.3.4	Effect of HPTP on texture .....	53
5.3.4.1	The effect of salt concentration on texture.....	53
5.3.4.2	The effect of HPTP and salt on texture .....	54
5.4	Colour.....	56

5.4.1	Influence of cooking time and temperature on meat colour in relation to pH	56
5.4.2	Influence of cooking time and temperature on meat colour in relation to <i>Bos indicus</i> content .....	58
5.4.2.1	Colour of raw samples .....	58
5.4.2.2	Colour of cooked samples.....	60
5.4.3	Influence of cooking time and temperature on meat colour in relation to Intramuscular Fat (IMF).....	60
5.4.3.1	Colour of raw samples .....	60
5.4.3.2	Colour of cooked samples.....	61
5.4.4	Influence of cooking time and temperature on meat colour in relation to interventions .....	62
5.4.4.1	The effect of PEF on meat colour.....	62
5.4.4.2	The effect of HPTP and brine concentration on meat colour.....	62
5.5	Modelling .....	66
5.5.1	Introduction .....	66
5.5.2	Modelling approaches .....	66
5.5.2.1	Empirical modelling.....	66
5.5.2.2	Semi-parametric modelling.....	68
5.5.2.3	Using Laplace models to model heat transfer .....	70
5.5.2.4	Numerical computational modelling .....	71
5.5.3	Conclusion.....	77
6.0	CONCLUSIONS & RECOMMENDATIONS .....	78
7.0	ACKNOWLEDGEMENTS .....	81
8.0	ABBREVIATIONS AND GLOSSARY.....	82
9.0	BIBLIOGRAPHY .....	84

## 1.0 EXECUTIVE SUMMARY

Raw meat is cooked to achieve a palatable and safe product. However, meat shrinks upon cooking due to protein denaturation which results in reduced yield by loss of liquid (cook loss). The moisture content of meat is also linked to the perceived juiciness by consumers. Therefore, it is important to understand the structural mechanisms behind the shrinkage and mass loss during cooking and subsequent storage, to retain a high yield as well as juiciness. Godsalve, Davis, and Gordon (1977) proposed a model for denaturing and shrinking of proteins at increased temperatures, forcing water from between-muscle fibre spaces, like a self-squeezing sponge. However, little information is available to predict the cook loss and product outcomes from different beef muscles destined to different end-markets.

The objectives of this project were to determine the underlying structural events that cause shrinkage of beef upon cooking, resulting in reduced yield by the loss of liquid, and investigate interventions to manipulate/minimise this. Moreover, the development of mathematical models for mass loss during cooking were to be investigated. Furthermore, use of new investigative tools for meat quality assessment such as confocal laser scanning microscopy, computer modelling and process engineering were at the core of the project and create capability for future projects for the Australian meat industry.

We investigated the impact of cooking temperature, cooking time, ageing, muscle type, ultimate pH, *Bos indicus* and intramuscular fat content and treatment with pulsed electric field (PEF) or high pressure thermal processing (HPTP) on mass loss, structure, texture and colour of beef muscle. The information resulting from this project complements and adds to existing knowledge and will enable beef processors to predict product performance.

### The key findings were:

- Denaturation of myofibrillar proteins were the primary source of structural changes and, hence, of the mass loss during heating, with only minor influence of connective tissue denaturation. The major factors influencing mass loss were cooking temperature and time. The ultimate pH (final muscle pH after slaughter) did influence the characteristics of raw and cooked meat with high pH displaying higher moisture content and lower mass loss than low pH meat. Neither *Bos indicus* nor intramuscular fat content affected the total mass loss and did not influence the dimensional changes of meat samples during cooking in this study.
- When cooking in a water bath, the most tender meat was achieved at temperatures ranging between 65 and 70 °C. In this study, meat with high pH (>6.0) retained more moisture in the structure upon cooking than medium (pH ~5.7), or low pH (~5.4) meat. This also increased the tenderness in some cases. With an increase in intramuscular fat (marbling score 4-5, compared to 0-3) the tenderness of some muscles (*e.g.* striploin) increased up to 32%, most likely due to a reduction in force required to split fat tissue compared to muscle fibres.
- In this study, HPTP (300-650 MPa, 60-89 °C, 5 min) of brine injected meat showed that only processing temperature had a significant effect on tenderness and mass loss, not the applied

pressure or brine concentration. Higher processing temperatures resulted in tougher meat and larger mass losses. All HPTP samples showed lower mass losses and higher tenderness than samples cooked in a water bath at corresponding temperatures.

**The following is recommended:**

- To limit mass loss and retain juiciness, it is important to avoid excessive shrinkage of meat. Therefore, it is crucial to keep core temperatures of meat under 70 °C during cooking. The ideal tenderness of cooked meat was achieved when the meat was cooked to a core temperature between 65 °C and 70 °C.
- Medium pH (5.7 – 5.9) and high pH (>6.0) meat retained more moisture when cooked at high temperatures (above 75 °C) than low pH (5.4 – 5.5) meat. Therefore, medium and high pH meat has greater potential to be sold as pre-cooked meat products.
- Meat from cattle with high *Bos indicus* content was slightly less tender (by 13% when cooked 60 min at 70 °C) than that derived from animals with low *Bos indicus* content, despite having the same mass loss. Therefore, it is recommended to keep cooking temperature below 70 °C for meat with high BI content, since the cooking temperature had larger influence on tenderness than the *Bos indicus* content.
- We recommend the use of HPTP (60 °C, 550 MPa) with brine injections (10% of total mass of either 0.2% PPI or 1.0% NaCl) as a treatment for meat tenderisation. This results in increased juiciness and is suitable for manufacturing ready-to-eat based meat products.
- We recommend further research into PEF processing as a method of value adding for the meat industry, such as tenderisation of raw meat as well as improved eating quality upon cooking. So far, the results from various studies are divergent and more knowledge is needed to deliver practical solutions to the industry.
- The predictive model developed in this work can be used for simulating cook loss of meat as a function of cooking conditions (cook temperature and time). It is flexible enough to account for other phenomena and extensible enough for complex meat geometries and shapes. We recommend coupling of a mechanical model to the mass and heat model for the prediction of meat tenderness and mass loss. Furthermore, incorporation of other food qualities (*i.e.*, sensorial, functional and nutritional) into the prediction would be important to enable the manipulation and control of meat quality to achieve desired attributes/value added meat products.

## 2.0 INTRODUCTION

Cooking generally makes meat more acceptable to consumers through the development of its specific flavour, tenderness, colour and appearance (R. Domínguez, Borrajo, P., Lorenzo, J. M., 2015). It is well known that a specific cooking condition (temperature and time) along with the specific meat composition (*e.g.* fat content, amount of connective tissue) has a significant impact on the final quality of the meat (R. Domínguez, Gómez, M., Fonseca, S., Lorenzo, J. M., 2014). Apart from inactivating pathogenic microorganisms, the optimal cooking mode of meat should meet two basic parameters; it should maintain a high yield (water retention), and have desirable sensory characteristics, namely tenderness, juiciness and flavour (Chiavaro, 2009).

Meat is composed of a large variety of proteins that can be classified into three main groups; myofibrillar, sarcoplasmic and connective tissue proteins. When meat is cooked by the application of heat, protein denaturation will take place. The higher the temperature and the longer the cooking time, the more denaturation will occur. The major proteins denature at different temperatures; from desmin at around 45 °C, followed by myosin, collagen, sarcoplasmic proteins, titin and finally actin at about 80 °C (Purslow, Oiseth, Hughes, & Warner, 2016). The denaturation temperature is influenced by the pH and ion concentration of the meat. The fibrillar proteins (actin and myosin) contract upon denaturation, and consequently, the piece of meat shrinks and squeezes out liquid (mass loss). This results in a stiffer structure containing less moisture, *i.e.* a tougher and less juicy piece of meat.

There is limited information available to predict the cook loss and product outcomes from muscles from beef carcasses destined to different end-markets. Meat processors are keen to extend their value adding and product opportunities from different muscles and carcasses. In particular, they want a consistent and reliable product. The information from this project complements and adds to existing knowledge and enables beef processors to predict product performance.

### 3.0 PROJECT OBJECTIVES

The objectives of this project were to:

- Determine the structural basis of dimensional changes leading to mass loss upon cooking
- Investigate the interventions to manipulate/minimise this
- Develop mathematical models for mass loss during cooking
- Incorporate new analytical tools to assess meat quality (Confocal laser scanning microscopy, mathematics, process engineering).

#### 3.1 Project background description

Muscle structure and water-holding capacity in relation to pre-processing and cooking were identified in discussions as being a shared strategic priority for AMPC, MLA and CSIRO. The expulsion of fluid from meat during pre-rigor processing, storage and cooking is economically important in terms of yield of raw and cooked products, and also in terms of consumer acceptability. Meat is sold by weight and up to 15% of weight loss can occur during storage, and up to 40% during cooking, both a consequence of mostly water loss. This project has focused on the basic mechanisms responsible for mass loss during meat cooking and subsequent storage, and characterised structural changes that occurs in meat during cooking. A series of six experiments was undertaken to elucidate the structural basis of mass loss. A mechanistic understanding of mass loss from cooking was developed by determining mechanical properties (Warner-Bratzler (WB) shear force) together with mathematical modelling of factors influencing mass loss.

The project focused on identifying the basic mechanisms responsible for mass loss during cooking of meat and investigated the relative importance of each structural change that occurred. These mechanisms were studied in a variety of ways, including the effect of microstructural changes (shrinkage in width and length at different length scales), the effect of physiological properties such as pH, ratio of *Bos indicus* cross-breed or intramuscular fat content and the impact of different processing interventions (PEF and HPTP).

#### 3.2 Ultimate pH

The pH of living muscle tissue is almost neutral (pH 7.1-7.2). After slaughter, glycogen in the cells continues to be used as an energy source which leads to the formation of lactic acid. The lactic acid production lowers the pH of the meat gradually until the cells are depleted of glycogen and the ultimate pH is reached. The ultimate pH of meat is linked to structural changes that relate to quality parameters such as water retention, colour and texture (tenderness). For example, high pH meat cooked to the same internal temperature as low pH meat, will show a different degree of doneness in the interior of the meat. The purpose of this project was to understand the impact of cooking

conditions (temperature and time) on meat of three different pH ranges; low (5.37 – 5.55), medium (5.71 – 5.93), and high (>6.00). The low pH range is the industry standard for meat with a Meat Standards Australia colour score of 2 or below (light red), which receives a premium price. The medium pH range colour score is 4 and the high pH range colour score is 6 (dark purple) (Meat Standards Australia, 2007). Both medium and high pH meat is downgraded and are marketed at a lower price.

### **3.3 *Bos indicus* and *Bos taurus***

The benefits of crossbreeding cattle suitable for tropical regions such as *Bos indicus* (BI) in comparison to cattle adapted to mild climate conditions, *Bos taurus* (BT), to improve cattle production through increasing disease and insect resistance, climatic tolerance, heterosis and genetic variation, are well documented (Arthur, Hearnshaw, Kohun, & Barlow, 1994; Highfill, Esquivel-Font, Dikeman, & Kropf, 2012). Common BI breed types in use for cross breeding with BT are high-grade BI Brahman and crossbreeds such as Santa Gertrudis, Droughtmaster, Bradford and Brangus (Holroyd, 2016). However, many studies show that crossbreeding BI and BT impacts eating quality of meat in a negative way by generating less tender meat (Aroeira et al., 2016; Gursansky, O'Halloran, Egan, & Devine, 2010; Highfill et al., 2012). Animals with different BI gene content are also known to vary in proteolysis. As proteolysis is considered to be an important factor for mass loss upon cooking, it was important to investigate the influence of BI on mass loss, texture, dimensional and colour change during cooking. The BI gene content of the animals was measured as hump height. Six muscle groups were studied within three hump height ranges; low (50 – 60 mm), medium (80 – 100 mm), and high (135 – 165 mm).

### **3.4 Intramuscular fat**

There is evidence that the amount of intramuscular fat (IMF), also referred to as marbling, in meat affects tenderness. Marbling is influenced by carcass weight and genotype. Therefore, nutrition, disease status and management influence marbling indirectly by affecting slaughter weight. Many studies evaluated the effect of marbling on sensory traits of the meat (Liang et al., 2016; Mao et al., 2016; Okumura et al., 2007). It is believed that marbling positively affects the eating quality of meat (Lambe et al., 2016). Generally, low IMF is more common in the food industry whereas medium and high IMF content are sought by “high end” meat consumers, as fat influences texture (acting as lubricant) and flavour (providing more flavour compounds), and thus increases the palatability of meat. In this study, we investigated the influence of marbling and cooking on mass loss, textural properties, dimensional and colour changes of commercially available beef in Australia.

### 3.5 Interventions

The Australian red meat industry has identified value-adding as a necessity to increase the profitability of non-premium cuts. If tougher cuts could be tenderised in a quick, safe way and transformed into valuable healthy products, there would be enormous opportunities for market growth. Implementation of novel technologies in the meat industry is a way of gaining a competitive advantage.

One such emerging processing technology is pulsed electric field (PEF) processing. Meat is treated with short high voltage pulses that aims to modify muscle structure to achieve tenderisation (Arroyo, Lascorz, et al., 2015; Faridnia et al., 2015; O'Dowd, Arimi, Noci, Cronin, & Lyng, 2013; Via Suwandy, Carne, van de Ven, Bekhit, & Hopkins, 2015; V. Suwandy, Carne, van de Ven, Bekhit Ael, & Hopkins, 2015). As muscle consists of parallel muscle fibres, the direction of the applied electric field may play a role in treatment effect (Bekhit Ael, Suwandy, Carne, van de Ven, & Hopkins, 2016).

Another novel technology to process food is high pressure thermal processing (HPTP), which combines high pressure and temperature to better retain food quality and freshness compared to conventional thermal processing, while ensuring a shelf stable and safe product (Farkas, 2000). Meat which has undergone HPTP exhibits lower mass loss than meat subjected to heat only (Buckow, Sikes, & Tume, 2013). In this project we investigated the influence of HTPT combined with of brine injection at various pressures and temperatures to determine optimum processing conditions to achieve maximum tenderness and minimal mass loss.

## 4.0 METHODOLOGY

There were six major milestones studies in this project investigating different aspects of the dimensional changes and mass loss upon cooking (Table 4-1). A wide range of beef muscles, cooking temperatures and cooking times were used. The influences of muscle pH, BI content and IMF on cook loss, water holding capacity (WHC), dimensional changes, texture and colour were also determined. The influence of two intervention processes – PEF processing of raw muscles and HTPP of brine injected muscles on meat quality were investigated. The large matrix of obtained data was to develop a computational model of mass loss as a function of cooking time and temperature. The specific experimental details of each milestone are outlined below, followed by descriptions of the processing and characterisation methods.

**Table 4-1.** Experimental overview of entire project.

Milestone	Study	Muscles	Cook temp (°C)	Cook time (min)
1	Fibre density	SM	65, 70, 80, 90	35
2	Cook loss	BF, ST	55, 60, 65, 70, 75	60
3	Ultimate pH	ST	55, 65, 70, 75, 85	20, 40, 60
4	<i>Bos indicus</i>	ST, LD, GM, SM, PP, IS	65, 70, 75	20, 40, 60
8	Intramuscular fat	ST, LD	65, 70, 75	20, 40, 60
9	Interventions	ST	70, 75	30, 60

SM – *semimembranosus*, **topside**; BF – *biceps femoris*, **outside flat**; ST – *semitendinosus*, **eye round**; LD – *longissimus dorsi*, **striploin**; GM – *gluteus medius*, **rump**; PP – *pectoralis profundus*, **brisket** and IS – *infraspinatus*, **oyster blade**.

### 4.1 Experimental design

#### 4.1.1 Impact of cooking temperature on meat structure and tenderness including density, cook loss, and shear force

##### 4.1.1.1 Experimental material

Two topside muscles, left and right, were collected from a yearling (2-tooth) heifer carcass, weighing 230.4 kg and with a P8 fat depth of 4 mm at a local abattoir 24 hours post slaughter. From each topside muscle (left and right), twenty blocks of meat, each about 65 x 35 x 30 mm and weighing approximately 65 g, were cut along the muscle fibre direction, as well as 20 strips, about 60 x 15 x 6.7 mm and

weighing approximately 7 g. The blocks and strips were randomly allocated to one of four cooking temperatures; 65, 70, 80 or 90°C ensuring that equal numbers of left and right sides were in each temperature treatment.

#### 4.1.1.2 Method

The meat blocks were cooked in plastic bags in a water bath for 35 min, while the strips were cooked for 8 min at 65 °C and 7 min at 70, 80 and 90 °C to ensure the same amount of percentage mass loss at each cooking temperature. After cooking, strips and blocks were cooled overnight at 4°C. Cook loss, weep loss, dimensional changes, sarcomere length (by laser method P. E. Bouton, Harris, Shorthose, and Baxter (1973)), moisture content, WB shear values and microstructure of muscle tissue were investigated.

### 4.1.2 Cook loss in relation to cooking temperature and ageing

#### 4.1.2.1 Experimental material

Outside flat (n = 1) and Eye round (n = 5) muscles were collected from both sides of beef carcasses (British breeds, a mix of steers and females, average weight 248 kg, average fat 16 mm, zero dentition) on six separate occasions from a processing plant at 24 hours post-mortem. The muscle from one side was used immediately and the muscle from the other side was vacuum packed and stored at 2 °C for 14 days (aged samples). Each muscle was cut into 18 blocks (about 50 x 30 x 30 mm) for subsequent heating. The blocks were cut along the muscle fibre direction from each muscle. Other samples were removed from the centre of the muscle for processing into muscle fibre fragments (1 g), myofibrils (7 x 1.5 g) or endomysial ghosts (1 g) and were all maintained on ice prior to processing.

For preparation of epimysial fragments, connective tissue from inner and outer sinew of beef yearling oyster blade steak and gravy beef/boneless shin yearling were collected with as little muscle tissue as possible attached.

#### 4.1.2.2 Method

The experiment consisted of three stages:

**Stage 1** – Blocks of meat were cooked in plastic bags in a water bath for 60 min at 55, 60, 65, 70 or 75 °C or subjected to microwave cooking in a Menumaster 3100i Microwave oven for 5 min at 30% of maximum power (*i.e.* 465 W). Cook loss, dimensional and structural changes were measured after cooking.

Myofibril slurries of cooked meat were prepared by removing 0.5 g of meat of each heat treated block and combined (3 x 0.5 g) for homogenisation (see section 4.3.9.1) to get one myofibril sample/temperature treatment. Myofibril sarcomere lengths were determined by optical microscopy (see section 4.3.9.7).

**Stage 2** - Seven batches of raw myofibril slurries were prepared by homogenisation of 1.5 g raw muscle in 15 ml ice cold mannitol buffer (see section 4.3.9.1). One tube was kept as a control (raw, non-treated) and the remaining tubes were placed into floating racks for 60 min in water baths (55°C, 60°C, 65°C, 70°C, 75°C) or subjected to microwave treatment as above. Myofibril sarcomere lengths were determined by optical microscopy (see section 4.3.9.7).

**Stage 3** – Heating of muscle fibre fragments and connective tissue fragments (up to 90 °C) while observing changes to microstructure in-situ with a confocal laser scanning microscope (CSLM).

### 4.1.3 Cook loss in relation to ultimate pH

#### 4.1.3.1 Experimental material

Beef eye round muscles from both the left and right side of the carcass were sourced from 18 domestic trade animals (0 – 4 tooth, males) from a local abattoir (Brisbane, Queensland). The pH of each animal was measured in the striploin muscle at the abattoir 24 hours post mortem in order to assign individual carcasses according to three pH range groups, low (5.37 – 5.55), medium (5.71 – 5.93), and high (>6.00), *i.e.*, 6 carcasses in each pH range group.

Each eye round muscle was trimmed of excess fat and connective tissue and 15 portions, about 55 x 35 x 40 mm and weighing approximately 85 g, were cut along the muscle fibre direction from both left and right sides and were randomly allocated to different cooking regimes.

#### 4.1.3.2 Method

Samples of various ultimate pH were subjected to cooking temperatures of 55, 65, 70, 75 or 85 °C for 20, 40 or 60 min respectively. Cook loss, dimensional changes, WB shear force values, colour and myofibril structural changes were measured after cooking.

### 4.1.4 Cook loss in relation to *Bos indicus* (BI) content

#### 4.1.4.1 Experimental material

Six muscles groups; eye round, striploin, rump, topside, brisket and oyster blade were sourced from 18 domestic trade animals (0-4 tooth, males, left side carcass) from local abattoir (Brisbane, Queensland). In order to classify the BI content according to MSA grading procedure, the hump height of each individual carcass was measured. The carcasses were then assigned to three individual to BI range groups, (low, medium, high) see Table 4-2. The muscles were stored frozen at -20 °C and then thawed at 4 °C for 48 hours prior to analysis.

**Table 4-2.** Values of selected MSA grading parameters of beef carcasses used in the experiment (carcass weight of left side, dentition, pH, *Bos indicus* content as hump height, fat colour, meat colour, ossification) and collagen content of the eye round

<i>Bos indicus</i> content	Carcass Side weight (kg)	Dentition	pH	Hump height (mm)	Fat Colour	Meat Colour	Ossification	Collagen content (%)
Low	101.6	1	5.48	50	1	2	140	2.95
	131.6	0	5.45	50	1	2	150	3.14
	172.2	2	5.5	60	1	2	170	3.46
	132.6	2	5.55	55	1	3	190	2.95
	127.0	2	5.52	55	1	2	160	3.11
	144.8	0	5.49	55	1	2	150	3.07
Medium	182.6	4	5.44	80	1	1C	200	3.25
	198.2	4	5.46	100	1	1C	170	3.22
	177.2	4	5.57	90	1	2	150	2.98
	189.0	4	5.55	90	2	2	180	3.13
	167.8	0	5.47	80	1	1C	140	3.45
	183.4	4	5.62	85	1	3	180	3.52
High	180.4	4	5.45	135	1	1C	160	3.39
	166.6	3	5.49	140	1	2	170	3.58
	204.2	2	5.39	140	1	1C	150	2.50
	147.8	0	5.45	165	1	1C	170	3.22
	205.0	4	5.46	150	1	1C	150	3.31
	193.2	4	5.47	140	1	1C	170	3.74

#### 4.1.4.2 Method

The experiment was done in two stages:

**Stage 1.** Muscle samples from beef eye round from animals with three different hump heights, were cooked at three different temperatures (65, 70 or 75 °C) for three different times (20, 40 or 60 min) to evaluate the influence of cooking temperature and time on cook loss in relation to BI content. The eye round muscle is believed to be closer to the median value of evaluated parameters for all muscles in the carcass (Shorthose, 1991), so was chosen for the stage 1 analysis.

**Stage 2.** Five different muscle groups, from animals varying in BI content, were cooked at one temperature (70 °C) for 60 min to evaluate the influence of muscle types on cook loss in relation to BI content.

Quality parameters such as collagen content, cook loss, moisture content, WHC, dimensional changes, colour, WB shear values, compression measurements, myofibrils structure and changes in structure of muscle fibre fragments upon heating/cooking, were investigated.

#### 4.1.5 Cook loss in relation to marbling

##### 4.1.5.1 Experimental material

Two muscles groups, eye round and striploin, were sourced from 14 domestic trade animals (stunned by non-penetrative bolt, Halal sticking method, electrically stimulated, 0-2 tooth, males, left side carcass) from a local abattoir in Oakey, Queensland. The pH of the striploins was measured at the abattoir 18 hours post mortem and animals with pH of greater than 5.8 were rejected. The marbling score was determined according to the MSA method (Meat Standards Australia, 2007) where the grader visually assessed the cut surface of the striploin muscle (cut between the 12<sup>th</sup> and 13<sup>th</sup> rib). Carcasses were then grouped into three individual marbling score groups, low (0 - 1), medium (2 - 3) and high (4 - 5), see Table 4-3 and Figure 4-1. It is important to acknowledge that the marbling scores were linked to the carcass weights, final feeding regimes and pH values. The muscles were stored frozen at -20 °C after collection and then thawed at 4 °C for 48 hours prior to analysis.

**Table 4-3.** Values of selected MSA grading parameters of beef carcasses used in the experiment. Intramuscular fat content (IMF), carcass weight, days of grain feeding, dentition, pH (18 hours post slaughter), meat colour (MSA), fat colour (MSA), Rib fat, Fat colour, AUS-MEAT marbling score, MSA grade of the eye round (ST) [LOW 0-1, MED 2-3, HIGH 4-5], Average fat content. Mean  $\pm$  S.E. calculated from Eq. 4-1.

IMF	Carcass weight (kg)	Grain feed (days)	Dentition	pH	Meat Colour	Fat Colour	Rib fat (mm)	AUS-MEAT marbling score	Fat content Average $\pm$ SE (%)
Low	384.5	130	2	5.57	2	0	11	1	3.45 $\pm$ 0.29
	315.0	130	2	5.54	1C	1	10	0	5.09 $\pm$ 0.08
	357.5	130	2	5.48	1C	0	12	1	5.44 $\pm$ 0.01
	295.5	130	2	5.45	1C	0	9	1	4.01 $\pm$ 0.15
	375.0	130	2	5.51	1C	0	12	1	5.21 $\pm$ 0.25
Medium	363.0	130	2	5.49	1C	1	10	3	6.90 $\pm$ 0.38
	349.5	130	0	5.43	1C	0	13	2	9.77 $\pm$ 0.02
	354.5	130	2	5.51	1C	0	21	2	7.89 $\pm$ 0.14
	384.5	130	2	5.47	2	0	15	3	8.27 $\pm$ 0.27
	381.0	130	2	5.50	1C	0	14	3	8.09 $\pm$ 0.02
High	386.0	200	2	5.48	1C	1	13	4	18.95 $\pm$ 0.06
	405.5	200	2	5.49	1C	1	25	5	15.03 $\pm$ 0.35
	387.0	200	2	5.42	2	1	17	4	17.08 $\pm$ 0.03
	390.0	200	2	5.39	2	0	22	4	12.21 $\pm$ 0.07

#### 4.1.5.2 Method

The experiment was divided into two separate stages:

**Stage 1** - Cook loss and structural changes of eye round muscle were studied, within the three IMF ranges (low, medium and high). Blocks of eye round were cooked at different temperatures (65, 70 or 75 °C) and cooking times (20, 40 or 60 min).

**Stage 2** - Two muscle groups, striploin and eye round from the three IMF ranges were cooked at 70 °C for 20, 40 or 60 min.

Cook loss, dimensional changes, WB shear value, compression tests, colour changes, and microstructural changes were measured after cooking in both stages.



**Figure 4-1.** Steaks of striploins from beef carcasses with different intramuscular fat content (L – Low, M – Medium, H – High).

#### 4.1.6 Influence of interventions on the structural basis of cook loss

The influence of two interventions, PEF and HPTP, on the structural basis of cook loss in beef were studied.

##### 4.1.6.1 Pulsed electric field (PEF) - Experimental material

A total of ten eye round muscles was sourced from five domestic trade animals (0-2 tooth, steers) from a local abattoir (Melbourne, Victoria) from both left and right sides of the carcass. The carcass weights ranged from 313 to 363 kg, with an average of  $327.6 \pm 20.6$  kg.

The pH of each muscle was measured on collection (*i.e.* 48 hr post mortem) and muscles with a pH of greater than 5.8 were rejected. The muscles were trimmed of excess fat and connective tissue and twelve portions were cut in approximately 65 x 30 x 25 mm blocks. Of the twelve samples, six were cut in the longitudinal fibre direction and another six in the cross-sectional (perpendicular) fibre direction. The average weight of the samples was  $67.5 \pm 9.9$  g.

#### 4.1.6.2 PEF - Method

The impact of PEF processing on beef eye round was evaluated by measuring WB shear force, colour, mass loss, and macro- and microstructural changes of treated meat before and after cooking (70 °C, 60 min). Two aspects were studied: a) whether the positioning of the samples (perpendicular or longitudinal to the electric field) during PEF processing had an impact, and b) whether the PEF processing conditions had an impact on the macro- and microstructure of the meat. Based on previous experiments, the PEF processing was conducted at 0.25 kV/cm, pulsed frequency of 100 Hz, pulse width 10 µs, and a total treatment time of 30 or 60 ms, respectively. The process details are described in section 4.2.2.

#### 4.1.6.3 High Pressure Thermal Processing (HPTP) - Experimental materials

In this study we investigated the impact of HPTP in combination with two salt solutions (sodium chloride or sodium pyrophosphate) injected to 110% of the original weight on cook loss, colour changes, texture and microstructural changes in beef eye round. The experiment was divided into two stages:

**Stage 1** – Four eye round muscles were sourced from four domestic trade animals (0-2 tooth, steers) from a local butcher (Werribee, Victoria). The average weight of the carcasses was 241 kg and the pH of the muscles was  $5.48 \pm 0.02$ . The muscles were trimmed of excess fat and connective tissue and then cut into 36 blocks (60 x 30 x 30 mm). Samples were injected with a brine solution containing 0, 0.2, 0.6, 1.0 or 1.2% sodium chloride (NaCl) or a solution containing 0, 0.1, 0.2, 0.3 or 0.4% sodium pyrophosphate (PPi) to 110% weight of the sample. Samples were placed into polyethylene (PE) bags and salt solutions were injected through the cross-sectional side of the samples with a single-needle syringe inside the bag to avoid any loss. After injection, samples were gently massaged for about 15 min to ensure the brine to be absorbed. After salt injection, the samples were vacuum packaged and stored at 4 °C overnight until processing on the following day.

**Stage 2** – Three eye round muscles were cut into 39 (sub-stage 1), 42 (sub-stage 2) and 39 (sub-stage 3) blocks, respectively (Table 4-4). Sample preparation and injection procedure applied were as above. The samples were injected to 110% of initial weight with a brine solution containing either 1.0% NaCl or 0.2% PPi.

#### 4.1.6.4 HPTP - Method

**Stage 1** – HPTP at 600 MPa, 75 °C for 5 min or conventional cooking in a water bath at 75 °C for 30 min, where the internal temperature of the meat samples reached 75 °C in both cases.

**Stage 2** – Due to the complexity of experimental design (eight combinations of pressure and temperature settings within two different solutions), the experiment was divided into three sub-stages (Table 4-4) carried out on different days. A set of control samples was cooked for 30 min in a water bath at temperatures that were similar to those used for HPTP.

**Table 4-4.** Experimental design of HPTP and control (cook-only) treatment parameters

Sub-stage	Number of samples	Brine (type)	HPTP (5 min)		Control (cook-only) (30 min) Temperature (°C)
			Pressure (MPa)	Temperature (°C)	
1	48	PPi (0.2%)	300	75	60, 64, 75
			350	64	
			470	75	
			470	60	
			590	64	
			640	75	
2	30	PPi (0.2%) or NaCl (1.0%)	350	85	75, 85, 89
			590	85	
			470	75	
			470	89	
3	48	NaCl (1.0%)	300	75	60, 64, 75
			350	64	
			470	75	
			470	60	
			590	64	
			640	75	

The equipment details are described in section 4.2.3.

In both stages the effect of HPTP was evaluated in relation to cook loss, colour, textural and microstructural changes.

## 4.2 Methods – cooking and processing

### 4.2.1 Cooking in water baths

Before cooking, fresh meat blocks were stored at 4 °C for at least 30 min to equilibrate. Samples were then cooked in PE plastic bags in circulating water baths using a digitally controlled heater with a temperature variation of  $\pm 0.5^{\circ}\text{C}$ . The cooking temperature and time varied between experiments (see specific descriptions Table 4-1) but in most cases the blocks were cooked for either 20, 40, or 60 min, at 55, 65, 70, 75 or 85 °C, respectively. After cooking, samples were shock chilled in ice slurry (0 °C) for 15 min.

### 4.2.2 Pulsed electric field processing

The PEF processing of meat was performed (using the conditions in 4.1.6.2) using a Diversified Technologies Power Mod™ 25 kW Pulsed Electric Field System (Diversified Technologies, Inc., Bedford, MA, USA), consisting of a PEF treatment chamber and a modulator cabinet described elsewhere (Buckow, Schroeder, Berres, Baumann, & Knoerzer, 2010). The treatments were performed in a treatment chamber (Figure 4-2), designed and manufactured by CSIRO to allow PEF applications of high electrical field strengths to solid foods.

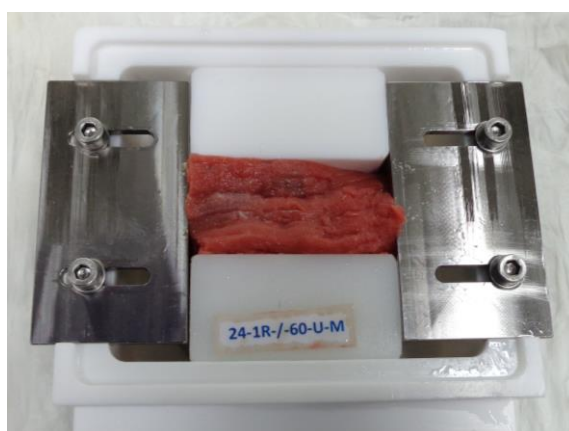


**Figure 4-2.** Eye round meat sample (longitudinal orientation of the muscle fibres) in a modified PEF treatment chamber for treatment of solid foods.

All meat samples were conditioned to approximately 4 °C overnight. The PEF treatment chamber was also conditioned to approximately 2 °C in an ice slurry before each treatment, and excess water removed prior to use. Samples were placed into the PEF treatment chamber with no air pockets at the surface of the electrodes. Square wave pulses of 10  $\mu\text{s}$  width at a peak voltage of 1,500 V were applied, resulting in an electrical field strength of 0.25 kV/cm. The pulse repetition rate was set to 100 Hz for all treatments in this trial. PEF was applied to the meat for different treatment times, 30 or 60 ms, resulting in two different energy inputs, 3.2 or 7.5 J/g respectively. Pulse shape, frequency, peak

voltage and electrical currents were recorded with an oscilloscope (#GDS-1102, GW Instek, Taipei, Taiwan) attached to the output port of the PEF system.

#### **4.2.3 High pressure thermal processing**

Samples were treated at high pressure in a 35 L high pressure system (QFP 35 L-600-S Food Press, Avure Technologies AB, Kent, USA). Vacuum-packed sample blocks were pre-heated to a core temperature of 50 °C or 60 °C (11 min at 55 °C or 65 °C in a conditioning tank) and were immediately transferred into the high pressure vessel. The pressure ramp-up rate was approximately 4 MPa/s. HPTP conditions were varied between 300 – 640 MPa and 60 – 89 °C. Once the maximum pressure was reached and the holding time was complete (5 min), the pressure was immediately released. Samples were then transferred into a cold water tank to be cooled for 10 min at 4 °C to avoid over cooking.

### 4.3 Characterisation methods

#### 4.3.1 Drip loss, cook loss and weep loss

Samples were weighed before and after overnight storage and cooking to determine drip loss and cook loss, respectively. Cooked samples were also weighed the following day to record any weep from storage overnight at 4 °C. The **total mass loss** was calculated as the difference between weights of raw and cooked meat samples (cook loss + weep loss) after overnight cold storage.

#### 4.3.2 Dimensional changes

The length, width and breadth of the individual blocks (as shown in Figure 4-3) were measured with digital Vernier callipers before and after cooking as well as before and after processing intervention to determine dimensional changes.

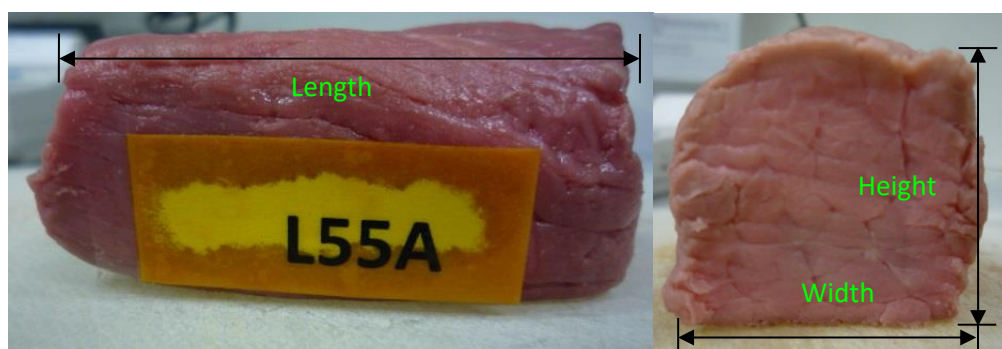


**Figure 4-3.** Blocks of samples showing the length, height and width measurements.

#### 4.3.3 Moisture content

Samples were measured in duplicate using the drying method described by (Thornton, 1981).

#### 4.3.4 Expressible moisture

Meat samples were cut using a scalpel into oblong pieces weighing  $3.0 \text{ g} \pm 0.2 \text{ g}$ . Strips of filter paper (approximately 175 mm X 15 mm) were cut from Whatman No. 1 filter paper and the meat sample pieces were then placed in the middle of a strip of filter paper, and the filter paper folded over so that the sample was resting in a sling formation. The sample and doubled-over filter paper were then placed into a 45 ml centrifuge tube. Samples were centrifuged at 5000 g for 15 minutes at 18 °C (Beckman Coulter J6-MI centrifuge). Immediately after centrifugation, the samples were removed from the tubes and weighed. The expressible moisture (EM) was calculated as weight change before and after centrifugation. Three sub-samples were cut and analysed from each sample.

#### 4.3.5 Colour measurement

The colour of each sample block was measured using a Minolta Chroma Meter CR-400 (Minolta Co., Ltd, Japan). Measurements were taken before and after cooking. The instrument was equilibrated in a 10 °C cool room / 20 °C laboratory, calibrated with a standard white plate under D65 illumination ( $Y = 92.0$ ,  $x = 0.3163$ ,  $y = 0.3328$ ) before use. Colour measurements were taken across the muscle fibres, avoiding areas of visible fat. Triplicate colour measurements were taken and the mean recorded. The colour was presented as values of: coordinate of the red colour lightness –  $L^*$ , redness –  $a^*$ , and yellowness –  $b^*$ .

#### 4.3.6 pH measurements

Muscle pH was measured by directly inserting a spear pH probe (IJ44C probe, Ionode, Pty Ltd., Australia) and temperature probe, connected to a WP-80 pH-mV-Temperature meter (TPS Pty Ltd, Australia), into the sample. The unit was calibrated with pH 4.00 and pH 7.00 buffer standards at 8 °C.

#### 4.3.7 Fat content

The fat content (FC) was calculated from the moisture content (4.3.3) applying the following equation for beef adopted from (Thornton, 1981):

$$FC = 95.6 - (\text{moisture content } (\%) \times 1.24) (\%)$$

Eq. 4-1

#### 4.3.8 Mechanical measurements

Meat tenderness was measured using an Instron 5564 fitted with a 500 N load cell (Instron, Norwood, Massachusetts, USA) and a modification of the WB shear device (P. E. Bouton, Harris, P.V. , 1972; Bratzler, 1932). The samples were cut into a rectangular shape (15 mm width x 6.7 mm height) giving a cross-sectional area of 1.0 cm<sup>2</sup>, and at least 25 mm long. A triangular shaped blade with a thickness of 0.64 mm was attached to an overhead clamp and was pulled up through the muscle fibres, perpendicular to the fibre direction, at a speed of 100 mm/min. The maximum peak force (PF) was objectively determined using the Bluehill® 3 software (Instron®, Illinois Tool Works Inc., USA), while the initial yield (IY) was determined by the operator as the height of the first peak from the curve. The difference between these measurements (PF-IY) was also calculated. Six determinations were made on each sample and the mean recorded.

### **4.3.9 Microstructural characterisation**

#### **4.3.9.1 Myofibril preparation**

About 1 g of muscle (raw or cooked) was homogenised in 15 ml ice cold Mannitol buffer (380 mM mannitol, 50 mM potassium acetate, adjusted to pH 5.6 with acetic acid) using an Ultra-turrax homogeniser (Ultra Turrax, T25 basic from IKA Laborotechnik, Germany) with a 18 mm head at 16,000 rpm for 3 times (10 s, followed by 10 s rest). The Mannitol buffer used for homogenisation was matched to muscle sample pH to prevent unwanted structural changes due to osmotic effects. The sample tubes were kept on ice at all times.

#### **4.3.9.2 Muscle fibre fragment preparation**

Muscle fibre fragments were prepared by homogenisation of 1 g of raw muscle 10 ml cold mannitol buffer (380 mM mannitol, 50 mM potassium acetate, with/without protease inhibitor) using an Ultra-turrax homogeniser (18 mm head, 11 000 rpm, 3 x 10 s) to make suspensions of muscle fibre fragments. The sample tubes were kept on ice during homogenisation to keep the suspension cold.

#### **4.3.9.3 Endomysial ghost preparation**

“Endomysial ghosts” were prepared from 1 g samples, using the method of (Champion, Purslow, & Duance, 1988). Briefly, 1 g of raw muscle was homogenised as in 4.3.9.2, in 10 ml of ice cold 50 mM CaCl<sub>2</sub>. The homogenate was filtered through a copper filter (1 mm<sup>2</sup> perforations) and the material remaining on the filter re-homogenised in CaCl<sub>2</sub> and re-filtered. This process was repeated three times. The filtrate was centrifuged and the sedimented endomysia was re-suspended in 25 mM NaCl, 2.5 mM histidine chloride buffer, pH 7.4. The suspension was then centrifuged and incubated at 37 °C for 30 min. After centrifugation, five washes were conducted in histidine buffer followed by three washes in distilled water adjusted to pH 7.4-7-8 with 1 M Tris.

#### **4.3.9.4 Epimysial fragment preparation**

1 g of connective tissue was added to 15 ml ice cold Mannitol buffer (380 mM, pH 5.6). Samples were blended by using an Ultra Turrax homogeniser (Ultra Turrax, T25 basic, IKA Laborotechnik, Germany) at 22,000 rpm with an 18 mm head. The samples were blended for 15 s, followed by a pause of 15 s. This procedure was repeated three times whilst the samples were cooled on ice at all times.

#### **4.3.9.5 Endomysial fragment preparation**

For each sample, 20 g of muscle tissue without any visible epimysium, perimysium or fat was cut into small pieces (1-5 mm) and homogenised for 30 s in 180 ml Mannitol buffer (380 mM, pH 5.6) using a Waring type blender. The connective tissue fraction was collected with an Abichem test sieve with 150 µm aperture. The sample was then rinsed with Mannitol buffer (380 mM mannitol, 50 mM

potassium acetate, adjusted to pH 5.6 with acetic acid) several times before resuspending it in mannitol buffer.

#### **4.3.9.6 Structure of myofibrils by confocal laser scanning microscopy**

Small aliquots of suspended myofibrils were diluted (1:4) with Mannitol buffer and stained with fluorescein isothiocyanate (FITC, 10 ppm). A sample drop was added to a microscope slide and sealed with nail polish. The myofibrils were observed under a 63× water immersion objective of a Leica TCS SP5 confocal laser scanning microscope (Leica Microsystems, Germany) using a 488 nm Ar-laser for dye excitation, 500 – 535 nm for detection. Myofibril sarcomere lengths were measured from images using Leica LAS AF software (Leica Microsystems, Germany). At least twelve myofibrils were observed in each sample.

#### **4.3.9.7 Structure of myofibrils by optical microscopy**

Small aliquots of suspended myofibrils were placed on flat microscope slides and sealed with nail polish. The myofibrils were observed in phase contrast mode by a Leica DM6000 microscope (Leica Microsystems, Germany). At least five images per slide were captured with an attached Leica DFC450 C camera. Images were analysed for average myofibril diameter and sarcomere length using ImageJ software (open source image processing program built by Wayne Rasband, National Institute of Mental Health, Bethesda, Maryland, USA).

#### **4.3.9.8 In-situ heating of muscle fibre fragments**

A drop of muscle fibre fragment suspension was mounted on a cavity slide and sealed with nail polish. The slide was placed on a Linkam THMS600 temperature stage (Linkam Scientific Instruments Ltd, UK) and under a 20× air objective (Leica 566049, N PLAN, L 20×/0.40) of a Leica TCS SP5 CLSM (Leica Microsystems, Germany). Images were captured simultaneously in Scan-BF transmission and fluorescence mode, using a 488 nm Ar-laser during heating (10 °C/min). Changes in length, diameter and sarcomere length of the fibre fragments with temperature were measured from the images using Leica LAS AF software (Leica Microsystems, Germany).

#### **4.3.9.9 Fluorescent labelling of connective tissue**

For fluorescein labelling of epimysium, 10 drops of suspended connective tissue solution were diluted in 1 ml Mannitol buffer and stained with 1 drop of 0.4% Fast Green stain. For endomysium, 1 drop of 0.4% Fast green stain was added per 2 ml of homogenised endomysium. One drop of stained suspension was then placed on a cavity slide and sealed with nail polish to prevent evaporation.

#### **4.3.9.10 Plastic embedding of muscle tissue for light microscopy**

Two subsamples (3 x 3 x 10 mm) of meat per experimental treatment were cut lengthwise along the muscle and put into 2.5% glutaraldehyde in 0.1 M Sorensen's buffer (pH 5.6) for resin embedding.

Glutaraldehyde fixed samples were dehydrated with increasing concentrations of ethanol (50, 75, 95% and Absolute alcohol) and then followed by infiltration of Technovit 7100 resin at different concentration ratios (1:2, 1:1 and 2:1 resin: ethanol for at least 2 hours in each step, followed by 100% resin for 30 hours). The samples were transferred to moulds for polymerisation at room temperature.

#### **4.3.9.11 Light microscopy of embedded samples**

Sections (1  $\mu\text{m}$ ) were cut from each resin blocks using glass knives in an Ultracut E ultramicrotome. Both longitudinal and cross-sectional sections of the muscles were floated onto water droplets and dried to glass microscope slides. The sections were stained with Orange G and Aniline blue for muscle and connective tissue, respectively. A Leica DM6100 microscope was used to image the sections using 10, 20 and 40X air objectives. Images were captured using Leica LAS V4.9 software.

#### **4.3.9.12 Transmission Electron Microscopy**

The method used to prepare the samples was previously described by Jung, de Lamballerie-Anton, and Ghoul (2000). After the treatments, meat samples were cut into sections with a razor blade (1 x 1 x 10 mm) and fixed immediately in Kanovsky's fixture (2% paraformaldehyde, 2.5% glutaraldehyde in a 0.1 M sodium cacodylate buffer, pH 7.4) overnight, at room temperature. The next day, the fixture was rinsed with a 0.1 M cacodylate buffer (3 times) and post-fixed in 1% osmium tetroxide and 1.5% potassium ferricyanide in distilled water for 1.5 hours. The samples were washed (3 times) in distilled water and stored in the refrigerator overnight (5 °C). Samples were then dehydrated with ethanol (50, 70, 90, 95, and 100%) and further dehydrated with absolute acetone (100%). Subsequently, the samples were placed in a mixture of acetone and Spurr's resin (1:1) with lids on, rotating, overnight. The next day, the samples were further exchanged with the same solution with lids off for 2 hours.

Finally, the samples were infiltrated via vacuum and then embedded in low viscosity Spurr's resin (Spurr, 1969). The blocks were cured at 70 °C and ultrathin sections (90 nm) were cut using a diamond knife. Subsequently, the thin sections were mounted onto a copper grid and observed using the JEOL 1010 transmission electron microscope (TEM) operated at 80 kV. TEM micrographs were captured with a Gatan Orius SC600 CCD Camera.

## 5.0 PROJECT OUTCOMES & DISCUSSION

### 5.1 Mass loss upon cooking

It is well-known that meat shrinks and loses moisture when cooked. This project have investigated the influence of factors such as cooking time and temperature, ageing, muscle type, ultimate pH, marbling, BI content on the mass loss upon cooking. Furthermore, interventions such as PEF and HPTP were used to reduce cooking losses.

Two different measurements of mass loss were used (Figure 5-1). Firstly, cook loss, which corresponds to the amount of liquid that was released during cooking, and secondly, subsequent weep loss, the further release of liquid as the samples were stored at 4 °C overnight(see 4.3.1). The combination, cook loss + weep loss, was referred to as total mass loss. Most of the lost mass is water but it also contains water soluble proteins and minerals.

A third measurement relating to moisture content and juiciness is WHC. This is the ability of meat to retain either inherent or added water upon the application of forces, *e.g.* pressure or centrifugation. In this project, WHC was measured as EM (see 4.3.4).

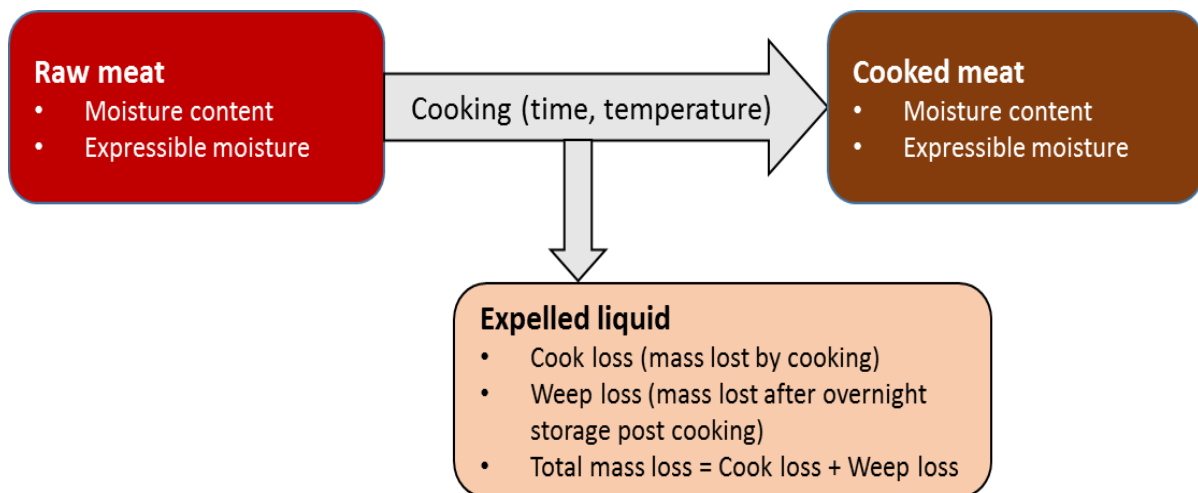


**Figure 5-1.** Schematic diagram showing measurements carried out in relation to weight loss due to cooking.

### 5.1.1 Influence of cooking time and temperature

As expected, the cooking time and temperature had a great impact on the total mass loss. The total mass loss increased with cooking temperature (Figure 5-2), with over 1/3 of the initial mass lost when meat was cooked at 85 °C for 40-60 min. Overall, a shorter cooking time resulted in lower losses which was more pronounced at higher cooking temperatures. The data presented here are further discussed in section 5.5.

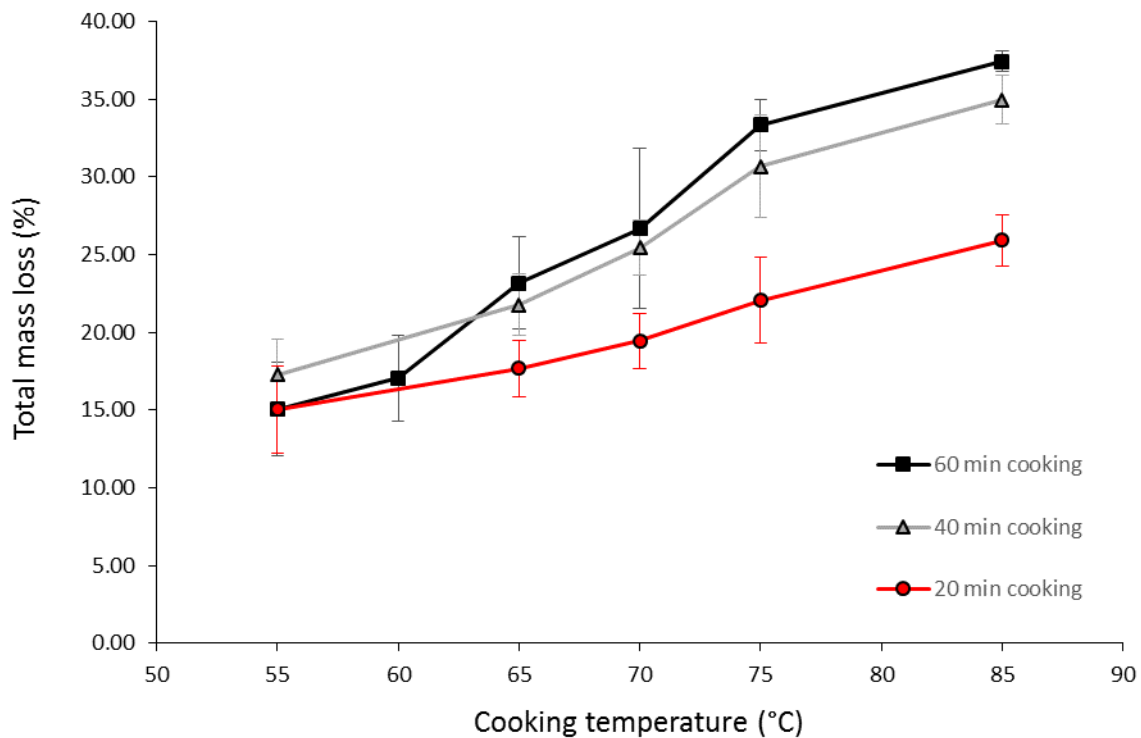


**Figure 5-2.** Mean total mass loss (%) of blocks of eye round cooked in a water-bath at various temperatures and time intervals. Error bars show standard deviation.

The cook loss was the major component of the total mass loss and, consequently, determined the result. The weep loss trend was inverse to the cook loss trend, *i.e.* the largest weep loss was observed after cooking at 55 °C and more weep loss was observed after cooking for 20 min, than for 40 or 60 min (data not shown). The combination of low temperature (55 °C) and short time (20 min) probably affects the equilibrium point of water retention in meat. In other words, the meat does not have a chance to reach a reasonable equilibrium during the cooking phase and will continue to exude water during the storage phase.

### 5.1.2 Influence of ageing

Ageing of eye round muscle for 14 days led to 1.5-3% higher total mass loss in comparison to the control samples (non-aged) upon cooking when blocks of meat were cooked for 60 min at 55-75 °C. Findlay and Stanley (1984) reported that ageing reduces the denaturation temperature ( $T_{max}$ ) of myosin and actin peaks in DSC studies, as well as denaturation enthalpy. This may reflect destabilisation of the structure of filamentous actin and myosin, hence denaturation is achieved faster at a given temperature. This may explain the increased cook loss seen in aged muscle.

### 5.1.3 Influence of muscle type

The mass loss of different beef primal muscles (*i.e.* striploin, rump, topside, outside flat, brisket and oyster blade) upon cooking at 70 °C for 60 min was investigated. The total mass loss ranged between 26-30% and no statistically significant difference between muscles was observed.

### 5.1.4 Influence of ultimate pH

#### 5.1.4.1 Cook loss

The cook loss increased with increasing cooking temperature and time within each pH range, see Figure 5-3. In the low, medium and high pH ranges, the cook loss varied from  $6.5 \pm 0.8\%$  (55 °C/20 min) to  $36.9 \pm 0.9\%$  (85 °C/60 min),  $4.4 \pm 1.5\%$  (55 °C/20 min) to  $34.0 \pm 1.6\%$  (85 °C/60 min) and  $2.5 \pm 1.2\%$  (55 °C/20 min) to  $30.5 \pm 6.1\%$  (85 °C/60 min), respectively. In general, high pH meat had the lowest cook loss at each time/temperature mode, followed by medium and low pH meat had the highest cook loss. Comparing the cook loss amongst pH ranges within cooking modes, several 'overlapping' areas can be found: For example, cook loss values for low pH meat cooked for 20 min show similar values as for high pH meat cooked for 40 min at the same temperature. A similar result occurs for medium pH meat cooked for 40 min compared to high pH meat cooked for 60 min, as well as for low pH meat cooked for 40 min compared to medium pH meat cooked for 60 min. This might be due to the fact that protein denaturation is pH dependant, and consequently, has an impact on cook loss as well.

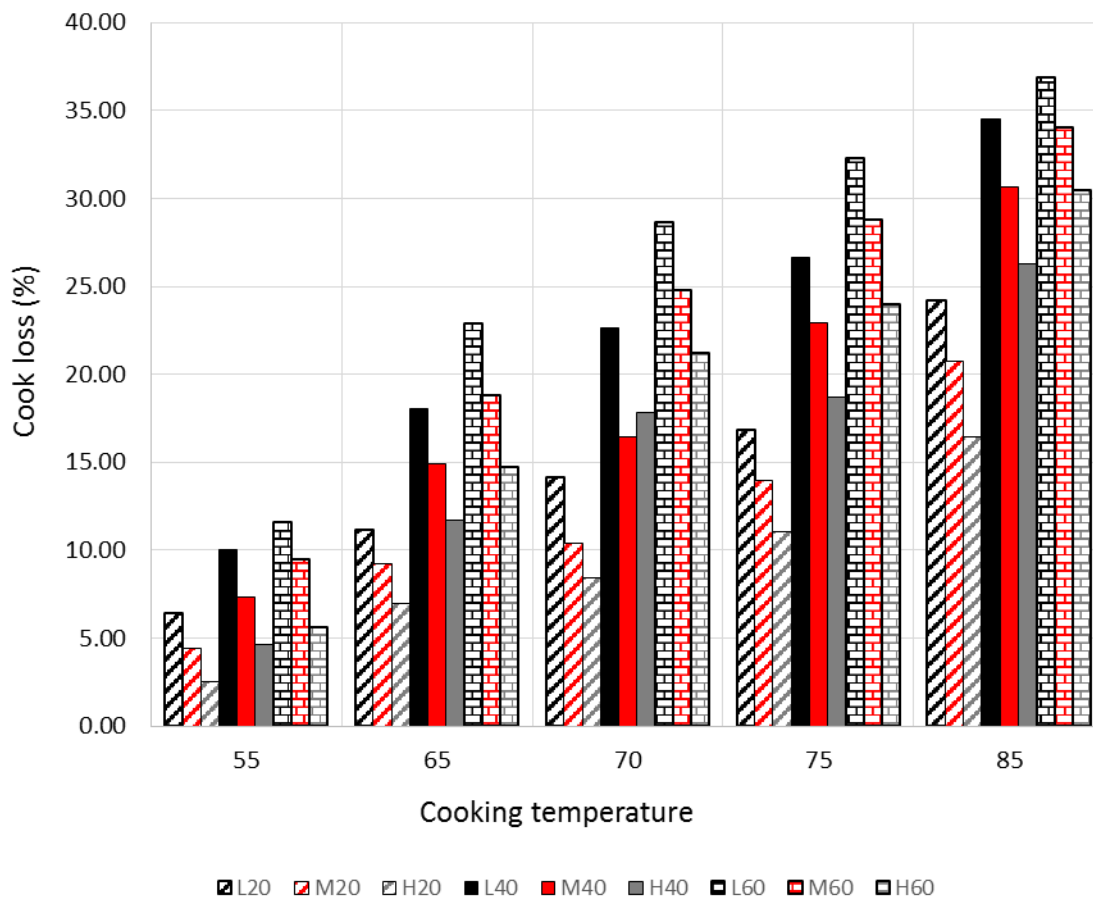


**Figure 5-3.** Cook loss of meat samples with different pH ranges, cooked at different temperatures and times. (L = Low pH, M = Medium pH, H = High pH, 20, 40 and 60 min).

#### 5.1.4.2 Weep loss.

The weep loss that exuded from the cooked samples during overnight storage was inversely related to the percentage of cook loss in each pH range, *i.e.* the higher the cook loss, the lower the weep loss. Comparing samples by temperature, the most significant weep loss was recorded for samples cooked at 55 °C (5.0 – 9.6%) regardless of pH and cooking time. When considering the influence of cooking time, the highest weep loss was observed for samples cooked for 20 min. Here, the meat did not have a chance to reach equilibrium during the cooking phase and continued to exude water during the storage phase. Overall, the high pH samples showed a lower weep loss (0.4 – 6.2%) compared to the medium (0.6 – 9.6%) and low pH meat (0.5 – 8.6%).

#### 5.1.4.3 Total mass loss

The total mass loss (cook loss + weep loss) showed a similar pattern to cook loss in relation to temperature, time and pH, as the cook loss was the dominant factor. This confirmed the trend that highest mass loss was observed in low pH samples, whereas high pH samples showed minimal losses.

#### 5.1.4.4 Moisture content.

The highest moisture content of cooked meat ( $74.0\% \pm 0.6$ ) was reported for the high pH meat cooked at  $55\text{ }^{\circ}\text{C}$  for 20 min. This was only 1.9% units lower than the corresponding raw sample ( $75.9\% \pm 0.6$ ). On the other hand, the lowest moisture content ( $63.0\% \pm 1.3$ ) was found in low pH meat cooked at  $85\text{ }^{\circ}\text{C}$  for 60 min. The corresponding raw samples had a moisture content of  $75.1\% \pm 0.8$  which led to a calculated mass loss of 33.4% during cooking. This was within the error range of the measured total mass loss ( $37.2\% \pm 0.7$ ) for these samples. As expected, the total moisture content data were in agreement with the total mass loss results across the range.

#### 5.1.4.5 Expressible moisture

The EM of low pH samples was higher ( $10.9 \pm 1.8\%$ ) than for medium pH ( $7.6 \pm 1.8\%$ ) and high pH samples ( $8.0 \pm 0.9\%$ ). This is because low pH meat has a pH that is closer to the isoelectric point of the major proteins in the muscle. Therefore, the protein conformation is denser and provides less space to retain water compared to high pH meat (Hamm & Deatherage, 1960).

For cooked samples, the WHC was significantly influenced by cooking time and temperature. Increased cooking times and higher temperatures resulted in reduced water content and lower EM.

Cook loss, weep loss, total mass loss and EM were significantly ( $P < 0.001$ ) influenced by cooking temperature, time and pH. Low pH meat exhibited a higher cook loss, lower moisture content and EM of cooked samples than high pH meat.

### 5.1.5 Influence of *Bos indicus* content

#### 5.1.5.1 Raw meat

The moisture content and the WHC of raw meat did not depend on the BI content. The moisture content was 75 – 76% and the WHC (measured as expressible moisture) was 22 – 23% for all samples.

#### 5.1.5.2 Cooked meat

There were no differences in total mass losses between different BI content for all cooking regimes employed; temperatures (65, 70 and  $75\text{ }^{\circ}\text{C}$ ) and times (20, 40 and 60 min) as shown in Figure 5-4. Accordingly, there were no significant ( $P > 0.001$ ) differences in the moisture content nor in the WHC after cooking in relation to the different level of BI content. Hence, it can be concluded that there was

no relationship between BI content and mass loss, and that the cooking time and temperature determined the degree of mass loss.

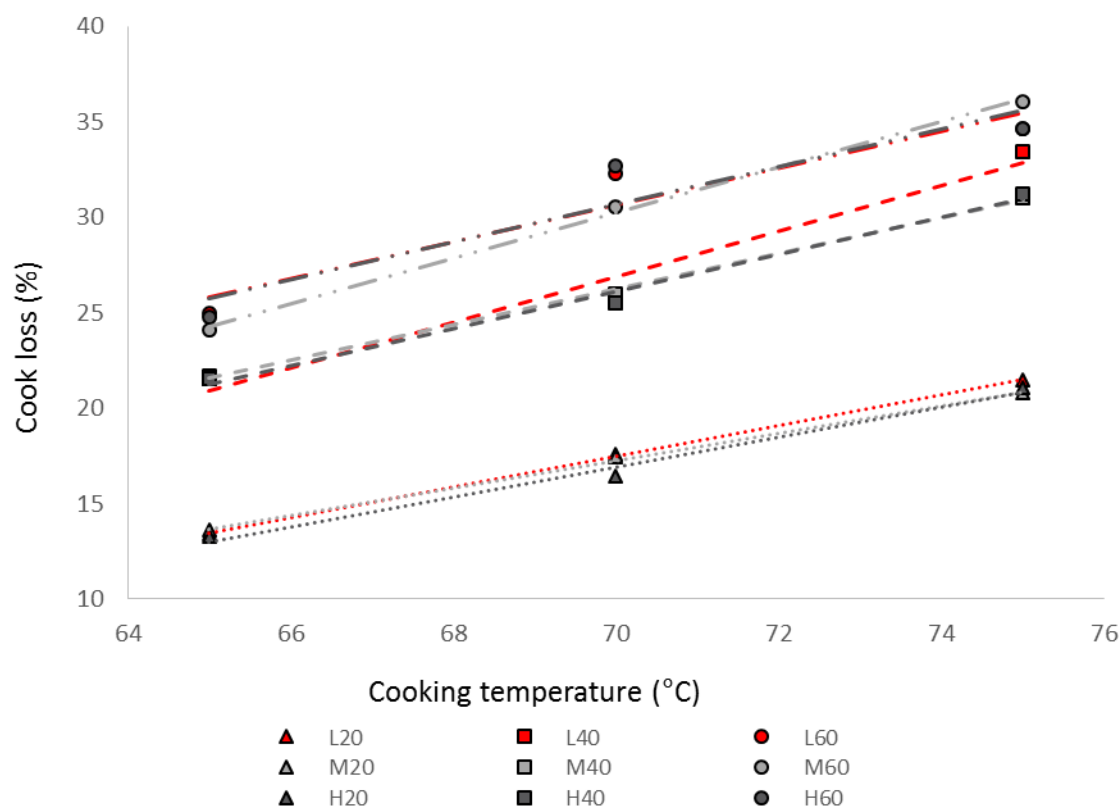


**Figure 5-4.** Effect of *Bos indicus* content (L – low, M – medium, H – high) on cook loss upon cooking at different temperatures (65, 70 and 75 °C) and times (20, 40 and 60 min) of beef eye round (n = 6).

## 5.1.6 Influence of intramuscular fat

### 5.1.6.1 Raw meat

The moisture content and EM of raw eye round were 73-75% and 21-22%, respectively. For striploin, the moisture content varied greatly from 64 to 73% for high and low IMF content, respectively and EM from 21 to 25% (Thornton, 1981). The greater variation in the moisture content of striploin compared to eye round was a reflection of the amount of fat and different accumulation of IMF in different muscle types, with more fat in the striploin than in the eye round. The moisture content was significantly lower ( $P < 0.001$ ) at higher IMF for both raw muscle types while the WHC did not depend on the IMF content ( $P > 0.05$ ).

### 5.1.6.2 Cooked meat

There were no differences in total mass losses between the three groups with different IMF contents for any of the cooking regimes; temperatures (65, 70 or 75 °C) and times (20, 40 or 60 min). However, the final moisture content of high IMF meat was lower ( $P < 0.001$ ) than for low IMF meat due to its higher amount of fat. This suggested that high IMF meat requires shorter cooking times than meat with lower IMF to obtain an equivalent moisture content in the cooked product and this could, potentially, influence tenderness. It must be noted that the lower moisture content could be counteracted during mastication by the higher fat content, which facilitates lubrication.

The WHC was not dependent on IMF content. This result was unexpected, as it was anticipated that at a lower moisture content, water would be more tightly bound and less expressible compared to higher moisture contents. In conclusion, results showed that at cooking temperatures between 65 and 75 °C for times between 20 and 60 min, the total mass loss and water retention were independent of the IMF content but influenced by actual cooking temperature and time.

### 5.1.7 Effect of interventions

#### 5.1.7.1 Pulsed electric field treatment

PEF processing can cause electroporation in biological cells, which can increase the amount of water expelled from meat during storage (*i.e.* drip loss) or cooking (*i.e.* total mass loss) (Arroyo, Eslami, et al., 2015). In our study, the application of PEF processing did not significantly ( $P < 0.001$ ) affect drip loss (1-1.5%) or total mass loss (25 – 32%) of cooked beef eye round compared to non-PEF pre-processed, cooked samples. However, the orientation in which the meat blocks were cut for PEF processing (either cross-sectionally or longitudinally in relation to its fibre direction) had an effect on the cook loss but not on the weep loss. The cook loss was greater in meat blocks treated cross-sectionally (~31%) compared to longitudinally treated meat blocks (within the range 24 – 27%). The higher water loss in cross-sectionally treated meat blocks could be due to the flow of electric current perpendicular to the muscle fibre orientation. However, all cross-sectional meat blocks including the control (untreated) had a higher cook loss. Consequently, it is likely that there are other reasons for this effect. To fit the treatment chamber, the blocks that were PEF treated cross-sectionally had to be cut differently from the primal muscles compared to the ones for longitudinal PEF processing. Although having the same volume, the cuts for cross-sectional treatment resulted in blocks with a larger surface area of exposed fibre ends (Rowe, 1978). Assuming that the majority of water released during cooking is expelled from the cross-sections rather than from the side of the fibres, the higher cook loss for cross-sectionally PEF treated blocks could be explained by their larger cross-sectional areas compared to the longitudinally PEF treated blocks.

In addition to drip, cook and weep loss, water binding was also measured as moisture content and WHC. The results from these measurements showed that the application of PEF processing did not

have a significant ( $P < 0.001$ ) effect on water binding and blocks with a larger cross-sectional fibre area had a lower moisture content after cooking, in agreement with the above results.

### 5.1.7.2 High pressure thermal treatment

#### Effect of salt concentration and HPTP on liquid loss

Blocks of eye round were injected with salt solutions, either PPI or NaCl at various concentrations, prior to HPTP. The amount of liquid lost after HPTP was compared to cook loss for samples cooked in a water bath to reach the same core temperature. As seen in Figure 5-5, no significant differences ( $P < 0.001$ ) were found between the different injected salt concentrations (18-24% mass loss for NaCl (A) and 23.0-23.9% for PPI (B)). However, the cook loss was greater (26-32% mass loss) in the control samples (cook-only) compared to the HPTP samples.

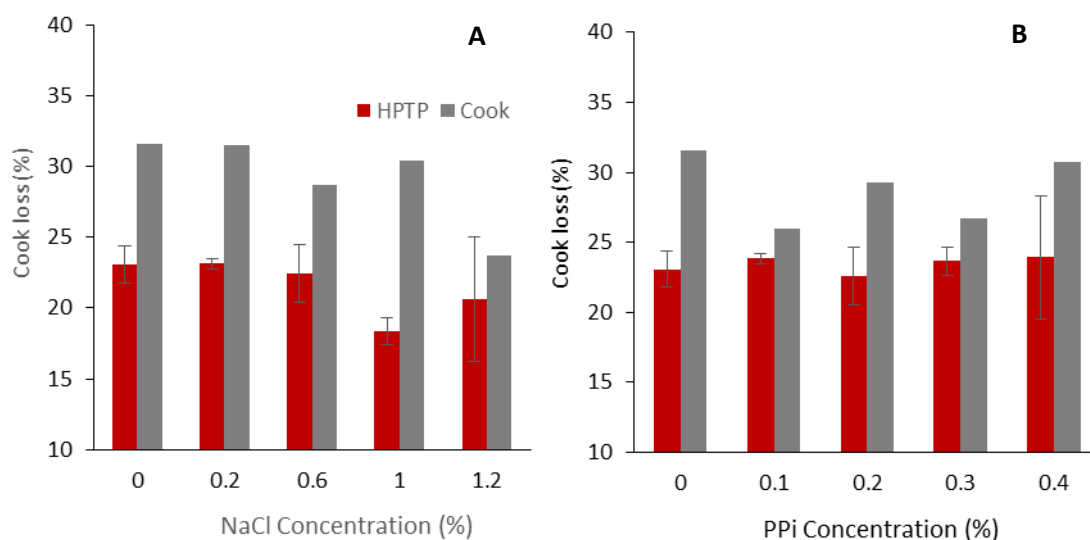


**Figure 5-5. (A)** Effect of NaCl concentration on the loss of liquid after treatment, HPTP (600 MPa, 75 °C, 5 min) or cook-only (75 °C, 30 min). **(B)** The effect of PPI concentration on the loss of liquid after treatment, HPTP (600 MPa, 75 °C, 5 min) or cook-only (75 °C, 30 min).

#### Effect of various HPTP pressures and temperatures on mass loss

In the next stage, various pressure and temperature combinations were investigated in relation to mass loss after processing. The results after HPTP : pressure (300, 350, 470, 590 or 640 MPa), temperatures (60, 64, 75, 85 or 89 °C) and processing time (5 min) or control cooking: pressure (0.1 MPa), temperature (60, 64, 75, 85 or 89 °C) and processing time (30 min), injected with either 1.0% NaCl or 0.2% PPI, are shown in Table 5-1.

The HPTP samples had lower mass loss compared to the control samples for both salt types. Samples injected with 0.2% PPI and treated at 640 MPa at 75 °C for 5 min had a similar cook loss ( $25.45 \pm 3.44\%$ ) as samples cooked at ambient pressure at 60 °C for 30 min ( $25.75 \pm 1.67\%$ ) and lower losses than

samples cooked at ambient pressure at 75 °C for 30 min ( $31.27 \pm 3.34\%$ ). Similar results were reported for the samples injected with 1.0% NaCl. There were no significant interactions between pressure and temperature for either PPI or NaCl injected samples. Furthermore, the brine/salt type did not have a significant ( $P > 0.05$ ) influence on the mass loss after HPTP. Furthermore, the cooking temperatures significantly ( $P < 0.001$ ) influenced cook loss, but the cook loss was not significantly ( $P < 0.05$ ) affected by the brine type used.

**Table 5-1.** Main effects of HPTP (300, 350, 470, 590 or 640 MPa and 60, 64, 75, 85 or 89 °C for 5 min) and control (cook-only, 0.1 MPa and 60, 64, 75, 85 or 89 °C for 30 min) on mass loss of processed beef eye round, injected with 0.2% PPI or 1.0% NaCl (Mean  $\pm$  S.E.)

	Pressure (MPa)	Temp (°C)	Mass Loss (%)	
			PPI 0.2%	NaCl 1.0%
HPTP	300	75	25.01 $\pm$ 3.79	21.66 $\pm$ 1.9
	350	64	17.96 $\pm$ 2.48	21.45 $\pm$ 5.67
	350	85	23.94 $\pm$ 2.37	23.61 $\pm$ 5.42
	470	60	18.31 $\pm$ 3.12	24.52 $\pm$ 1.81
	470	75	23.06 $\pm$ 4.75	23.23 $\pm$ 2.95
	470	89	24.12 $\pm$ 3.73	22.58 $\pm$ 2.92
	590	64	22.55 $\pm$ 5.55	19.54 $\pm$ 2.95
	590	85	22.81 $\pm$ 2.21	24.12 $\pm$ 5.71
	640	75	25.45 $\pm$ 3.44	24.67 $\pm$ 0.44
Cooking	0.1	60	25.75 $\pm$ 1.67	23.96 $\pm$ 3.1
	0.1	64	25.31 $\pm$ 1.58	22.34 $\pm$ 3.55
	0.1	75	32.26 $\pm$ 5.68	26.26 $\pm$ 6.39
	0.1	85	35.07 $\pm$ 4.31	33.77 $\pm$ 3.05
	0.1	89	31.27 $\pm$ 3.34	34.02 $\pm$ 3.44

## 5.2 Dimensions and microstructure

Meat is known to shrink upon cooking due to protein denaturation. This section reports the dimensional changes both of large scale (blocks of meat) and small scale (isolated muscle fibre fragments and myofibrils). The impact of cooking temperature, cooking time, ageing, muscle type, ultimate pH, BI and IMF content and pre-processing by PEF processing or HPTP on the structure of beef muscle were studied. Godsalve et al. (1977) proposed a model for denaturing and shrinking of proteins at increased temperatures, forcing water from between-muscle fibre spaces to the surface of the meat – “a self-squeezing sponge” , resulting in mass loss and shrinkage of meat. In the present study, the squeezing/shrinkage could be divided into two types; a cross-sectional shrinkage and a lengthwise shrinkage. As meat is a highly ordered structure, it is likely that different types of proteins are responsible for the changes in width and length.

### 5.2.1 Influence of cooking time and temperature

#### 5.2.1.1 Cross-sectional shrinkage

Meat changes its dimensions upon heating/cooking, initially through shrinkage across the muscle fibres (Purslow et al., 2016). This shrinkage starts at around 50 °C and is most likely driven by the denaturation of myosin. From 55 °C there was no remarkable additional shrinkage with increased temperature in the large scale cross-sectional area, as shown in Figure 5-6. The average reduction in cross-sectional area after 60 min of cooking was 15-18% independently of cooking temperature. However, there were large differences in shrinkage between individual blocks of meat as may be seen by the large standard deviation (Figure 5-6). When blocks of meat were cooked for a shorter time less shrinkage was observed, about 2-10% decrease in cross-sectional area after 20 min of cooking and about 8-16% after 40 min. These results are further discussed in relation to the mathematical modelling in Section 5.5.

On a smaller scale, the individual muscle fibres in cooked samples had a smaller cross-sectional area compared to raw samples, see Figure 5-7. Moreover, the separation of the muscle fibres was larger for the cooked than for the raw sample. Image analysis of micrographs confirmed these observations. The average fibre density for raw samples was 326 fibres/mm<sup>2</sup>. Cooked blocks (65-90 °C for 35 min) had a larger average fibre density, 436-507 fibres/mm<sup>2</sup>, which related to the large scale cross-sectional shrinkage observed in Figure 5-6, *i.e.*, when a sample block shrinks in diameter, the fibres occupy a smaller space, which results in a higher fibre density. No significant difference in fibre density between samples cooked at different temperatures (65-90 °C) was observed.

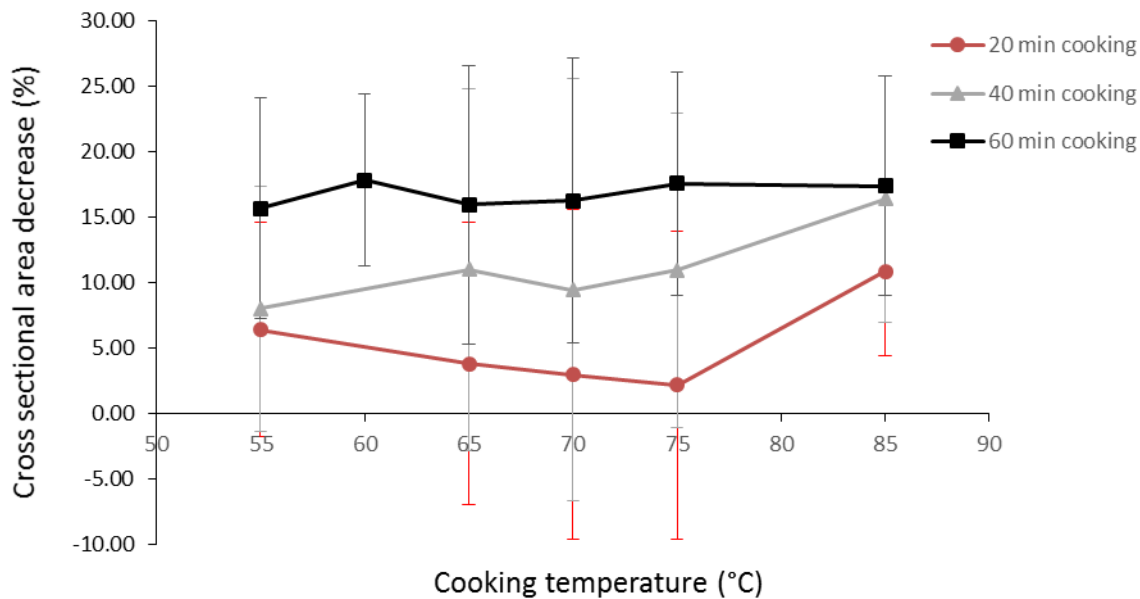


**Figure 5-6.** Cross-sectional area decrease of eye round blocks cooked for 20, 40 or 60 minutes at various temperatures. Error bars show standard deviation.

The increase in fibre density was greater than the corresponding large scale shrinkage. This could be explained by the sampling areas for the micrographs for the density measurements, as they were chosen from areas with good muscle fibre coverage and not from areas that included perimysium. The connective tissue in the perimysium is likely to swell and occupy a larger volume after cooking, as can be seen for the endomysium in Figure 5-7b. The discrepancy in shrinkage at different length scales could, be explained by the heterogeneity of the muscle structure, with a decrease in muscle fibre area and an increase in connective tissue occupied area upon heating.

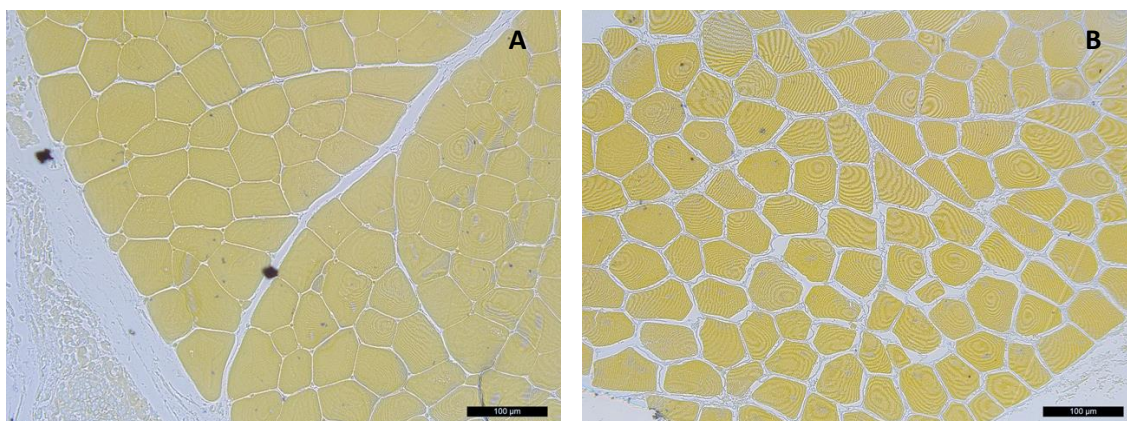


**Figure 5-7** Cross-sections of (A) raw and (B) cooked (60 min at 70 °C) eye round muscle tissues showing shrinkage and separation of muscle fibres due to cooking. Muscle tissue is stained yellow and connective tissue pale blue. Scale bars: 100 µm.

### 5.2.1.2 Longitudinal shrinkage

When the muscle tissue was heated, initially there was shrinkage across the muscle fibres followed by a decrease in length along the muscle fibres (longitudinal shrinkage), see Figure 5-8. This lengthwise decrease started around 65 °C and continued with increasing cooking temperature to about 20% at 85 °C. Blocks of meat cooked for 60 min shrank more than blocks cooked for 20 or 40 min, as the proteins were exposed for longer time to heating which resulted in muscle proteins fully reaching their new conformation. The longitudinal shrinkage is likely to be related to the denaturation of actin. The maximum longitudinal shrinkage was around 30%. This was for meat cooked in a microwave oven to reach a point where no further shrinkage occurred.

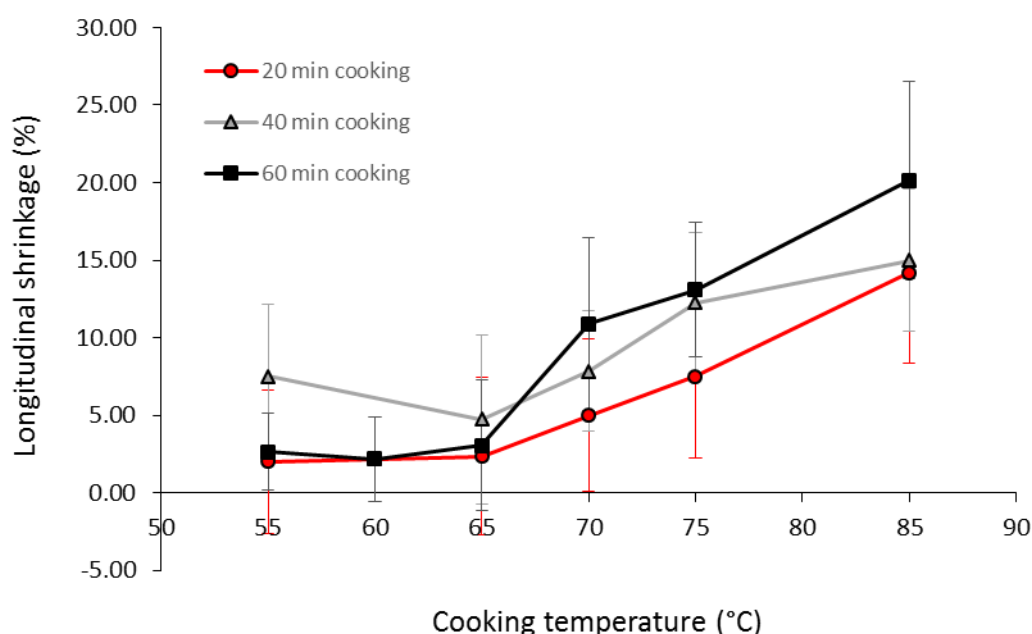


**Figure 5-8.** Length decrease of eye round blocks cooked for 20, 40 or 60 minutes at various temperatures. Error bars show standard deviation.

At the extreme point, 60 min at 85 °C, the blocks of meat decreased in length about 20% whereas the sarcomere length of individual muscle fibres decreased by approximately 30%. The discrepancy could be explained by gaps formed in the muscle microstructure between cells due to heat-induced disintegration of the structure, and solubilisation of surrounding collagen that keeps muscle fibres aligned within the muscle fibre bundles, and the entire muscle, prior to cooking.

The beef muscles samples decreased in length, width and sarcomere length upon heating. In Figure 5-9, a series of micrographs of a muscle fibre fragment show the changes with temperature. Note, specifically, the change in width between 55 °C and 60 °C and the change in length between 75 °C and 90 °C.

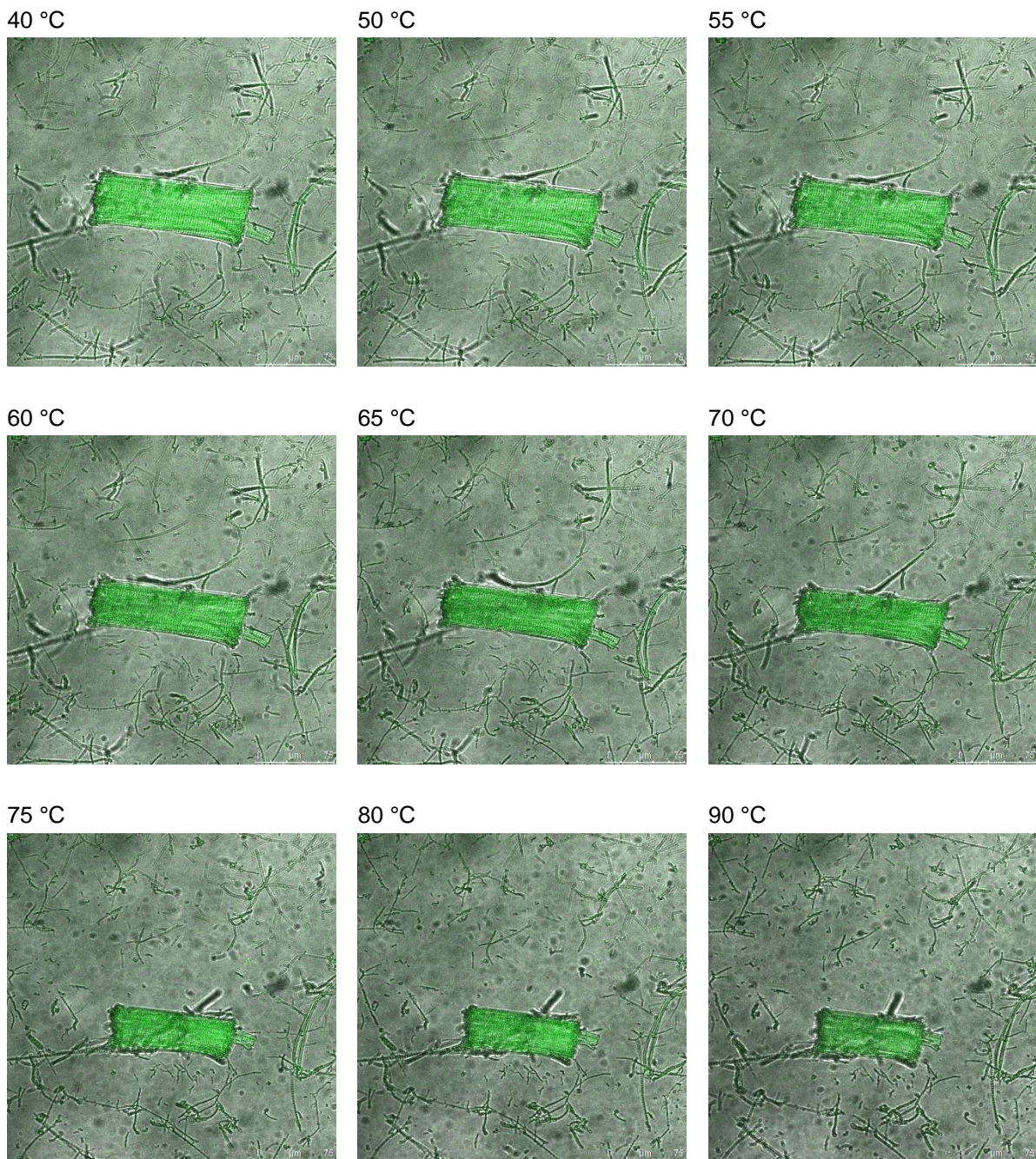


**Figure 5-9.** Micrographs of muscle fibre fragments (Eye round – *M. semitendinosus*) captured during heating to observe structural changes. Shrinkage in width starts around 50 °C and length around 70 °C. Size of images: 310 μm x 310 μm.

In general the calculations of the volume lost (%) on cooking were in fair agreement with weight losses (%) at 55 °C (assuming a density of 1 gram equal 1 ml), but considerably underestimated the weight loss at higher temperatures. This may have indicated some hardening of the meat block as the temperature increased. Fluid may have drained out of the meat and decreased the weight of the block, but this may only be partly reflected in the volume change, as a stiffer block structure will not shrink as much.

Comparison of the maximum changes in cross-sectional area, length and volume between the meat cooked as blocks and the same changes in fibre fragments heated under the microscope revealed very similar magnitudes in shrinkage. Taken together, the data suggests that the macroscopic shrinkage of meat was largely dominated by shrinkage within individual muscle fibres by myofibrillar proteins, and that the role of heat-induced shrinkage in the intramuscular connective tissue (both endomysium and perimysium) was not a major driver of cook losses, although it may have a minor role.

Rhee, Wheeler, Shackelford, and Koohmaraie (2004) showed that there is considerable variation in mass loss between different muscles from the same animal. However, over the eleven beef muscles they studied, there was not a significant correlation between mass loss and collagen content of the muscle, which weighs against a dominant role for heat-induced shrinkage of intramuscular connective tissue in driving variations of mass loss. Similarly, Tornberg (2005) showed that the mass loss is similar between whole meat (connective tissue networks intact) and minced meat (connective tissue networks disrupted).

### 5.2.1.3 Influence of muscle type

Seven different beef muscles; eye round, striploin, rump, topside, brisket, outside flat and oyster blade were investigated in relation to their dimensional change upon heating. The decrease in length of various muscles after cooking is shown in Figure 5-10. The same trend as in Figure 5-8 was observed, *i.e.* a marked decrease in length above 65 °C. However, most of muscles were only measured after cooking at 70 °C. The striploin and oyster blade appeared to shrink more than the other muscles but there was large variability between samples, especially for the oyster blade that has a line of gristle running through the middle of the muscle that clearly effected the shrinkage behaviour deforming the blocks, leading to large standard deviations. Hence, no significant ( $P > 0.05$ ) variation in either cook loss or dimensional changes could be observed between the seven muscles in this study. Other studies have reported differences in behaviour for different muscles during cooking (P. E. H. Bouton, P.V.; Shorthose, W.R., 1976; Rhee et al., 2004). The discrepancy between the results of our study and data reported by others researchers might be explained by the long cooking time (1 hour in a water bath) used in our study compared to the shorter heating/cooking time applied in other studies, *e.g.* 5.5 min heating by a belt grill used by (Rhee et al., 2004). A longer heating time allows for internal processes and reactions in the samples to come closer to equilibrium.

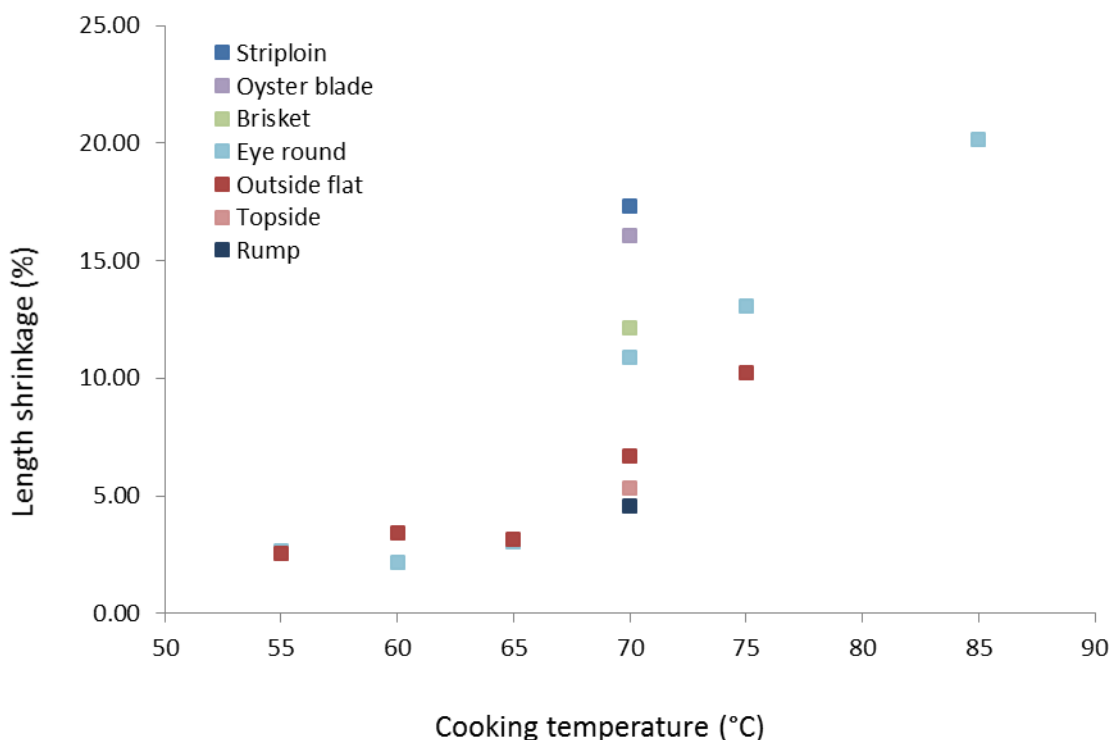


**Figure 5-10.** Decrease in length of various beef muscles after cooking as blocks for 60 min in a water bath.

#### 5.2.1.4 Dimensional changes of aged meat upon heating

Ageing of eye round and outside flat muscles for 14 days led to higher mass losses upon cooking but showed no significant ( $P > 0.05$ ) difference in shrinkage behaviour compared to meat aged for 1 day post mortem (Figure 5-11). During post-mortem aging the cytoskeletal proteins (titin, nebulin and desmin) are rapidly and preferentially degraded by calpains (Huff-Lonergan & Lonergan, 2005). If thermally initiated shrinkage of titin or nebulin was a strong driver of longitudinal shrinkage, or desmin was a strong contributor to transverse shrinkage, then the degradation of these proteins during ageing would be expected to reduce the amount of shrinkage in length or cross-sectional area when aged meat is cooked. Our results are contrary to their hypothesis, inferring that thermal shrinkage of these cytoskeletal proteins is not a strong contributor to the shrinkage of meat upon cooking.

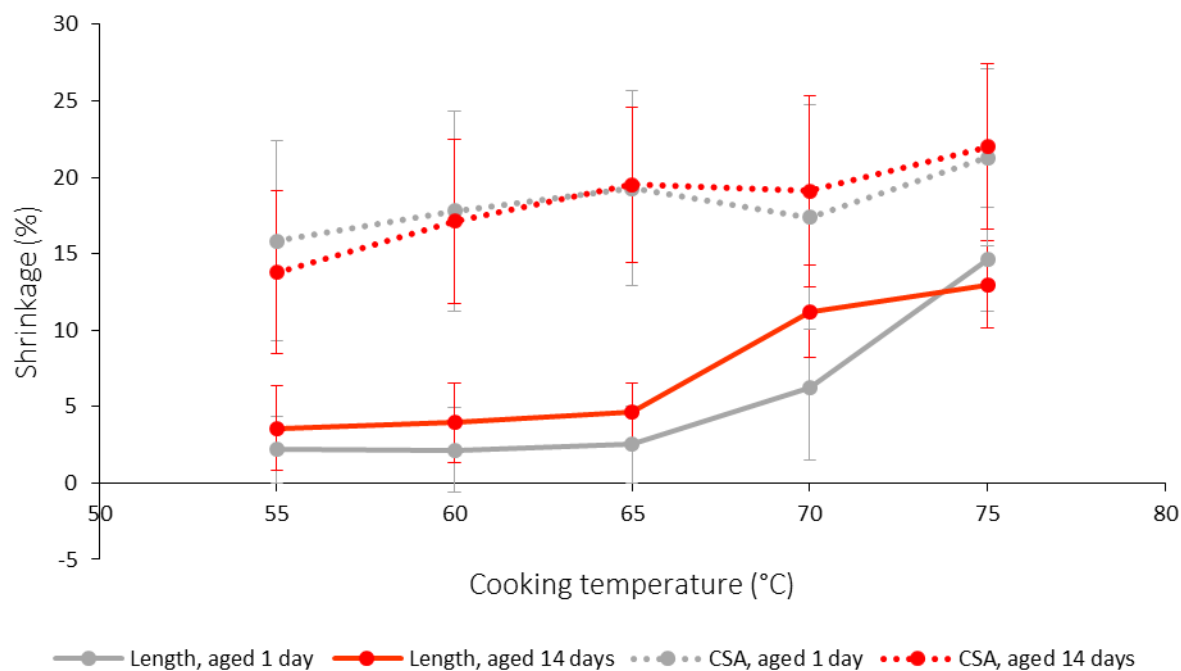


**Figure 5-11.** Dimensional decrease in length and cross-sectional area (CSA) of eye round aged for 1 or 14 days of ageing as a function of cooking temperature. Samples cooked in water bath for 60 min.

### 5.2.1.5 Effect of heating on connective tissue

Isolated fragments of connective tissue were heated and the structural changes studied by microscopy. During heating, the connective tissue fragments expressed granulation and denaturation of fibres resulting in more compact structures. Unordered fibres of epimysium and endomysium shrank significantly upon heating (up to 87%), while thicker more structured fibres were less affected by heating and decreased less than 30%. As seen in Figure 5-12, heating to 50 °C did not cause any structural change to the connective tissue. Between 65 and 75 °C, the shrinkage of endomysial fibres was fast. At 75 °C, the majority of the transition appeared complete with only a slight change observed with increasing temperatures (up to 90 °C). On the other hand, the muscle fibre fragment present in the same image series (Figure 5-12) showed a very different behaviour upon heating, with a clear longitudinal shrinkage from 75 °C. Moreover, the muscle fibre fragment did not shrink to the same extent as the connective tissue when not constrained by muscle tissue.

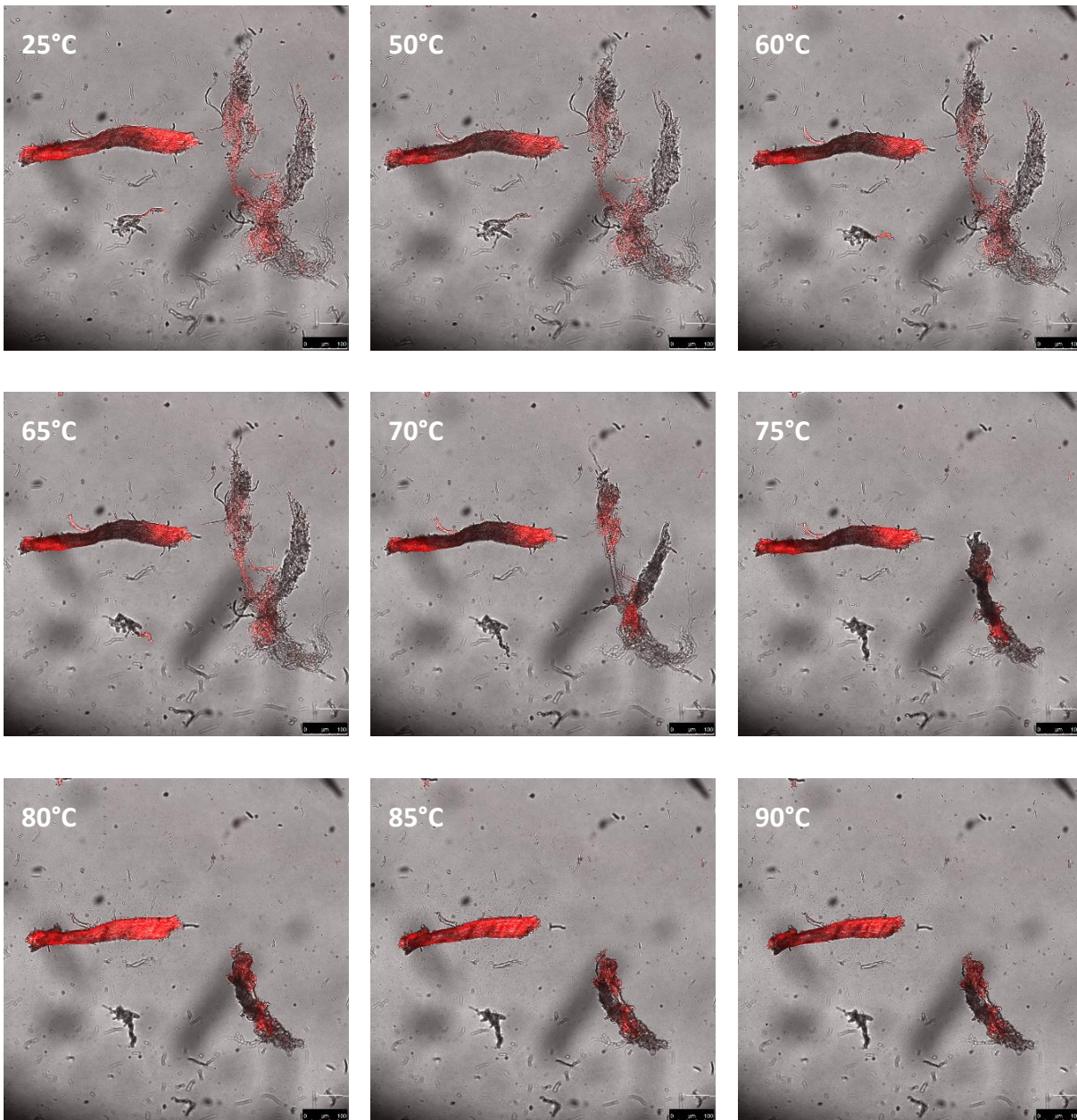


**Figure 5-12.** Micrographs of muscle fragments during heating from 25 to 90 °C. The feature to the left in each image shows a muscle fibre fragment and the one to the right in each image is a connective tissue fragment assembly. Size of images: 775  $\mu$ m x 775  $\mu$ m.

## 5.2.2 Influence of pH, *Bos indicus* content and Intramuscular fat

### 5.2.2.1 Ultimate pH

The effect of ultimate pH on the dimensional changes of meat during cooking was investigated. Statistical analysis of the results showed that shrinkage of the muscle fibre length was independent of pH and depended only on the cooking temperature and time. With increasing cooking temperature and time the length of the fibre decreased for all pH values. These results indicate that longitudinal muscle shortening is dictated by the acto-myosin complexes formed in the sarcomeres at the on-set of rigor. Hence, the longitudinal sarcomere shrinkage is not pH dependent.

Conversely, the change of width and height of the blocks showed a different behaviour. The low pH samples showed an increased shrinkage in the cross-sectional area compared to the medium and high pH meat. This is largely due to the transversal size of fibres being dependent on post-mortem lactic acid formation in the muscle and thus pH dependent. Consequently, protein solubility, electrostatic interactions and water binding are all pH dependent and favoured at higher pH values (~ 7.0, physiological pH of muscle).

### 5.2.2.2 *Bos indicus* content

A comparison of longitudinal and cross-sectional shrinkage amongst BI ranges showed that the shrinkage of muscle tissue only depended on the cooking temperature and time. Therefore, increasing cooking temperature and time will increase the extent of shrinkage, regardless of the BI range.

### 5.2.2.3 Intramuscular fat content

Comparing the dimensional changes (longitudinal and cross-sectional) across various muscle groups and intramuscular fat contents showed that the reduction in dimensions of the muscle structure was not significantly ( $P > 0.05$ ) influenced by the IMF content, only by cooking time and temperature.

### 5.2.3 Effect of interventions

#### 5.2.3.1 Pulsed electric field treatment

The influence of PEF processing and cooking on dimensional changes was investigated. No significant ( $P > 0.05$ ) changes in block dimensions nor microstructure could be observed after PEF processing. Following a subsequent cooking step (60 min at 70 °C), no significant ( $P < 0.05$ ) dimensional changes between the PEF treated and non-treated control were observed. This may be a positive asset of the PEF technology and warrants further investigation.

#### 5.2.3.2 High pressure thermal processing

The influence of HPTP on dimensional changes as was studied at a microscopic scale by TEM. Samples from the most diverse conditions were chosen. No large scale dimensional measurements were carried out on HPTP blocks.

Muscle fibres consist of long cylindrical structures called myofibrils. Each myofibril consists primarily of two types of protein filaments, thick and thin filaments which are positioned along the myofibril in alternating groups with some overlap at the ends. Each such repeat unit is called a sarcomere. By microscopy these alternating structures of thin and thick filaments are seen as bands. The A-band is a relatively dark area within the sarcomere that extends along the total length of the thick filaments. The H-band (a region with only thick filaments) is at the centre of the A-band. In the middle on the H-band, the darker M-line can be seen. The I-band is the region between adjacent A-bands, in which there are only thin filaments. The Z-lines form the boundaries between adjacent sarcomeres and can be found in the middle of the I-band.

#### 5.2.3.3 Stage 1 – Effect of salt type

TEM images of the ultrastructure of muscle subjected to salt injection and subsequent HPTP or cooking are shown in Figure 5-13. The raw control sample (injected with water) showed parallel sarcomeres (Figure 5-13A). The Z-lines were well defined within the I-bands. A-, M- and H-bands were clearly visible. For the HPTP sample injected with water (Figure 5-13B), sarcomere lengths appeared about 40% shorter and A-bands were contracted compared to the control. I-bands had loosened with disrupted Z-lines and partial loss of M-bands could be observed.

When muscles were injected with brine and treated by HPTP, the ultrastructure of the muscle fibres was much more disrupted and clearly swollen compared to the samples injected with water. In Figure 5-13C & D, the micrographs of muscle fibres subjected to the highest salt concentrations (0.4% PPI and 1.2% NaCl, respectively) are shown. Here, the sarcomere lengths were 2.5 and 3.5 times greater for PPI and NaCl injected samples, respectively, compared to water injected ones. Disordered Z-lines and ruptured I-bands were seen. A clear loss of muscle structure integrity was observed as a result of HPTP as found in other studies summarised in (Buckow et al., 2013).

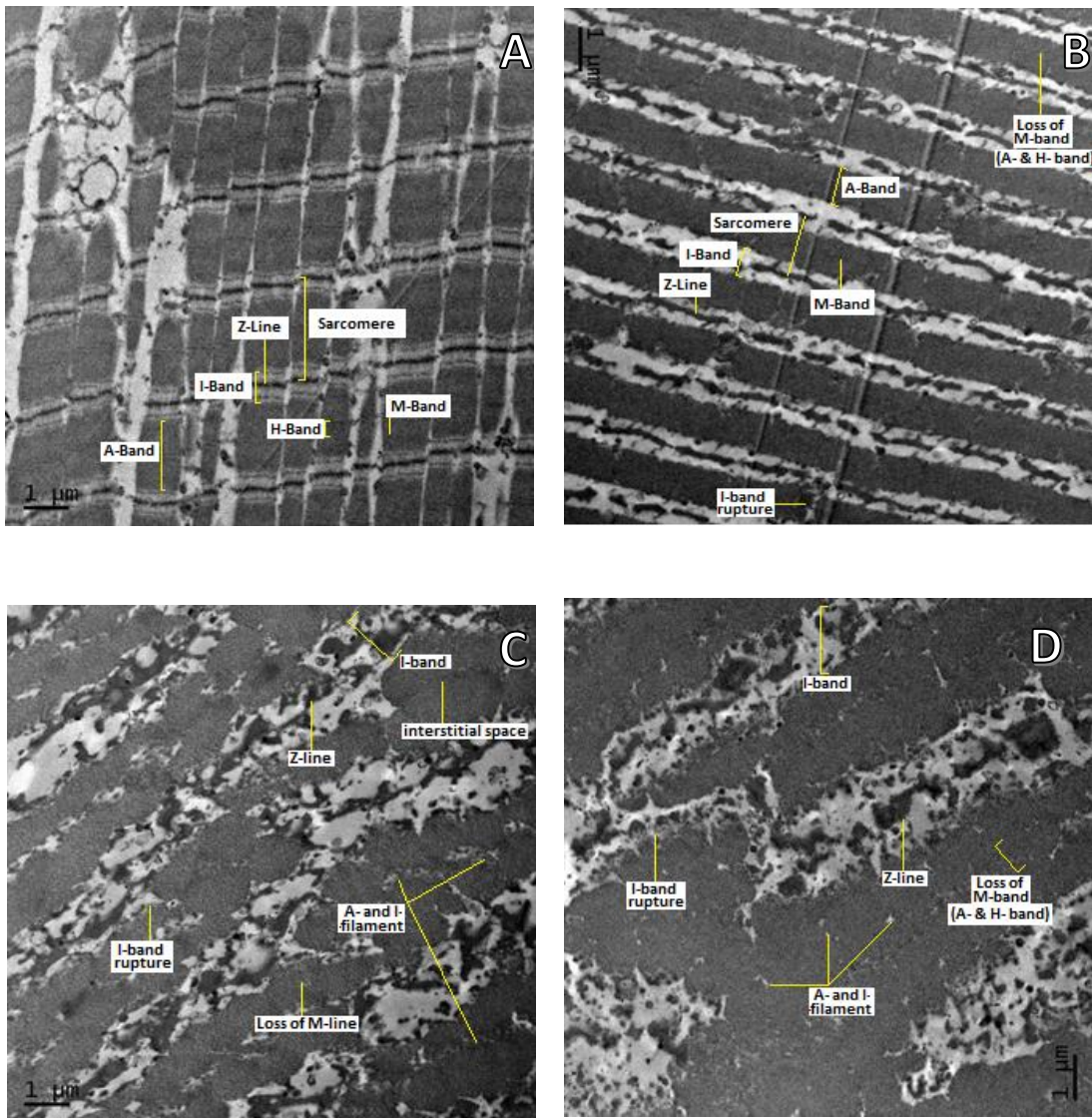


**Figure 5-13.** TEM micrographs (1500X) of eye round muscle injected with 10 % of; **(A)** water (no HPTP), **(B)** water + HPTP, **(C)** 0.4 % PPI + HPTP, and **(D)** 1.2 % NaCl + HPTP. HPTP condition: 600 MPa, 75 °C, 5 min. Scale bars: 1  $\mu\text{m}$ .

## 5.3 Texture

The measurement of texture using a WB device gave four values (P. E. Bouton, Harris, P.V. , 1972): (i) peak force (PF), the total amount of force required to shear through the sample; (ii) the initial yield (IY), a measurement of the myofibrillar resistance; (iii) the peak force minus initial yield (PF-IY), a measure of the contribution of connective tissue in muscles (where the sarcomeres have not shortened below 1.8  $\mu\text{m}$ ) to the overall texture; and (iv) work, the energy required or work done, in applying a force during the WB shear force test. The PF value is the accepted value used when discussing meat texture using the WB device and the convention used in this report. Samples with PF values lower than 40 N are considered tender, while values higher than 60 N are considered tough (Miller, Carr, Ramsey, Crockett, & Hoover, 2001).

### 5.3.1 Influence of cooking temperature

There was no significant effect of sample type (blocks or strips) on IY or PF values, though all were significantly ( $P < 0.05$ ) affected by cooking temperature. IY, related to the myofibrillar component of the muscle (Møller, 1981), showed an increase from about 35 N after cooking at 65 °C to about 52 N at 90 °C (results not shown). PF influenced by both myofibrils and connective tissue (Møller, 1981), showed a smaller increase with temperature than IY, from about 50 N at 65 °C to about 60 N at 90 °C. Cooking at 80 or 90 °C gave similar results for IY and PF, respectively.

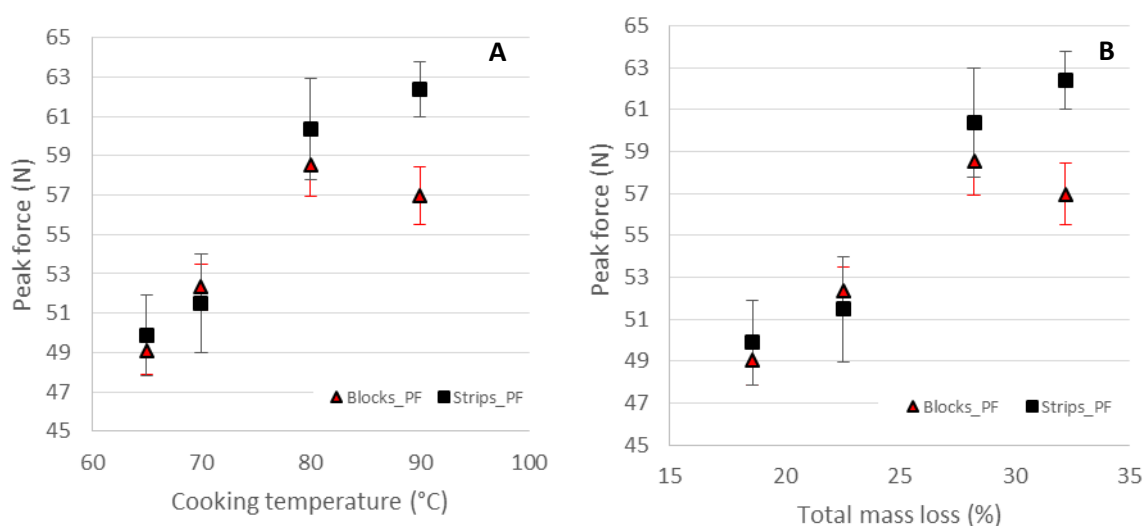


**Figure 5-14. (A)** Average PF values of cooked topside (*semimembranosus*) as obtained by WB shear force testing as a function of cooking temperature. **(B)** Average PF values of cooked topside (*semimembranosus*) as a function of average total mass loss.

The muscle fibre cross-sectional diameter decreased by approximately 20% during cooking compared to raw samples, but the actual cooking temperature (in the 65-90 °C range) had little effect on the fibre diameter and fibre density. This indicated that the number of fibres per  $\text{mm}^2$  of cross-sectional area

was not a factor in the increase of WB shear force IY or PF values with increasing cooking temperature. Instead, the toughening of the meat was more likely to be a result of the moisture loss.

When the PF values are plotted against the total moisture loss, as in Figure 5-14b, a steady increase was seen, up to 50 N, where the graph then levels off. This shows that the WB shear force data was highly influenced by the moisture content of the tested meat. Overall, there was a direct relationship between cooking temperature and weigh loss that resulted in increased peak force.

### 5.3.2 Influence of muscle type

The tenderness, as measured by PF, for different beef primal muscles (rump, striploin, oyster blade, brisket, topside and eye round) upon cooking at 70 °C for 60 min can be observed in Figure 5-15. The rump, striploin and oyster blade have lower connective tissue in comparison to the brisket, topside and eye round, which results in a lower PF value.

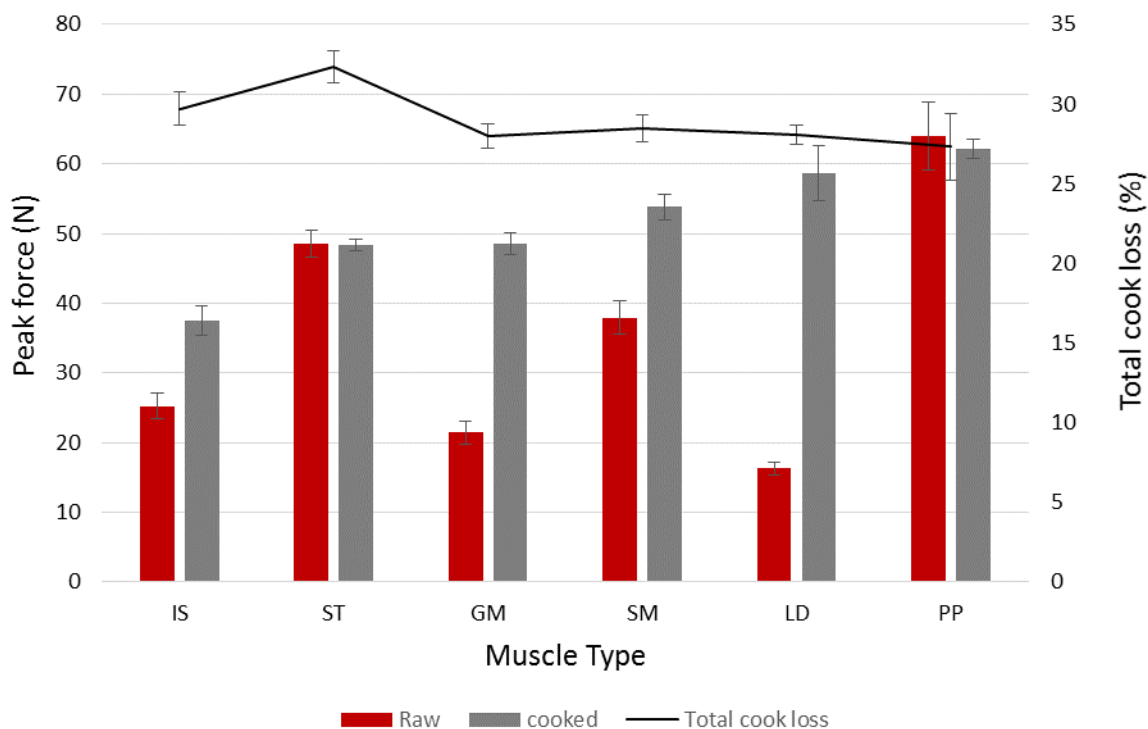


**Figure 5-15.** Average Peak Force (PF) values and total mass loss values of cooked beef topside (*M. semimembranosus*) as obtained by WB shear force testing. Rump – GM, Striploin – LD, Oyster Blade – IS, Brisket – PP, Topside – SM and Eye round – ST.

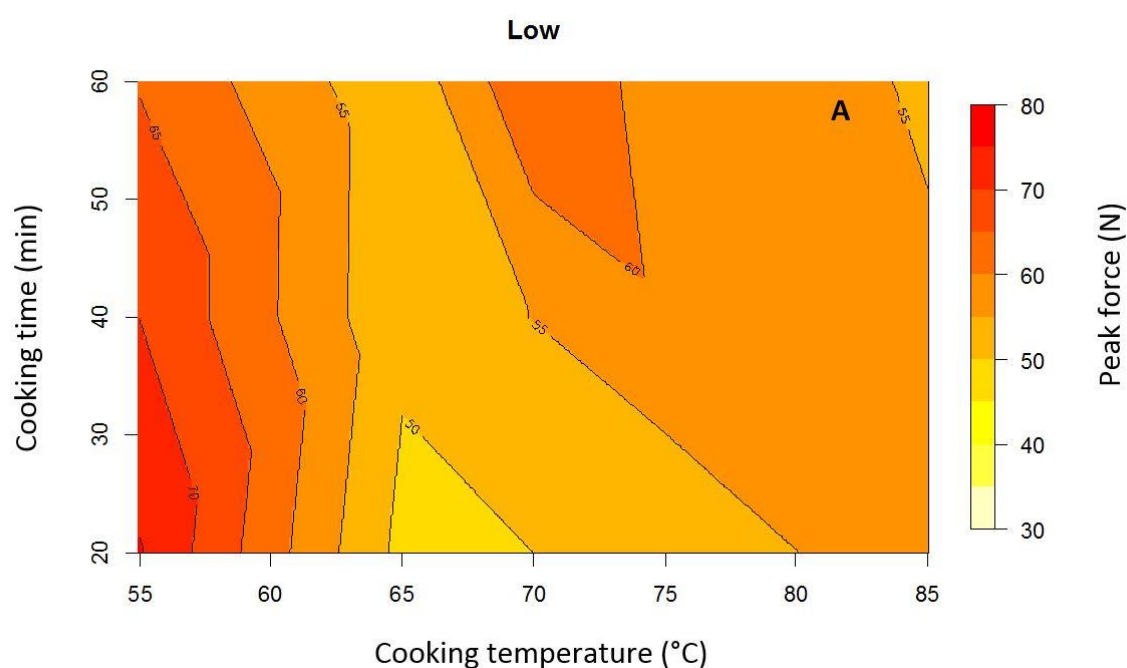
### 5.3.3 Influence of ultimate pH, *Bos indicus* content and Intramuscular fat

#### 5.3.3.1 Ultimate pH

Overall, in relation to temperature, the PF of samples cooked at 55 °C was higher compared to the PF of raw samples, ranging from 50.6 to 75.3 N and from 42.5 to 51.4 N, respectively. The PF for samples cooked at 65 °C was lower than for 55 °C samples, and then the PF slowly increased with increasing temperature.

Comparing the PF in relation to pH a similar trend was observed. The PF of raw low and high pH samples were both higher than of samples from the medium pH range. The same applied to samples cooked at 55 °C regardless of cooking time. However, a different scenario was seen when samples were cooked at 65 °C, the PF seemed to flatten out across the pH ranges, so the differences were not remarkable. When samples were cooked at temperatures above 65 °C the PF then seemed to increase again over all pH ranges. Moreover, the PF of low and high pH samples increased more than of the medium pH samples, as shown in Figure 5-16.

Comparing the PF to cooking time, a clear decrease occurred with increasing cooking time when cooked at 55 °C for low and medium pH samples, whereas for high pH samples the trend was the inverse. No clear pattern was seen at 65 °C; however, PF values of samples cooked at 70 and 75 °C did react in the same way; that is with increasing cooking time the PF increased as well. Whereas, for samples cooked at 85 °C, the PF trend reversed and decreased with cooking time. At higher temperatures, the effect on tenderness by increased cook loss due to longer cooking times appears to be overridden by solubilisation of the connective tissue leading to a more tender meat.



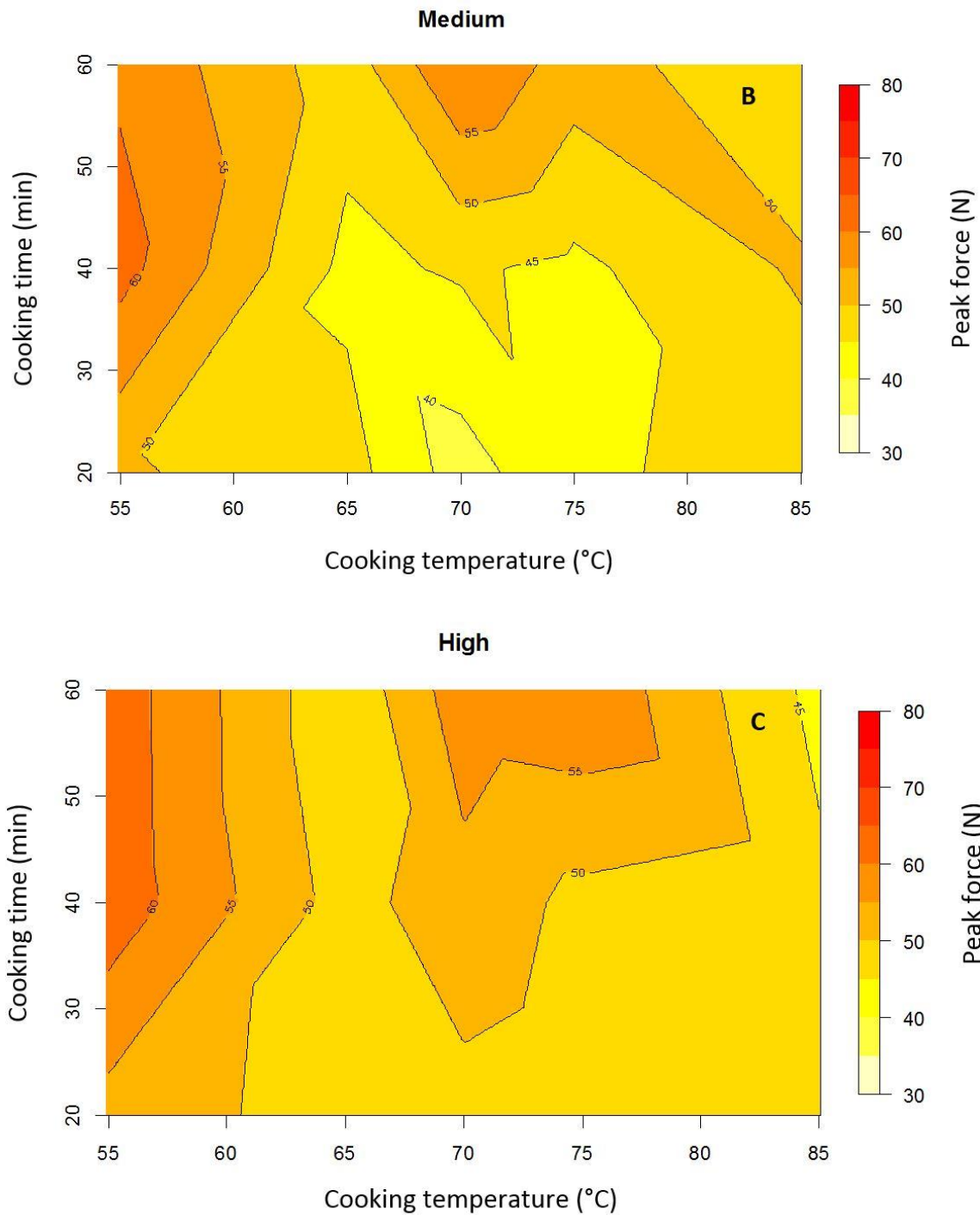


**Figure 5-16.** Peak force of (A) low, (B) medium and (C) high pH of eye round cooked at different temperatures (55, 65, 70, 75 and 85 °C) and time intervals (20, 40 or 60 min).

### 5.3.3.2 *Bos indicus* content

Eye round samples of low, medium or high BI content were cooked at one of three temperatures (65, 70 or 75 °C) and for one of three times (20, 40 or 60 min). As presented in Figure 5-17, the PF was significantly influenced by the cooking time, cooking temperature and proportion of BI.

In relation to the duration of cooking, the PF of samples cooked for 20 minutes for the low and medium BI content were more tender than the raw samples and only at high BI content did the PF become greater than for the raw samples. This was similar for the samples cooked for 40 minutes. All the samples cooked for 60 minutes had significantly greater PF values than raw samples, for all BI content.

Comparing the PF in relation to temperature, there was a similar trend. The samples cooked at 65 or 70°C had lower PF values than those cooked at 75°C. Comparing the effect of BI content on PF, only at 70°C for 40 or 60 minutes and at 75°C for all times was the PF decreased in comparison to the raw sample.

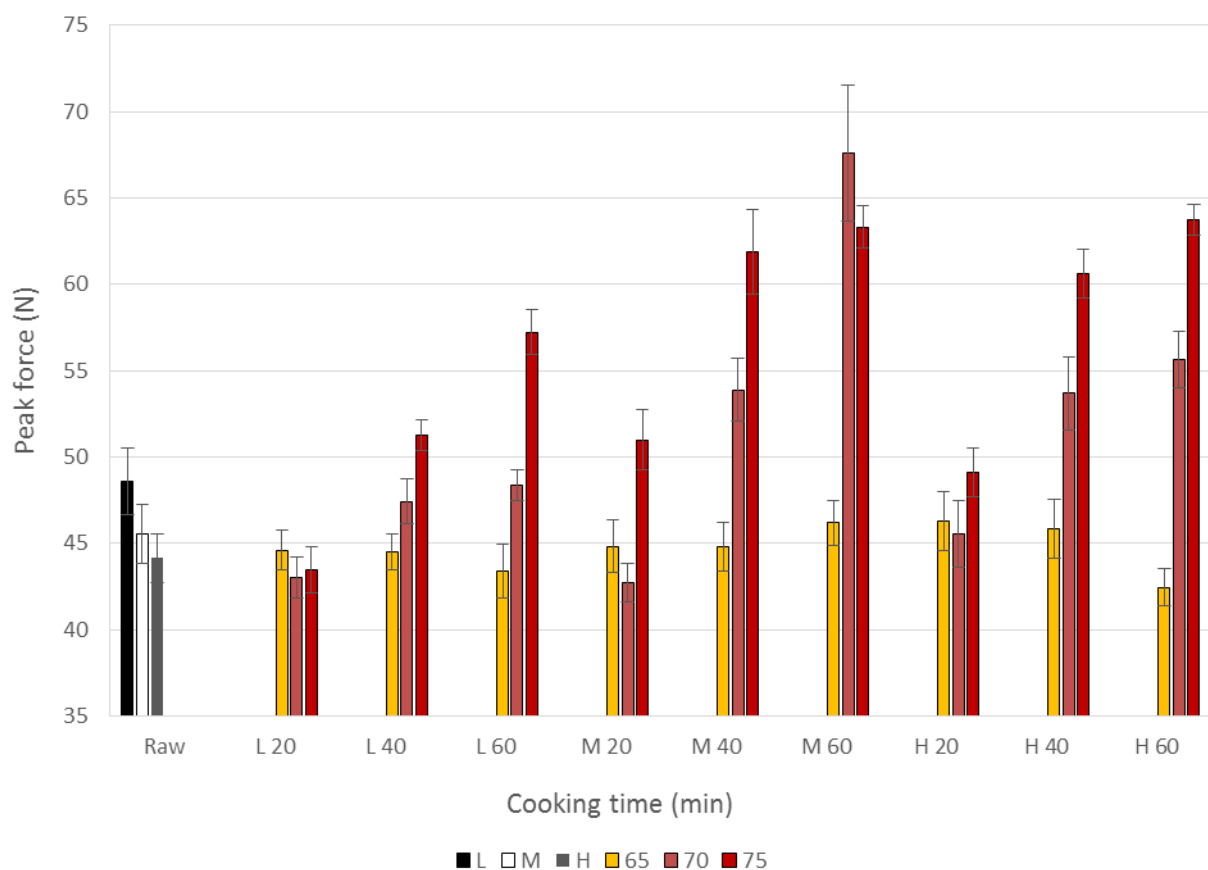


**Figure 5-17.** Peak Force (N) of low (L), medium (M), and high (H) *Bos indicus* content of beef eye round cooked at different temperatures (65, 70 and 75°C) and different times (20, 40 and 60 min).

When looking at different muscle types, the difference in PF values between the medium and high BI content was 1.6 N for the rump, 1.8 N for the striploin and 1.9 N for the brisket. These differences in texture were very small and unlikely to be detected by the average consumer.

### 5.3.3.3 Intramuscular fat (IMF)

#### Stage 1 - Eye round results

Eye round samples were cooked at three temperatures (65, 70 or 75 °C) and times (20, 40 or 60 min). Figure 5-18 shows that all eye round samples fell into the category between tender and tough, in the 40 – 60 N range, after cooking at 70 °C.

In relation to the duration of cooking, the PF of all eye round samples cooked for 20 min at 65, 70 or 75 °C were more tender than the raw samples across the IMF range (low, medium and high). The same applied for the samples cooked for 40 min in the low and high IMF range, whereas the PF of samples in the medium IMF range was slightly greater compared to the corresponding values of the raw meat. Samples cooked for 60 min, displayed a similar trend as those cooked for 40 min and had significantly lower PF values than the raw samples for low and high IMF contents. However, the samples cooked for 60 min at 70 °C had a greater PF compared to those cooked at 65 or 75 °C or even the raw samples.

Comparing the PF in relation to cooking temperature, a general trend could be seen. With increasing cooking temperature the PF of meat samples increased at all IMF ranges when cooked for 40 or 60 min. However, cooked samples (65, 70 or 75 °C) containing high IMF contents showed an opposite trend. These samples showed a decreased PF with increasing cooking temperature and the PF was significantly lower than of the raw samples.

Comparing the effect of IMF content on PF, only at 70 °C for 40 and 60 minutes the tenderness increased in comparison to the raw sample.

The initial yield (IY) results followed the same trend as the peak force values. The work increased with IMF content and tended to be more uniform in the samples cooked for 40 or 60 min. In samples cooked at 75 °C for 20 min, the reverse happened and work decreased as IMF content increased.

#### Stage 2 – Comparison of two different muscles cooked at 70°C

In stage 2 of the experiment, striploins from the same animals used in stage 1 were cooked at 70 °C for 20, 40 or 60 min. The differences in texture between muscles were significant with PF, IY and Work significantly influenced by the IMF content.

The mechanical properties of striploin and eye round muscles after cooking at 70 °C for 20, 40 or 60 min, can be observed in Figure 5-18. The striploins were considered tender (PF < 40 N) for all samples except the low IMF content cooked for 40 or 60 min. A lower connective tissue content in striploins in comparison to eye rounds could explain the lower PF.

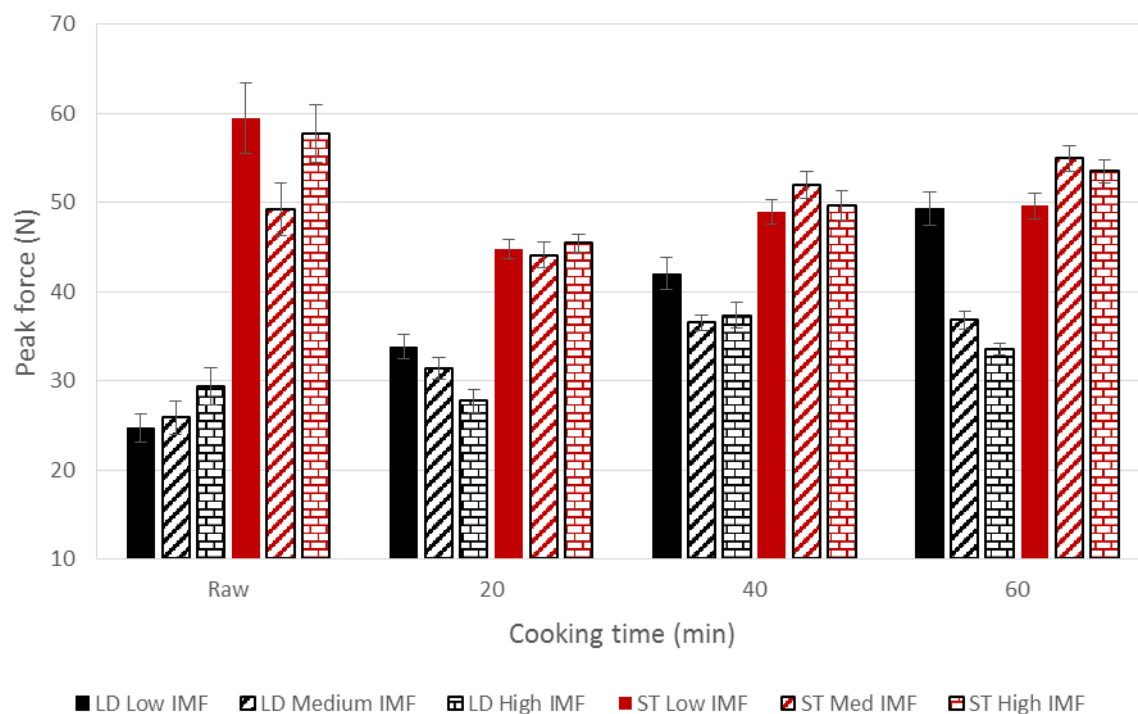


**Figure 5-18.** Peak Force (N) of different muscle (LD = striploin, ST = eye round) cooked at 70 °C for different cooking times (20, 40 or 60 min) and different intramuscular fat content (L = Low, M = Medium, H = High).

Interestingly, the influence of IMF on texture was more pronounced for the striploin than eye round, with clearly lower values for PF, IY and Work with increasing IMF content (Figure 5-18). This result might reflect the overall higher fat content of the striploin compared to the eye round.

### 5.3.4 Effect of HPTP on texture

#### 5.3.4.1 The effect of salt concentration on texture

Results for WB shear PF measurements on eye round muscle, after brine injection (NaCl or PPI) and HPTP or control (cook-only) treatments are shown in Figure 5-19 respectively.

HPTP had a significant tenderising effect on the PF of PPI samples, with HPTP samples having a significantly ( $P < 0.001$ ) lower PF than the control (samples cook in a water bath) (Figure 5-19).

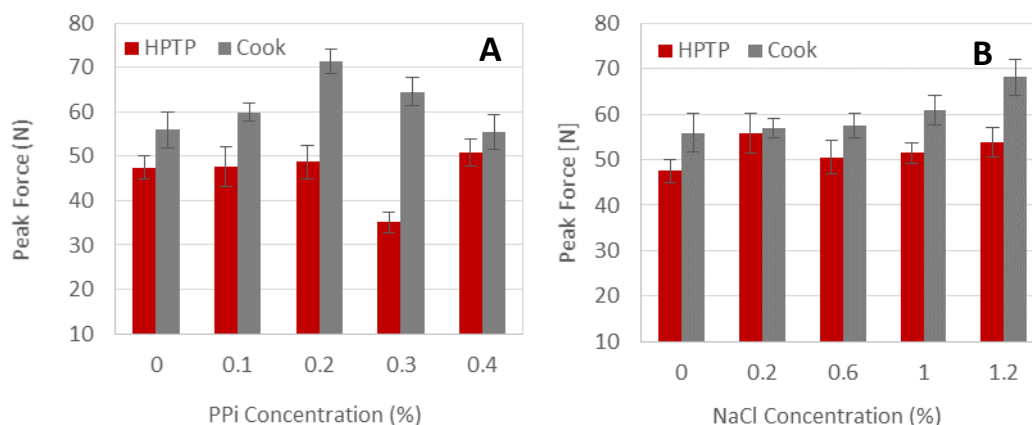


**Figure 5-19.** The effect of HTPP (600 MPa, 75 °C, 5 min) or Control (cook-only, 75 °C, 30 min) treatments, and PPI (A) and NaCl (B) concentration on the peak force.

Samples injected with NaCl (Figure 5-19B) did not show a significant difference in ( $P > 0.05$ ) PF when comparing the different brine concentrations. The same was observed for IY measurements. There were no interactions between pressure and brine concentration when the meat was injected with NaCl. In contrast, there was a significant difference ( $P < 0.05$ ) in the PF between control (cook-only) and HTPP samples.

#### 5.3.4.2 The effect of HTPP and salt on texture

Based on the results of cook loss from the Stage 1 experiment, muscles of eye round were injected with either 0.2% PPI or 1.0% NaCl. PF and IY values were significantly different ( $P < 0.05$ ) with changing temperature in the HTPP samples for both the NaCl and PPI injected samples, see Figure 5-20. The PF of control samples, increased with cooking temperature (results not shown). However, cooking at elevated pressures resulted in a lower PF; compared to the control, see Figure 5-20.

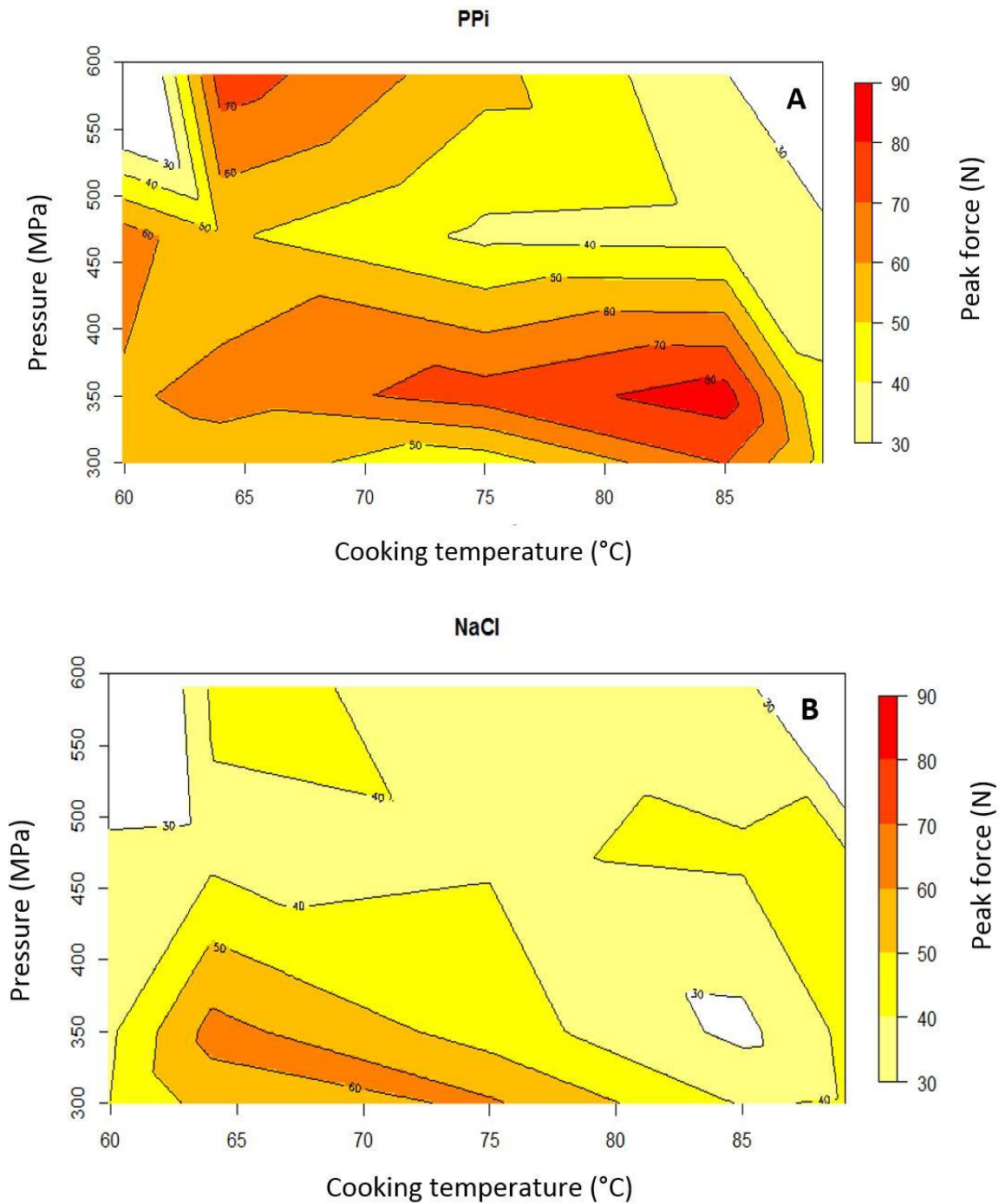


**Figure 5-20.** Main effects of HTPP (300, 350, 470, 590 and 640 MPa and 60, 64, 75, 85 and 89 °C for 5 min) on texture (PF) of processed beef eye round injected with 10% of either; **(A)** 0.2% PPI, or **(B)** 1.0% NaCl.

When reviewing the control (cook-only) samples it was evident that the PF and IY values were significantly affected by the cooking temperature ( $P < 0.05$ ) (results not shown). However, there were no significant differences ( $P > 0.05$ ) between the two salts (NaCl and PPI).

## 5.4 Colour

### 5.4.1 Influence of cooking time and temperature on meat colour in relation to pH

The influence of ultimate pH on colour change during cooking was investigated. Colour change was measured in four stages: 1) before cooking (raw meat), 2) after cooking, 3) after overnight storage, and 4) on a freshly cut surface after overnight storage.

Certain patterns were expected when comparing the colour of raw samples over a pH range. Low pH meat is known to be pale, whereas high pH meat has a darker colour. Generally, with increasing pH value, lightness ( $L^*$ ) and redness ( $a^*$ ) values decreased (Figure 5-21). This meant that the meat samples with low pH values were lighter, redder, and yellower than medium and high pH meat samples and, therefore had the highest hue and chroma values.

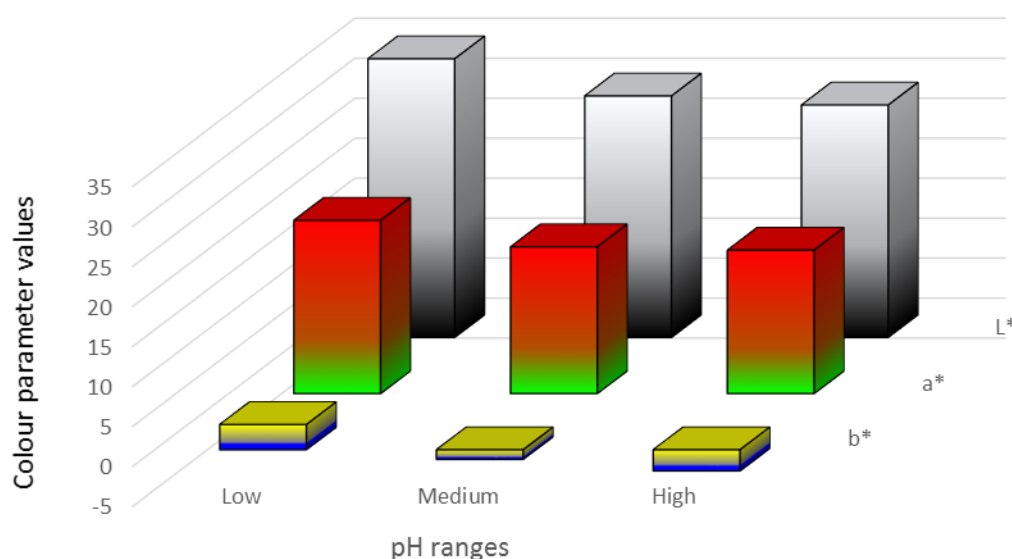


**Figure 5-21.** Colour parameter values of beef eye round (raw meat) in relation to pH.

The lightness ( $L^*$ ) of cooked samples was significantly ( $P > 0.001$ ) higher than the lightness of raw meat samples. However, the lightness of cooked samples did not change evenly over the applied cooking temperature range. The largest increase of lightness ( $L^*$ ) was reported at 55 °C and 85 °C for all pH ranges (Figure 5-22). When comparing lightness ( $L^*$ ) differences between pH ranges, the largest changes occurred within the medium pH range.

Unlike lightness ( $L^*$ ), redness ( $a^*$ ) showed an inverse pattern. The main changes in redness ( $a^*$ ) were recorded for low pH samples, whereas the smallest changes were observed at high pH samples. The differences in redness ( $\Delta a^*$ ) increased with increasing cooking temperature, regardless of the pH range. Although, the largest difference in redness ( $\Delta a^*$ ) was observed at high cooking temperatures (>70 °C), the absolute redness value ( $a^*$ ) for cooked meat was highest for meat cooked at 55 °C, with

high pH meat displaying the most red colour (see Figure 5-23). This could be related to the higher moisture content of high pH meats. Controlling the water release of meat during cooking can impact on the final colour and tenderness.

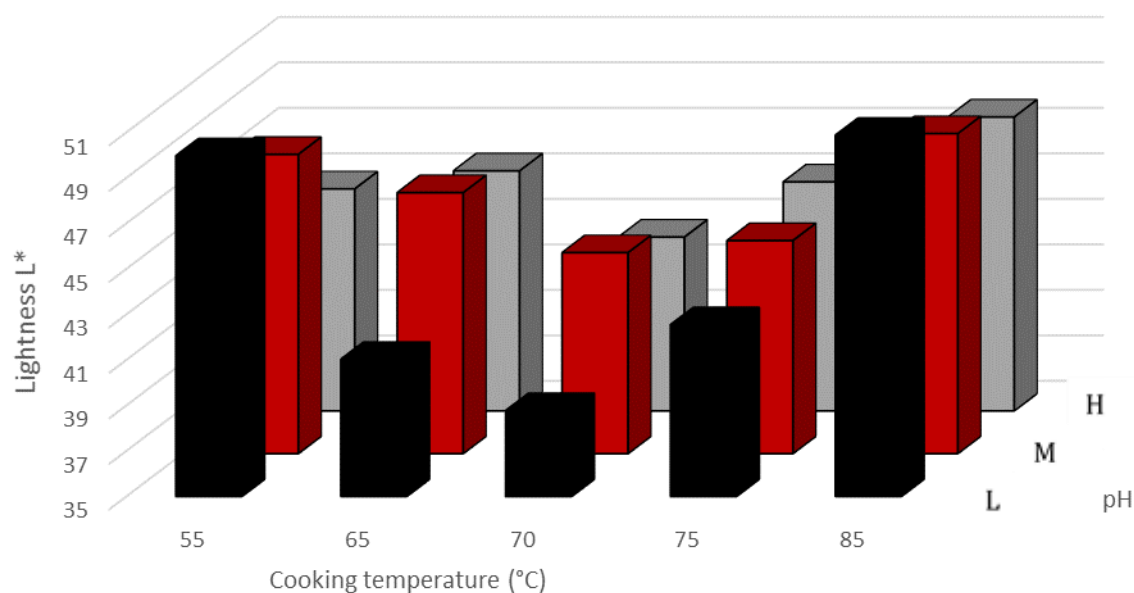


**Figure 5-22.** Lightness ( $L^*$ ) values after 40 min cooking amongst pH ranges (L – Low, M – Medium, H - High).

The colour of cooked samples was stable during overnight storage and no significant ( $P>0.05$ ) changes were recorded. Changes in redness  $\Delta a^*$  decreased with pH, cooking temperature and time. Low pH meat samples cooked at 85 °C showed the most significant differences in redness ( $a^*$ ), whereas differences in redness in high pH meat samples cooked at 55 °C for either 20, 40 or 60 min remained relatively constant. This indicates that low pH meat samples showed a more pronounced change in redness ( $a^*$ ) than high and medium pH samples. The absolute  $a^*$  values were also lower and consequently the cooked low pH samples appeared to be less red than the corresponding high pH meat.

In Figure 5-23, a photo of blocks of the three pH ranges cooked for the different time and temperature modes is shown. When comparing the high pH to the low pH samples, a clear difference in perceived ‘doneness’ (decrease in redness) by colour was visible. The low pH meat appeared more well-done than the high pH meat when cooked at similar conditions. It was observed that, high pH meat maintains its redness ( $a^*$ ) for longer during cooking and the most significant colour changes during cooking were observed in the temperature range of 55-65 °C and at temperatures  $\geq 75$  °C.



**Figure 5-23.** Samples of low (L), medium (M) and high (H) pH beef eye round cooked at different cooking modes (temperature (55, 65, 70, 75 and 85 °C) and time (20 min; yellow label, 40 min; pink label, and 60 min, white label).

#### 5.4.2 Influence of cooking time and temperature on meat colour in relation to *Bos indicus* content

The effect of BI content on colour changes during cooking was measured before cooking (raw meat) and after cooking. The aim of this analysis was to determine if the BI content had a significant influence on the initial colour (raw samples). Furthermore, it was investigated if the colour variation is carried through the cooking stage.

##### 5.4.2.1 Colour of raw samples

We found that the colour of raw cuts was significantly affected by the BI content ( $P < 0.05$ ). The lightness ( $L^*$ ) and redness ( $a^*$ ) values of both medium and high BI ranges were 0.5-2 units lower (darker) than of those cuts from the low BI range (Figure 5-24), which concurs with the results of the striploin in the study of (Gama et al., 2013).

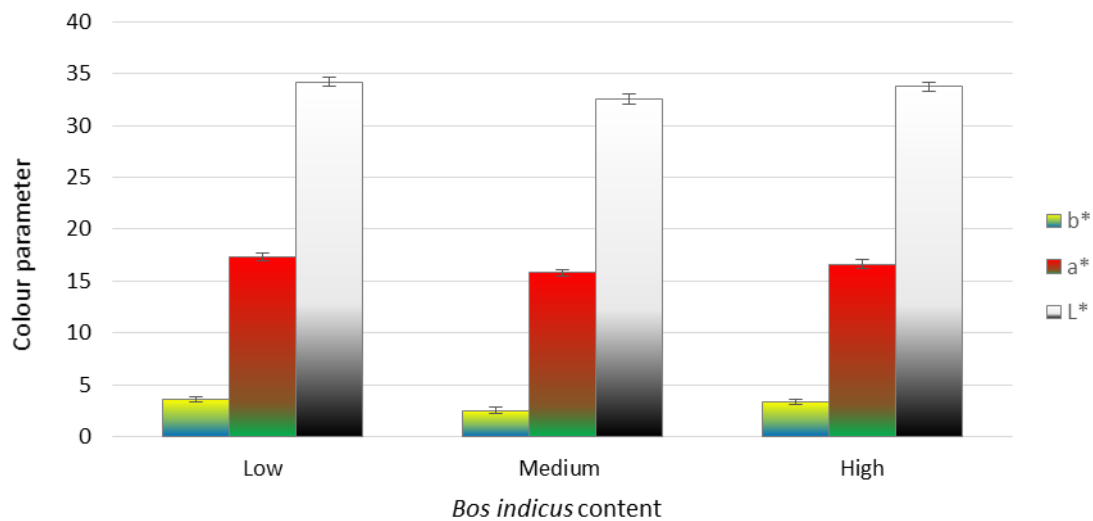


**Figure 5-24.** Colour parameter values of beef eye round *M. semitendinosus* (raw meat) in relation to *Bos indicus* content (lightness –  $L^*$ , redness –  $a^*$ , and yellowness –  $b^*$ ,  $n = 6$ ). Error bars represent standard error.

When comparing different muscle groups with different BI contents, the lightness values tend to be lower for the muscles originating from the crossbreeds (medium and high BI range), whereas the muscles from animals low in BI content were characterised by increased lightness values (lighter appearance). Other than for the brisket, the decrease in lightness within the BI ranges was observed in the striploin, rump, eye round, topside and the oyster blade.

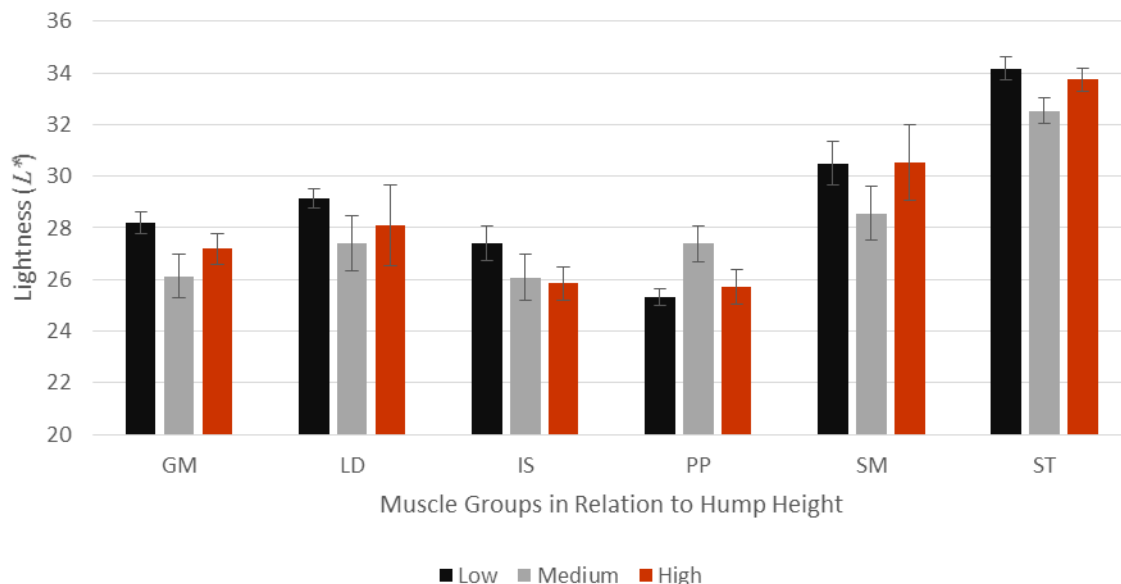


**Figure 5-25.** Lightness ( $L^*$ ,  $n = 6$ ) colour parameter of various muscle groups (GM – Rump, LD – Striploin, IS – Oyster Blade, PP – Brisket, SM – Topside, ST – Eye round) in relation to *Bos indicus* range. Error bars represent standard error.

Along with the lightness, a reduction in redness of the brisket, the striploin, rump, eye round and topside, did occur with the increasing BI content and ranged from 2.1 to 13.4%. These differences in redness were significant ( $P < 0.05$ ) for the rump, eye round, and topside.

#### 5.4.2.2 Colour of cooked samples

Samples of the eye round were cooked in a water bath under a range of conditions at 60, 70 or 75 °C for 20, 40 or 60 min. The  $L^*$  value of raw samples significantly ( $P < 0.001$ ) increased during cooking. However, it did not change evenly over the temperature range. The largest increase in lightness ( $L^*$ ) of the eye round over all BI ranges was reported after cooking at 65 °C for 20 min. As in previous findings with ultimate pH, the colour parameters did significantly change with cooking time ( $P < 0.001$ ) but were not significantly influenced by the BI range.

Unlike the lightness value, the redness value showed an inverse change pattern. The largest decrease in redness ( $a^*$ ) ( $10.39 \pm 1.03$ ) was recorded for low BI content samples (cooked for 60 min at 70 °C), whereas for the medium and high BI range, samples cooked under the same conditions the decrease was only  $7.70 \pm 1.38$  and  $8.59 \pm 1.01$  respectively. Based on our previous experiment, we expected that the differences in redness ( $\Delta a^*$ ) would increase with increasing temperature and time. This was clearly observed for low BI samples throughout the cooking temperature and time range applied. The decrease in redness ( $\Delta a^*$ ) was statistically significant within cooking time ( $P < 0.001$ ), but not with cooking temperature.

#### 5.4.3 Influence of cooking time and temperature on meat colour in relation to Intramuscular Fat (IMF)

The influence of IMF content on colour changes during cooking was investigated. Colour was characterised by  $L^*$ ,  $a^*$ , and  $b^*$  values of the blocks before (on raw meat) and after cooking. The aim was to investigate whether the IMF content did have an influence on the initial colour (*i.e.* raw samples) and whether a potential colour variation is carried through the cooking stage as well.

The experiment was divided into two stages: In stage one, samples from the eye round, within three IMF ranges (low, medium and high) were cooked at various temperatures (65, 70 or 75 °C) for different times (20, 40 or 60 min). Secondly a second muscle, striploin, within the IMF ranges, was cooked at 70 °C for different times (20, 40 or 60 min) to study quality changes during cooking.

##### 5.4.3.1 Colour of raw samples

The redness and yellowness values of the high IMF samples were significantly ( $P < 0.001$ ) higher than cuts containing medium and low IMF contents.

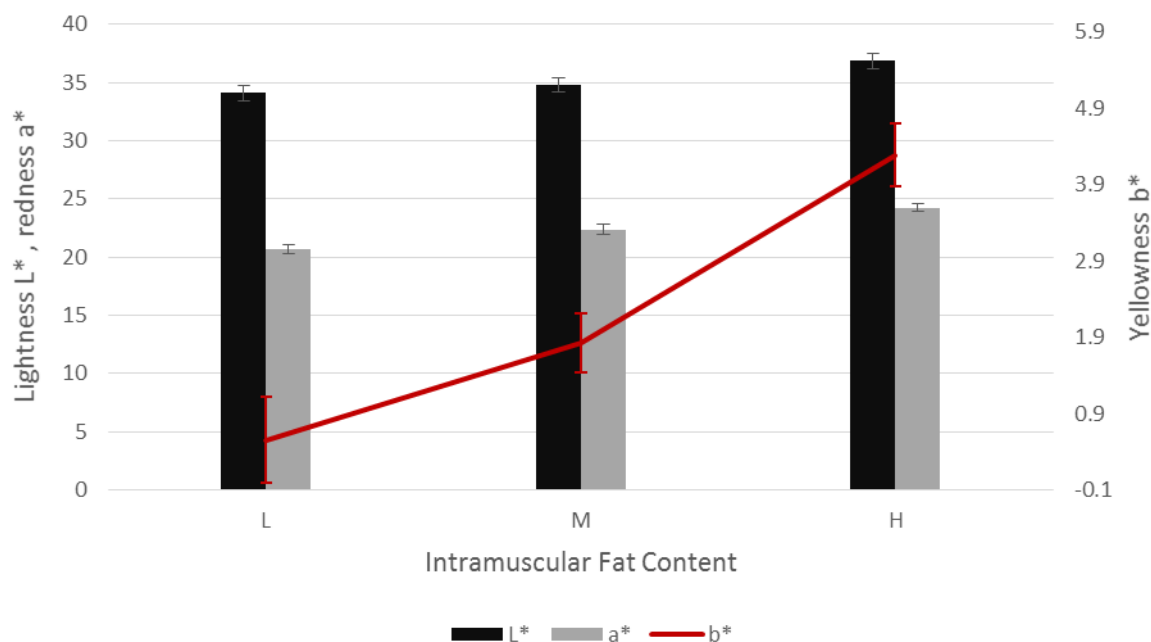


**Figure 5-26.** Colour parameter values (Lightness –  $L^*$ , redness –  $a^*$ , yellowness –  $b^*$ ,  $n = 6$ ) of raw beef striploin in relation to intramuscular fat content (L = Low, M =Medium, H = High).

The  $L^*$  values tended to be higher for the muscles with high IMF contents, than the lightness value of muscles containing low and medium IMF, which appeared darker. In the striploin, lightness increased more with increasing IMF content than in the eye round.

Along with the lightness, redness increased in both the striploin and eye round with increasing IMF.

#### 5.4.3.2 Colour of cooked samples

The striploin and eye round samples were cooked in a water bath of different cooking temperatures (60, 70 or 75 °C) and times (20, 40 or 60 min). The lightness ( $L^*$ ) of the cooked samples was higher compared to uncooked samples. The values of individual colour parameters did not change evenly over the temperature range and the highest increase in lightness ( $L^*$ ) of eye round meat samples was reported after cooking at 65 °C for 40 min. The colour parameters of raw samples changed significantly with cooking temperature, time and IMF content ( $P < 0.001$ ).

The redness ( $a^*$ ) of the meat changed similarly to lightness ( $L^*$ ). The largest decrease in redness ( $14.31 \pm 0.23$ ) was recorded for high IMF content samples (cooked at 75 °C for 60 min), whereas for the medium and low IMF range samples cooked under the same conditions had redness values of only  $11.66 \pm 1.41$  and  $12.23 \pm 0.94$ , respectively. Based on the studies of ultimate pH and BI content it was expected that the redness differences will increase with increasing cooking temperature and time. This was observed at all ranges of IMF content throughout the cooking temperature and time ranges. The decrease in redness was significant for cooking time, temperature and IMF content ( $P < 0.001$ ).

## 5.4.4 Influence of cooking time and temperature on meat colour in relation to interventions

### 5.4.4.1 The effect of PEF on meat colour

The effect of the PEF treatment on the colour of meat is shown in Table 5-2. PEF treatment did not have a significant effect ( $P > 0.1$ ) on the colour parameters ( $L^*$ ,  $a^*$ ,  $b^*$ ) of meat, that is, neither treatment time nor fibre direction showed any impact on colour.

**Table 5-2.** Effect of PEF treatment time (0, 30 and 60 ms) on colour parameters (lightness ( $L^*$ ), redness ( $a^*$ ) and yellowness ( $b^*$ ) on beef eye round (ST) for two different fibre direction cuts

Fibre direction	PEF treatment <sup>A</sup> (ms)	Colour parameters of beef					
		Before treatment			After treatment		
		$L^*$	$a^*$	$b^*$	$L^*$	$a^*$	$b^*$
Cross-sectional	0	41.08 ± 0.82	23.78 ± 0.58	13.06 ± 0.48	43.11 ± 0.63	25.00 ± 0.44	15.62 ± 0.46
	30	41.05 ± 0.75	23.29 ± 0.62	12.82 ± 0.51	42.38 ± 1.05	24.65 ± 0.53	15.57 ± 0.56
	60	41.74 ± 0.41	24.09 ± 0.40	13.25 ± 0.34	43.54 ± 0.60	25.68 ± 0.61	16.34 ± 0.38
Longitudinal	0	40.99 ± 0.77	22.75 ± 0.71	12.60 ± 0.55	42.50 ± 0.81	24.18 ± 0.67	14.98 ± 0.59
	30	42.08 ± 0.96	22.91 ± 0.57	12.67 ± 0.47	42.92 ± 0.71	26.02 ± 0.47	16.65 ± 0.32
	60	42.91 ± 0.60	24.27 ± 0.70	13.69 ± 0.49	43.75 ± 0.56	24.74 ± 0.62	15.92 ± 0.40
Statistical significance <sup>B</sup>							
PEF treatment time		-	-	-	n.s.	n.s.	n.s.
Fiber direction		-	-	-	n.s.	n.s.	n.s.

<sup>A</sup>PEF treatment settings - field strength of 0.25 kV/cm applied at 100 Hz with a pulse width of 10 µsec for different treatment times (0, 30 and 60 ms) <sup>B</sup> $P < 0.1$  \*  $p < 0.05$  \*\*  $p < 0.01$  \*\*\*  $p < 0.001$  n.s.= non-significant <sup>C</sup>Mean ± standard error

As PEF processing did not have a significant effect on the colour of the meat, this could be a positive attribute for future implementation of the technology, as it does not impact on one of the most important quality traits of the meat.

### 5.4.4.2 The effect of HPTP and brine concentration on meat colour

The results for change in lightness ( $L^*$ ) after HPTP, at varying PPI concentrations are shown in Figure 5-27. The colour of each sample was measured before and after HPTP.

In Figure 5-27 and Figure 5-28 the lightness ( $L^*$ ) and redness ( $a^*$ ) of raw beef and beef after HPTP (600 MPa, 75 °C, 5 min) and cooked beef (0.1 MPa, 75 °C, 30 min) are shown. Irrespective of the salt concentration, the lightness ( $L^*$ ) increased after HPTP when compared to the raw samples. A pressure treatment of 600 MPa significantly increased the  $L^*$  value of both brine injected meat samples

( $P < 0.05$ ). The HPTP treatment caused a significant ( $P < 0.01$ ) decrease in redness ( $a^*$ ), and an increase in yellowness ( $b^*$ ) for both PPI and NaCl injected beef. Despite investigating the interaction between pressure and brine concentration, it was evident that the changes in  $L^*$ ,  $a^*$  and  $b^*$  were due to the change in pressure ( $P < 0.05$ ), as opposed to the salt concentrations, which did not affect the colour. Similar results were observed for PPI and NaCl injected meat samples. Lightness ( $L^*$ ) and yellowness ( $b^*$ ) increased, while the redness ( $a^*$ ) decreased.

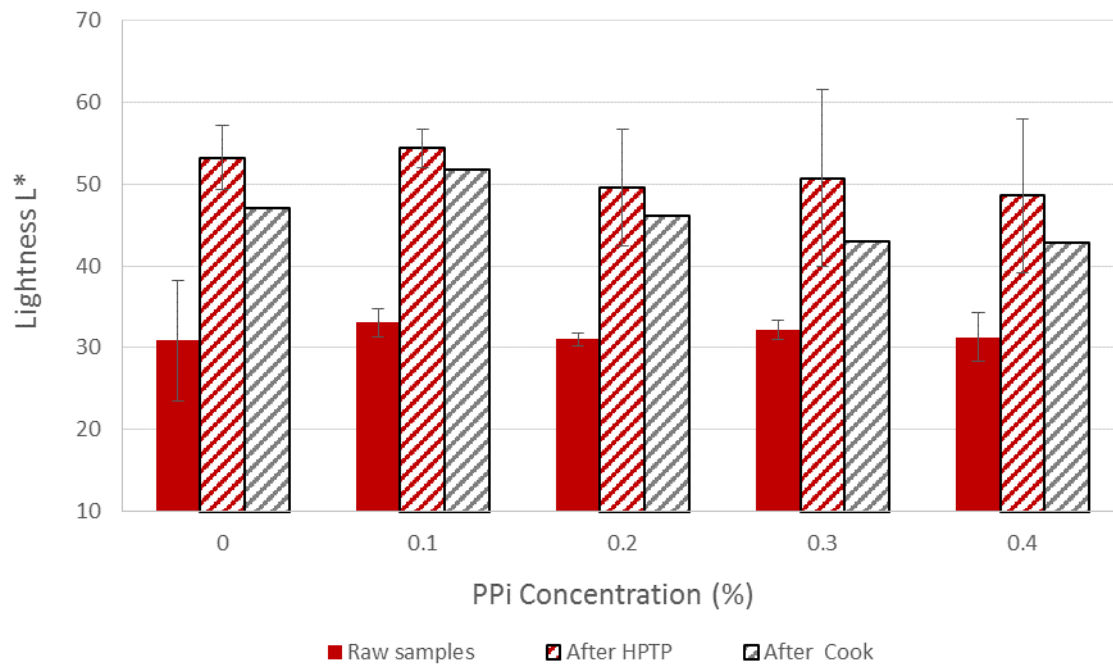


**Figure 5-27.** Changes in meat colour – Lightness ( $L^*$ ) with PPI concentration (%) and pressure (MPa). Meat injected with PPI to 110% of the original weight. HPTP (600 MPa, 75 °C for 5 min), cooking (0.1MPa, 75 °C, 30min), n = 15.

Furthermore, samples that received a control treatment (cook-only, 75 °C for 30 min, n= 5) and HPTP (600 MPa at 75 °C for 5 min, n = 15) were compared. Two-way ANOVA demonstrated there was an interaction between pressure and brine concentration ( $P < 0.05$ ). That is, when the pressure is increased the lightness ( $L^*$ ) increased.

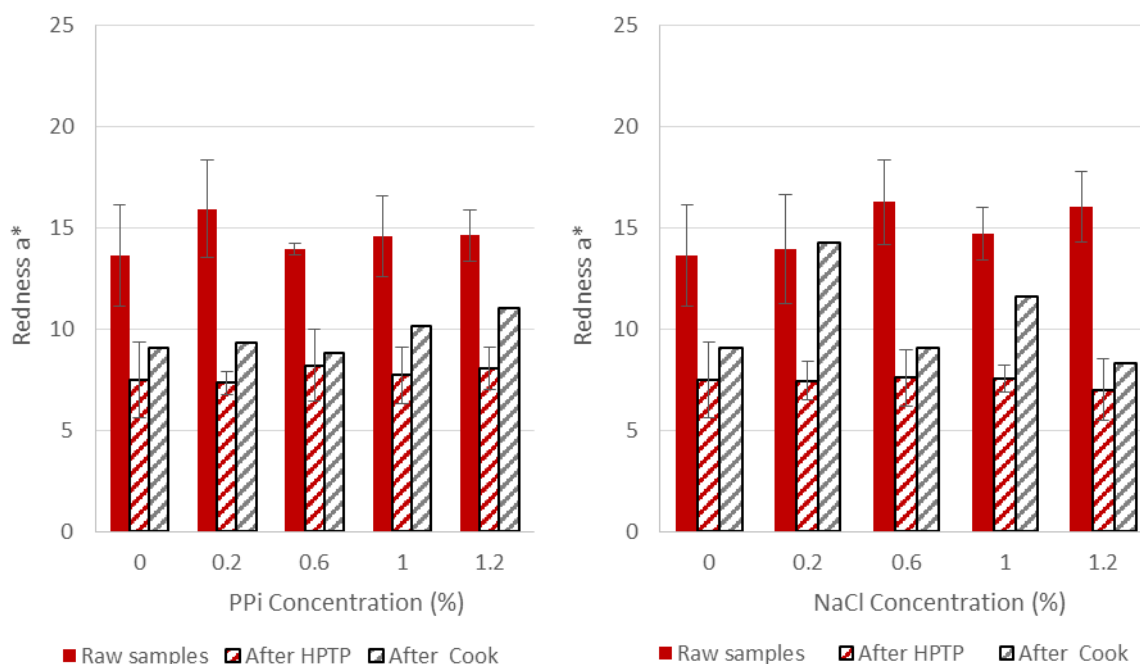


**Figure 5-28.** Changes in meat colour – Redness ( $a^*$ ), with PPI concentration (%) and pressure (MPa). Meat injected with PPI to 110% of the original weight. HPTP (600 MPa, 75 °C for 5 min), cooking (0.1MPa, 75 °C, 30min),  $n = 15$

The same analysis was conducted for NaCl injected samples. The combined effect of pressure and the brine concentration on lightness of brine injected meat was significant ( $P < 0.001$ ). An interaction was also seen in the NaCl injected beef for brine vs pressure where it significantly affected the lightness ( $L^*$ ) value, *i.e.* increasing pressure resulted in increased lightness ( $L^*$ ). In addition, unlike the PPI injected beef, the NaCl injected beef showed a significant effect of pressure on the redness ( $P < 0.001$ ) Figure 5-28B.

The effect of the cooking (0.1 MPa, 60, 64, 75, 85 or 89 °C for 30 mins) on colour is outlined in Table 5-3. The different salt types resulted significantly different  $b^*$ ,  $\Delta a^*$  and  $\Delta b^*$ . Salt type did not significantly affect  $L^*$ ,  $\Delta L^*$  or  $a^*$  values. However, the different processing temperatures did result in significantly different  $a^*$ ,  $b^*$ ,  $\Delta a^*$  and  $\Delta b^*$  values. Neither temperature nor salt type had a significant effect on  $L^*$  and  $\Delta L^*$  values. When comparing the salt type for the HPTP samples, there was no significant difference for the  $L^*$  and  $a^*$  values.

**Table 5-3.** Main effects of HPTP (300, 350, 470, 590 and 640 MPa and 60, 64, 75, 85 and 89 °C for 5 min) and control (cook-only, 0.1 MPa and 60, 64, 75, 85 and 89 °C for 30 min) on colour parameters of processed bovine *M. Semitendinosus*, injected with 0.2% PPI. Mean  $\pm$  S.E.

		Colour parameters after processing						
Pressure (MPa)	Temp (°C)	PPI (0.2%)			NaCl (1.0%)			
		<i>L*</i>	<i>a*</i>	<i>b*</i>	<i>L*</i>	<i>a*</i>	<i>b*</i>	
HPTP	300	75	59.36 $\pm$ 3.09	11.73 $\pm$ 1.66	16.39 $\pm$ 0.82	60.84 $\pm$ 1.90	11.91 $\pm$ 2.93	14.98 $\pm$ 1.59
	350	64	61.20 $\pm$ 2.16	16.91 $\pm$ 2.15	15.34 $\pm$ 0.72	60.63 $\pm$ 7.02	13.61 $\pm$ 2.84	15.88 $\pm$ 1.92
	350	85	61.46 $\pm$ 3.27	11.42 $\pm$ 0.79	15.00 $\pm$ 0.84	59.34 $\pm$ 3.41	12.16 $\pm$ 1.28	17.83 $\pm$ 1.40
	470	60	61.29 $\pm$ 2.73	13.78 $\pm$ 2.20	15.8 $\pm$ 0.94	60.44 $\pm$ 4.38	13.08 $\pm$ 1.15	16.95 $\pm$ 0.74
	470	75	56.58 $\pm$ 4.09	10.72 $\pm$ 1.41	16.5 $\pm$ 2.53	56.56 $\pm$ 6.06	11.12 $\pm$ 2.92	17.99 $\pm$ 2.37
	470	89	58.60 $\pm$ 7.15	11.23 $\pm$ 1.11	16.14 $\pm$ 1.40	55.80 $\pm$ 1.64	11.3 $\pm$ 2.29	16.5 $\pm$ 0.75
	590	64	59.87 $\pm$ 4.61	13.19 $\pm$ 0.71	16.2 $\pm$ 0.72	65.21 $\pm$ 3.43	9.64 $\pm$ 1.28	13.65 $\pm$ 1.56
	590	85	57.02 $\pm$ 1.71	11.64 $\pm$ 1.53	16.03 $\pm$ 2.00	60.6 $\pm$ 4.01	11.62 $\pm$ 2.84	16.78 $\pm$ 1.95
	640	75	57.49 $\pm$ 3.85	10.55 $\pm$ 1.65	15.72 $\pm$ 1.06	57.77 $\pm$ 2.14	12.31 $\pm$ 2.68	15.68 $\pm$ 0.93
	Cooking	0.1	60	60.94 $\pm$ 5.26	18.49 $\pm$ 0.41	15.33 $\pm$ 1.32	60.15 $\pm$ 4.66	23.16 $\pm$ 2.86
0.1		64	54.54 $\pm$ 7.51	21.21 $\pm$ 5.46	16.32 $\pm$ 2.14	58.96 $\pm$ 4.59	22.84 $\pm$ 4.43	17.33 $\pm$ 2.35
0.1		75	51.27 $\pm$ 8.03	10.71 $\pm$ 0.98	15.27 $\pm$ 0.40	58.36 $\pm$ 3.45	18.43 $\pm$ 3.74	16.97 $\pm$ 0.34
0.1		85	55.52 $\pm$ 3.72	11.61 $\pm$ 1.72	14.47 $\pm$ 0.28	57.46 $\pm$ 2.45	11.99 $\pm$ 0.82	14.56 $\pm$ 0.59
0.1		89	53.09 $\pm$ 1.16	9.50 $\pm$ 1.57	14.45 $\pm$ 0.68	55.38 $\pm$ 2.59	10.49 $\pm$ 0.89	14.63 $\pm$ 0.73

## 5.5 Modelling

### 5.5.1 Introduction

Most meat and meat-based products are cooked prior to consumption. The cooking process not only destroys pathogenic or spoilage microorganisms but also develops sensorial properties which are meat and processing specific (Kondjoyan et al., 2014). During cooking, meat can lose mass (*i.e.* cook loss), which determines the yield of the cooking operation, making it a critical factor for the meat industry. Cooking also affects the quality of meat (*e.g.* juiciness, tenderness, nutritional components, etc.). It is therefore important to know how variations of processing conditions and properties of the raw meat will affect the yield and quality of cooked meat to improve and optimise the cooking process. Extensive characterisation of the cooking process using a strictly experimental approach constitutes a formidable challenge due to the excessively large number of variables that must be considered.

The development of mathematical models is helpful to better understand of the underpinning physics affecting the cooking process and final product quality. Using optimum design and operating conditions of a cooking process is essential to achieve desired quality attributes of a cooked product. Such models would be of relevance and interest, to the meat industry to predict quality parameters of meat after the cooking process. In such cases, knowledge of the appropriate conditions could, when combined with an accurate predictive model, allow for the production of cooked meat products which can be targeted to consumers. A number of approaches have been used to develop predictive mathematical models, ranging from empirical, solely based on observed data, to semi-parametric, a hybrid approach consisting of parametric and non-parametric components, to computational, consisting of physics, mathematics and computer science, which aim to simulate and study the behaviour of complex systems. The latter approach is regarded as a useful decision-making tool which allows for the generation of tangible results for a wide range of scenarios through a virtual laboratory, without the excessive need for labour-intensive trial-and-error experimentation (H. T. Sabarez, 2015). It may also be utilised to develop new/improved conceptual designs and to optimise operating conditions in a cost-effective route to intensifying innovation with minimal investment of time, manpower, and funds.

The use of each of these three approaches, *i.e.* empirical, semi-parametric and computational, have been used to model the cooking of meat. These are described in this section.

### 5.5.2 Modelling approaches

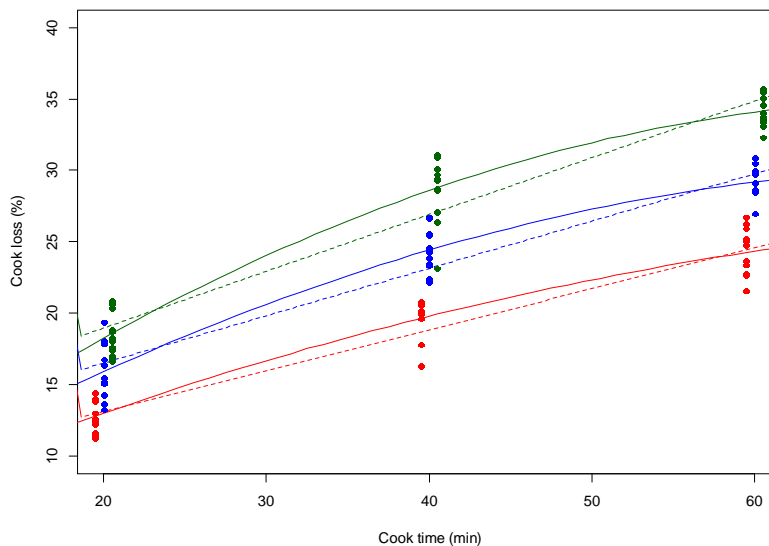
#### 5.5.2.1 Empirical modelling

Figure 5-29 shows the cook loss of eye round which increased with cooking time and cooking temperature. It was initially assumed that the loss was linearly related to the cooking time as this is the simplest model but this proved not to be the case. Instead, a quadratic function was found to best describe the relationship between cook loss and time, and of the form

$$y = b_0 + b_1x + b_2x^2$$

Eq. 5-1

where  $y$  is the cook loss,  $x$  is the cooking time in minutes,  $b_2$ ,  $b_1$ , and  $b_0$  are the coefficients for  $x^2$ ,  $x$  and the intercept, respectively, for each temperature ( $^{\circ}\text{C}$ ). Figure 5-29, illustrates that cooking temperature had an effect on cook loss, and the coefficients,  $b_i$ , were found to be related to the cooking temperature with  $b_1$  increasing with temperature, and  $b_0$  and  $b_2$  decrease with increasing temperature. This allowed the development of a predictive model relating cook loss to both cooking temperature and time. Figure 5-30 shows a contour plot of the predicted cook loss as a function of cooking time and temperature, indicating that cook loss increased with both cooking temperature and time.



**Figure 5-29.** A plot of cook loss (%) against cook time (min) for different cooking temperatures (65, 70 or 75  $^{\circ}\text{C}$ ). The points in red, blue and green represent 65, 70 and 75  $^{\circ}\text{C}$ , respectively, while the solid and dashed lines represents the line of best fit for the linear and quadratic models for each temperature. The points are offset for clarity.

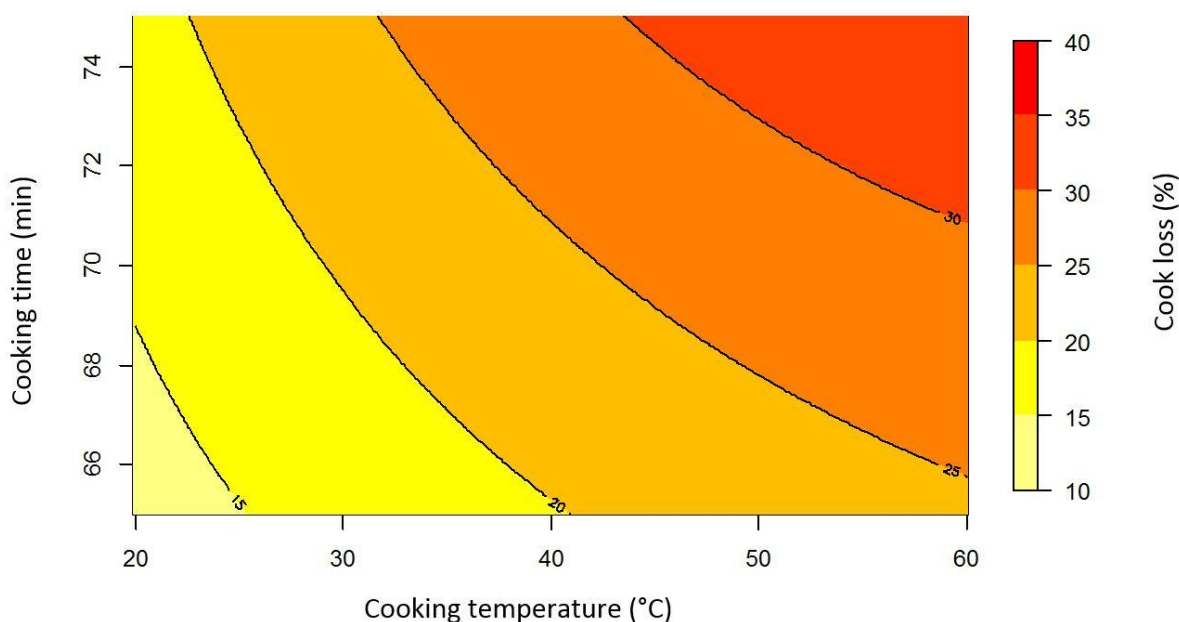


**Figure 5-30.** Contour plot showing predicted cook loss (%) of eye round as a function of cooking temperature (°C) and time (min).

### 5.5.2.2 Semi-parametric modelling

From a biophysical perspective, the cooking of meat can essentially be expressed with comparatively few factors. It is the process of denaturation and contraction of protein structures as a function of applied heat (Kondjoyan, Ouilic, Portanguen, & Gros, 2013; Tornberg, 2005; Vert et al., 2012). Sometimes pressure is applied in addition to heat, and meat's acidity and salinity manipulated, but the preceding definition captures the broad features of cooking meat. As a conceptual basis for semi-parametric modelling, the changes within the meat are perhaps best seen as two intertwined dynamical systems. One relates to heat transfer through the meat while the other relates to the process of localised protein denaturation and physical alteration within meat as a function of temperature. This framework is particularly useful for modelling mass loss during cooking as it is essentially water debinding and migration during protein denaturation (Bombrun, Gatellier, Portanguen, & Kondjoyan, 2015; Goñi & Salvadori, 2010; Kondjoyan et al., 2013; Ouilic, Lemoine, Gros, & Kondjoyan, 2011; Vert et al., 2012). This is depicted in Figure 5-31, with aspects of cooking as inputs, resultant mass loss and other sensory and nutritional qualities of meat as outputs, and the relevant intrinsic characteristics of raw meat depicted as two mutually causal dynamical systems with their own list of internal variables. Many factors appear as variables for both models highlighting the interconnectedness and mutual causality of heat transfer and protein denaturation processes.

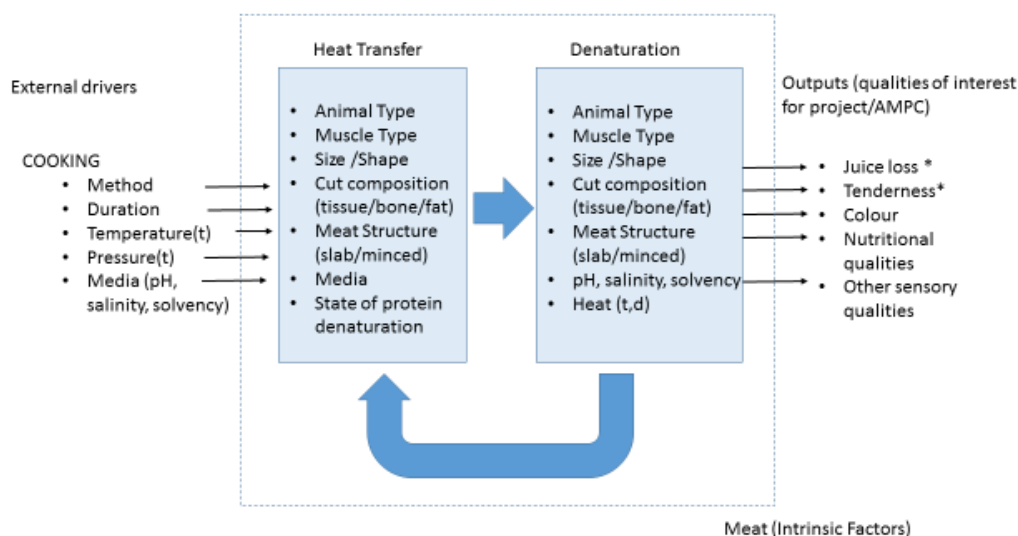


**Figure 5-31.** Conceptual biophysical model of cooking meat.

Being able to break down a complex process into simpler, functionally defined stages is useful in generating insights into the cooking process. However, it is generally difficult to express a compartmentalised model with distinct inputs, outputs and subsystems with differential equations. There is a well-established body of knowledge, including mathematical techniques and software for their implementation, from the field of systems and control engineering which serves to tackle this (Nise, 2004). The use of Laplace transform (Ljung, 2009) makes differential equations not only separable but also algebraic. These models in the Laplace domain are known as transfer functions, one for each subsystem, mapping the subsystems input onto its output. These transfer functions can then be combined in a relatively simple algebraic manner to represent the system as a whole. Once the transfer function representation is established, inverse Laplace transform may be applied to go back to a description of the process as a function of time, generating a more familiar mathematical representation.

Transfer function models are essentially linear, time-invariant (LTE) approximations. There are two important considerations. Firstly, cooking meat is not time-invariant, that is, heat conductivity and so heat transfer, along with protein structure will vary with cooking time and, as such, water loss may be non-linear and time-variant. Nevertheless, such systems can quite often be approximated as LTE systems. The overall fit of the transfer function output to the actual system output will be an objective measure of how well this can be achieved. Secondly, if the transfer function model is of a poor fit, it would still be a very helpful starting point for formulating a state-space model (Ogata, 2010) for the process. State-space models allow more design freedom in that they are not limited to LTE systems, but are more complex and perhaps less intuitive than transfer function models. Insights acquired from even a partially successful transfer function could help deal with the complexity of its state-space counterpart (Ljung, 2009).

### 5.5.2.3 Using Laplace models to model heat transfer

Using experimental data, second order transfer functions were found to provide very good fits to the measured data. The degree of variability of using this approach was assessed for the meat core temperatures at four different cooking temperatures; 55, 65, 70 and 75 °C. Figure 5-32 shows the predicted curves for each temperature, with each temperature normalised for comparison. While all the curves are very similar, there does appear to be two subgroups, 55 and 75 °C in one, and 65 and 70 °C in the other. This could either be due to random experimental variations, or to differences within the samples (*e.g.* physical dimensions of the cuts of meat, changes in protein structure or related properties).

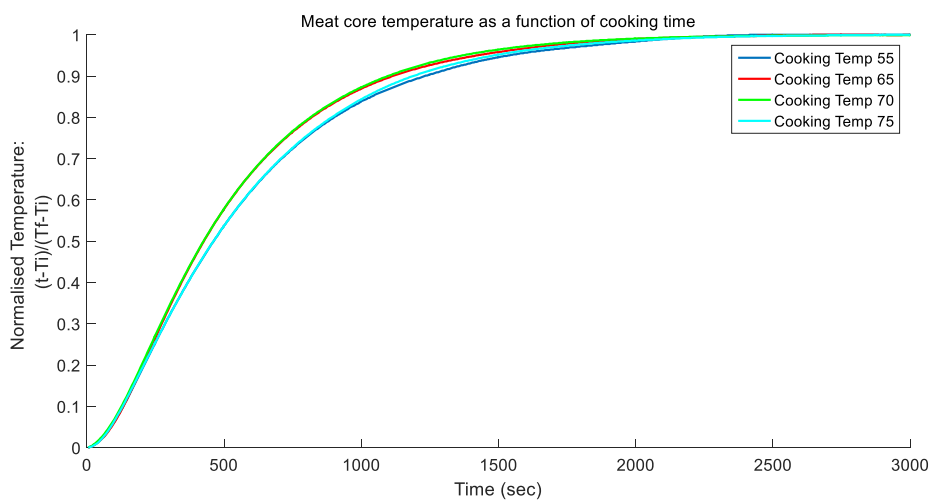


**Figure 5-32** Meat core temperature as a function of cooking time

The second order transfer function models were of the form, using 55 °C as example;

$$\frac{1.72 \cdot 10^{-5}}{s^2 + 0.010s + 1.72 \cdot 10^{-5}}$$

Eq. 5-2

With similar models described for the other temperatures. More intuitively, the above can be expressed as

$$\frac{1.72 \cdot 10^{-5}}{(s + 0.0021)(s + 0.0082)}$$

Eq. 5-3

By utilising these expressions as inputs to relevant transfer functions, it was possible to define

$$c(t) = [T_i + (T_c - T_i)(1 - 1.61 e^{-0.0022t} + .61 e^{-0.0059t})] * u(t)$$

Eq. 5-4

Where  $u(t) = 1$  for  $t > 0$ ,  $u(t) = 0$  for  $t < 0$ ,  $c(t)$  is the core meat temperature,  $T_i$  is the initial meat temperature (prior to cooking) and  $T_c$  is the set cooking temperature.

Considering all temperatures, it was feasible to derive:

$$c(t) = [T_i + (T_c - T_i)(1 - A_1 e^{(-.00225 \pm .00015)t} + A_2 e^{-.0074 \pm .0015t})] * u(t) \quad \text{Eq. 5-5}$$

where  $A_1$  and  $A_2$  were dictated collectively by the coefficients of  $t$  in the two exponential functions and could as a generalised model describe the cooking meat temperature with time.

Preliminary equations were developed using first order transfer functions to model denaturation and water but insufficient experimental data was available to develop generalised models as indicated above.

#### 5.5.2.4 Numerical computational modelling

A three dimensional (3D) geometric coordinate system was considered as an appropriate approach to describe the physics occurring during the cooking process of meat. The solution in 3D geometric coordinate was employed to represent the real system due to the dimension of the meat under investigation (*i.e.*, significant proportions in three coordinate lengths). The system under investigation was assumed symmetric, hence only half of the entire computational domain was considered for modelling.

For modelling, the cooking process can be considered as simultaneous heat and mass transfers between the food product and the environment. The coupled transfer of heat and mass, which simultaneously occurs both externally and internally to the food matrix during cooking, can be described as follows: (1) convective heat transfer between hot water and the product surface, (2) heat transfer mainly by conduction within the solid interior, (3) convective mass transfer between product surface and surrounding air, (4) mass transfer in the solid interior by diffusion (liquid or vapour), and (5) moisture evaporation at the product surface.

Obuz, Powell, and Dikeman (2002) consider water evaporation (a process driven by the moisture difference between the meat surface and air) for modelling moisture loss in meat cooking. To reduce the complexity of the problem, it was assumed that the beef meat is a continuum medium (where the micro-structure is neglected), and shrinkage due to fibre contraction and the associated loss were not considered. During cooking, mechanical deformation of the meat can be substantial and the underlying physics are not simple, as the meat contracts in the direction of the fibres, and expand in one of the directions perpendicular to the meat fibres (van der Sman, 2007). Considering the mechanical deformation was beyond the scope of the present modelling work.

The mathematical descriptions for a generalised geometry for simultaneous conductive heat and diffusive mass transfer in the interior of solid product are given below. The transient heat transfer

within the food matrix is modelled according to Fourier's law of heat conduction (Eq. 5-6), while the mass transport within the food matrix is modelled using the basic law governing the movement of mass according to Fick's law of diffusion (Eq. 5-7).

$$\rho C_p \left( \frac{\partial T}{\partial t} \right) + \nabla(-k \nabla T) = 0$$

Eq. 5-6

$$\left( \frac{\partial c}{\partial t} \right) + \nabla(-D \nabla c) = 0$$

Eq. 5-7

Where  $C_p$  is the specific heat capacity at constant pressure (J/kg·K),  $T$  is temperature (K),  $k$  is the thermal conductivity (W/m·K),  $t$  is time (s),  $\rho$  is the density (kg/m<sup>3</sup>),  $D$  is the effective water diffusivity in the food (m<sup>2</sup>/s) and  $c$  is water concentration (mol/m<sup>3</sup>).

The boundary condition at the surface (at  $t > 0$ ) for heat transfer, considering the mass transfer between the air stream and meat surface which couples the heat and mass transfer equations simultaneously, is given in Eq. 5-8. This means that the heat transported by convection from the hot water to the meat surface is partly used to raise the meat temperature by conduction and partly for water evaporation at the meat surface.

$$k \frac{\partial T}{\partial n} = h_c (T_w - T) + k_c \lambda (c_s - c_a)$$

Eq. 5-8

Where  $k$  is the thermal conductivity (W/m·K),  $T$  is temperature (K),  $n$  represents the direction normal to the surface,  $h_c$  is the heat transfer coefficient (W/m<sup>2</sup>·K),  $T_w$  is the water temperature (K),  $T$  is the food temperature (K),  $k_c$  is the mass transfer coefficient (m/s),  $\lambda$  is the latent heat of evaporation (J/kg),  $c_a$  is the water concentration in air (mol/m<sup>3</sup>), and  $c_s$  is water concentration on the meat surface (mol/m<sup>3</sup>).

The boundary condition at the surface (at  $t > 0$ ) for mass transfer is given in Eq. 5-9, which accounts for the balance between the diffusive flux of liquid water coming from the interior of the meat and the flux of vapour from the meat surface to the air stream.

$$D \frac{\partial c}{\partial n} = k_c (c_s - c_a)$$

Eq. 5-9

Where  $D$  is the effective water diffusivity in food (m<sup>2</sup>/s),  $c$  is the water concentration (mol/m<sup>3</sup>),  $n$  represents the direction normal to the surface,  $k_c$  is the mass transfer coefficient (m/s),  $c_a$  is the water concentration in air (mol/m<sup>3</sup>) and  $c_s$  is the water concentration on the meat surface (mol/m<sup>3</sup>).

The solution of the governing partial differential equations (PDEs) describing the cooking process requires knowledge of the thermophysical and transport properties of the product, air and water. In this case, the thermophysical properties of meat (*i.e.*, thermal conductivity, specific heat capacity and density) were assumed to be dependent on the composition of the meat (*i.e.*, water, protein, fat, carbohydrate and ash) expressed as a function of the local temperature (ASHRAE, 1995; Choi, 1987; H. T. Sabarez, 2012).

The transport coefficients for heat and mass required in the boundary condition were estimated from empirical equations involving dimensionless numbers. The convective heat transfer coefficient required for the boundary condition in the heat transfer equation was calculated using the Nusselt–Reynolds–Prandtl correlation for local convective heat transfer for a particular geometry of the food material given by Heldman (2007). The mass transfer coefficient, which describes the convective mass transfer at the surface of the product, was obtained using the Sherwood–Reynolds–Schmidt correlation for average convective mass transfer for a particular geometry of the food material (Heldman, 2007). The heat and mass transfer coefficients can vary significantly depending on the process parameters (*i.e.*, food size, fluid velocity, etc.).

The water vapour concentration of the air in equilibrium with the surface of the meat exposed to convection was estimated from the relationship given by Huang (1995). For meat, these authors reported the values for the empirical constants  $c$  and  $n$  to be 5222.47 and -1.0983, respectively.

$$RH = e^{\left( \left( \frac{-c}{R_g T} \right) M_e^n \right)}$$

Eq. 5-10

Where  $RH$  is the relative humidity (%),  $R_g$  is the universal gas constant (kJ/mol·K),  $M_e$  is the equilibrium moisture content (% dry basis),  $T$  is food temperature (K), and  $c$  is the water concentration (mol/m<sup>3</sup>).

The effective diffusion coefficient is the main parameter for the characterisation of mass transfer phenomena in solid foods. It is regarded as a lumped property that does not really distinguish between the transport of water by liquid or vapour diffusion, or capillary or hydrodynamic flow due to pressure gradient set up in the material (Mujumdar, 2008). However, the effective diffusivity depends on geometric shapes and process conditions, and it is strongly a function of both temperature and moisture content. In some cases, the well-known Arrhenius equation is used to quantify the influence of temperature on moisture diffusivity (Sablani, 2007). In the cooking process, the effective diffusion coefficients were estimated according to the relationship for drying processes reported elsewhere (H. T. Sabarez, 2012; Henry T. Sabarez, 2014; H. T. Sabarez, 2015) by a least squares fit between the predicted and experimental moisture loss data, assuming the dependence on both moisture concentration and temperature of the product. Moisture loss during cooking can be considered analogous to moisture loss during drying, thus the use of the equation here is justified (Shilton, 2002).

$$D = e^{\left(\frac{c}{c_i}\right)} e^{\left(\frac{E_a}{RT}\right)}$$

Eq. 5-11

Where  $D$  is the effective water diffusivity in food ( $\text{m}^2/\text{s}$ ),  $c$  is the water concentration ( $\text{mol}/\text{m}^3$ ),  $c_i$  is the initial water concentration ( $\text{mol}/\text{m}^3$ ),  $E_a$  is the activation energy ( $\text{kJ}/\text{mol}$ ),  $R$  is the universal gas constant ( $\text{kJ}/\text{mol}\cdot\text{K}$ ) and  $T$  is the food temperature ( $\text{K}$ ).

Thus, the influence of temperature and moisture content on the effective diffusivity could be established from a single experiment, as the change in temperature and moisture content of the product during cooking depends on the operating conditions. It is apparent from the relationship that the effective diffusion coefficient values gradually increased with temperature and decreased with the decreased in moisture content. The  $D$  values obtained in this study were in the range of  $2.63 \times 10^{-9}$  to  $1.42 \times 10^{-7} \text{ m}^2/\text{s}$  with a value for  $R^2$  of 0.9652, indicating a good fit of the model to the experimental moisture loss data.

For regularly shaped geometries with proper initial and boundary conditions, together with appropriate simplifications and assumptions of the mathematical models of a system, it is possible to derive information about the system by analytical means, which produce general solutions. However, for complex geometries and equations, it is necessary to use numerical computational methods to provide approximate solutions for the problem under investigation. The fundamental concept of numerically solving the complex systems is the discretisation of the geometry of interest to a number of finite elements or cells, thus reducing the complex governing equations to sets of simple linear or polynomial equations by employing appropriate approximation techniques. The numerical methods produce solutions in steps, with each step providing the solution for one set of conditions and the calculation repeated to expand the range of solutions.

For this study, the resulting systems of highly coupled non-linear PDEs in the space-time domain together with the set of initial and boundary conditions were numerically solved by finite element method (FEM) using a commercial software package (COMSOL Multi-physics™, Comsol AB, Stockholm, Sweden) (Multiphysics, 2007). A preliminary grid independency test was carried out to ensure that the solution is independent of grid or cell size and to verify whether the numerical solution basically remains the same with further grid or cell refinements. The time-dependent problem was solved by an implicit time-stepping method. The resulting systems of non-linear equations were solved using Newton's method while a direct linear system solver was adopted to solve the resulting systems of linear equations. The relative and absolute tolerances were set to 0.001 and 0.0001, respectively to control the error at each integration step.

When a model (particularly the one based on fundamental physics) is properly validated, one can extrapolate a system's behaviour to a range of parameters not tested in the experiment. A parametric sensitivity study can be undertaken to further investigate the effects of the uncertainties of various input parameters on the model's predictions and to demonstrate the usefulness of the predictive tool

in identifying critical operational factors affecting the process. The model can then be used to test a number of scenarios (different operating conditions and material properties) to study the interactions between the factors in the system and to examine the critical parameters affecting the cooking process.

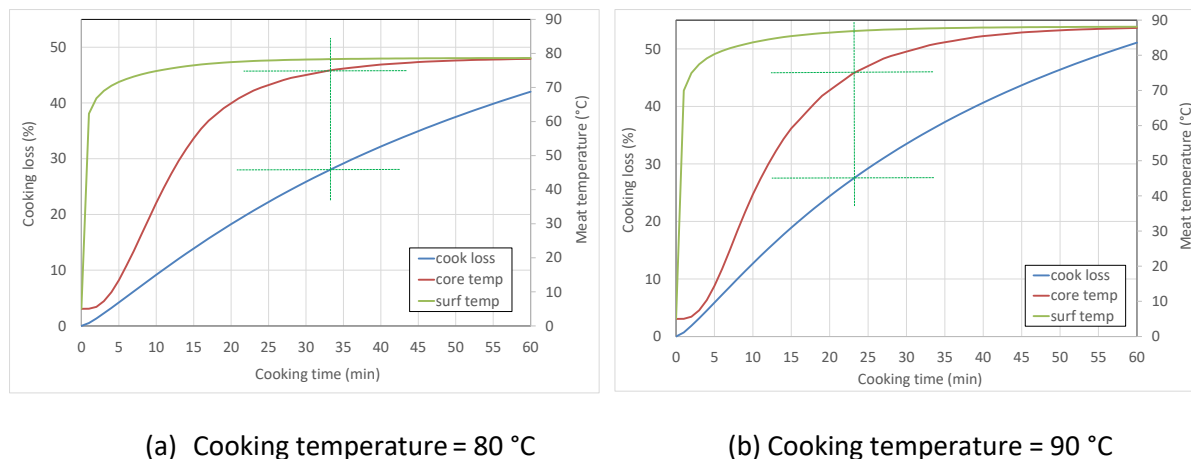


**Figure 5-33.** Plots of the predicted cooking kinetic losses and temperatures (core and surface) of beef meat (55 x 35 x 40 mm) for two cooking temperatures (80 and 90 °C)

For illustration purposes, the modelling tool was used to predict the important operational parameters (product temperature, cook loss and cooking time) during the cooking process of a meat sample at two different cooking temperatures. It should be emphasised that the temperature at the centre of the product is often used to determine the required cooking time (Kondjoyan, Ouilic, Portanguen, & Gros, 2013). In cooking food, the most important requirement is to achieve a final internal temperature of 75 °C at the centre to ensure microbiological safety (ASHRAE, 1989). This requirement is obviously dependent on the type of food products. Figure 5-33 demonstrates the usefulness of the predictive tool to evaluate the effect of cooking temperatures to achieve the required cooking time and the impacts on cook loss during meat cooking. The simulations show that an increased cooking temperature shortens the time required to reach the target centre temperature of 75 °C. It can be seen from Figure 5-33 that cooking meat at 80 °C temperature would take about 33 minutes for the meat centre temperature to reach 75 °C, while cooking at 90 °C temperature would require just 23 minutes to heat the centre meat temperature to 75 °C (Figure 5-33b). This represents a difference of about 10 minutes in the time needed to cook the meat between the two temperatures.

On the other hand, it can be seen that the cook loss was not affected by the increase in cooking temperature, resulting to a similar cook loss of about 27% to reach to the required cooking time for both cooking temperatures. The drawback is that cooking at 90 °C resulted in a much higher meat temperature (about 88 °C at the surface) with larger temperature gradients between the centre and the surface (about 12 °C difference) compared to cooking at 80 °C with meat surface temperature of 79 °C and temperature gradient of about 3 °C. This could have implications on the quality of the cooked

product. For example, cooking at 90 °C exposes the product to higher temperature (although for a shorter time) with less uniformity in heating (large temperature gradient) at the end of the required cooking time compared to cooking at 80 °C. However, it should be noted that in thermal processing the product quality changes are usually affected by temperature-time combination.

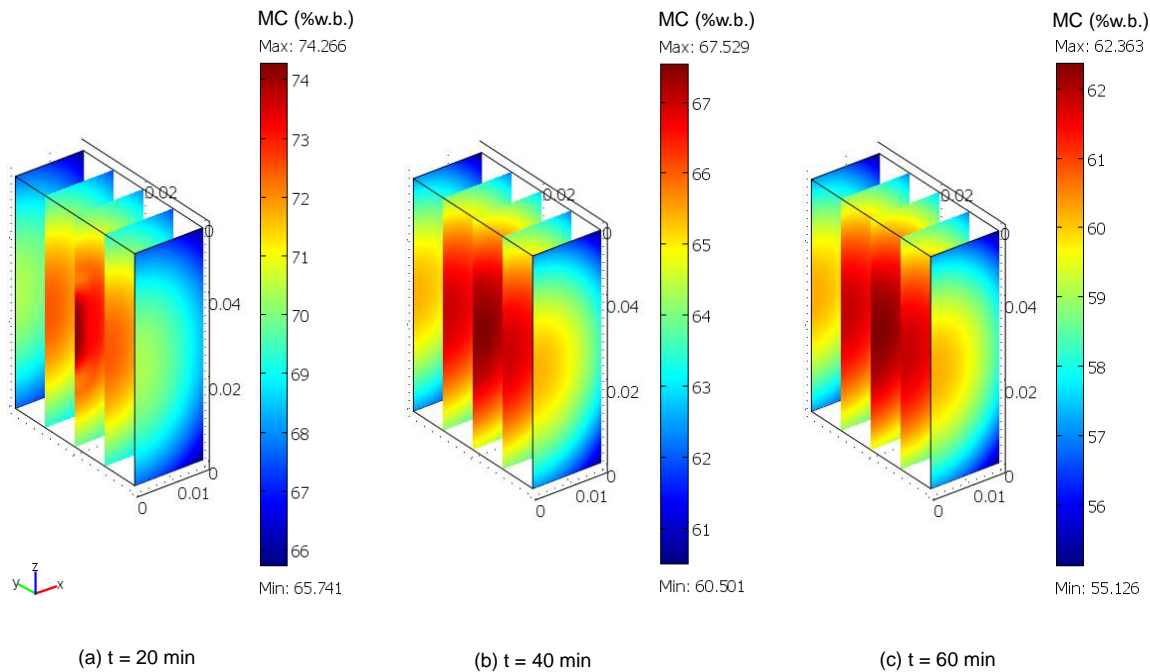


**Figure 5-34.** Predicted moisture content distribution during cooking of meat (55 x 35 x 40 mm) at 75 °C.

The advantage of the numerical modelling approach is that the temperature and moisture distributions across the solid food domain can be established at any time during cooking. Figure 5-34 depicts the corresponding progress of the moisture content distribution within the meat during the cooking process. It shows that a moisture content gradient exists across the meat sample with the external surface was more dried than the centre. For example, cooking at 75 °C for 60 min would lead to a moisture content difference between the surface and the centre by about 7%. Several authors have also reported a variation in the water content locally in the meat sample during cooking (Bisceglia, 2013; Kondjoyan et al., 2013).

Quality is often analysed averagely while its evolution is local and depends on the complex thermal and water gradients generated in the meat during cooking (Kondjoyan et al., 2014). From a quality point of view, it is of interest to minimise the moisture loss during cooking. The prediction in the distributions of moisture content and temperature across the food matrix is therefore important in characterising the quality changes during cooking for achieving the optimal design and operating conditions of a cooking system which maximises the retention of the desired quality attributes of the product.

### 5.5.3 Conclusion

Three modelling approaches have been used to model the cooking of meat. The first was an empirical approach where a quadratic equation was utilised to relate cook loss with the cooking time, and a linear relationship between the quadratic equation coefficients and the cooking temperature. When combined, these two equations are able to demonstrate the behaviour related to the cook loss of meat with cooking temperature and time.

The second approach was semi-parametric and the cooking process was defined as a cascade of heat transfer and denaturation subsystems. Laplace transform equations were deployed to make this separability possible, and transfer function models were developed for each subsystem. Inverse Laplace transform equations were used to define the variables of interest (core meat temperature and water loss) as functions of time and cooking conditions. This approach demonstrated the overall excellent fit of the models and that this was a very useful approach to take, providing an empirically validated framework within which impact of biophysical attributes of meat, relevant to meat scientists, industry and the consumer, can be well understood.

The third approach was computational and based on a mathematical model developed from fundamental physical laws which described the simultaneously coupled heat and mass transfer mechanisms occurring during the meat cooking process. In this numerical model, the governing partial differential equations for heat and mass transfer were numerically solved by a finite element method implemented in a commercial software package. This allows predictions of transient temperature and moisture content distributions across the product in a space–time domain during the cooking process as a function of various cooking conditions.

The numerical model developed in this work can be used as a predictive tool for the simulation of the important transport phenomena in optimising the design and operation of the cooking process of meat that minimises the cook loss. The model can readily be adapted to account for other phenomena and can be extended for other geometries in complex shaped systems. During cooking of meat, significant structural changes occur. Coupling a mechanical model for prediction of the meat tenderness and the effect of contraction on water transport would allow better predictions. In addition, modelling the cooking process in a way that incorporates the prediction of food qualities (*i.e.*, sensorial, functional and nutritional) will be important to enable the manipulation and control of food quality to achieve the desired attributes.

## 6.0 CONCLUSIONS & RECOMMENDATIONS

### Summary

The major findings of the project were:

#### Dimensions and Cook loss

Meat changes its dimensions upon heating due to protein denaturation. Firstly, shrinkage across the muscle fibres was initiated at approximately 50 °C, most likely driven by the denaturation of myosin. Secondly, a lengthwise shrinkage along the muscle fibres occurred from 70 °C (denaturation of actin). The ageing of meat resulted in a small increase in cook loss (1.5 – 3% higher total mass loss) and had a minor impact on shrinkage of muscle fibres, since cytoskeletal proteins, which are known to break down during ageing, were not major players in the dimensional changes upon heating. Therefore, the main source of structural changes, and hence responsible for the cook loss during heating, was the denaturation of myofibrillar proteins, with only minor influence of connective tissue denaturation.

As expected, cook loss increased with increasing cooking temperature and time. The ultimate pH did influence the characteristics of raw and cooked meat, while high pH meat (> 6.0) exhibited higher moisture contents and lower cook losses than low pH (5.37 – 5.55) meat. Neither *Bos indicus* nor intramuscular fat content affected the total mass loss and did not influence the dimensional changes during cooking. There were some differences in the moisture content and water holding capacity meat when comparing the different primal cuts after cooking. We found that the oyster blade and striploin tended to have less moisture than the rump, topside and brisket after cooking under the same conditions.

#### Texture

The most tender meat was achieved by cooking in the temperature range of 65 – 70 °C. There were significant differences in texture between different muscles of cooked meat. Rump, oyster blade and striploin were more tender than topside, brisket and eye round cooked under the same conditions (70 °C / 60 min). This was probably due to the different amount of connective tissue in these muscles. Meats with higher pH retain more moisture in the structure upon cooking which might benefit the tenderness. With an increase in intramuscular fat the tenderness increased, most likely due to the decrease in force required for the blade to cut through fat rather than cutting through meat fibres.

#### Colour

Cooking temperature affected the colour of the cooked meat primarily as a result of the denaturation of myoglobin, resulting in a lighter and less red colour of meat. Major colour changes upon cooking occurred in two steps: when meat was cooked at temperatures within 55-65 °C, and when temperatures were ≥ 75 °C. As expected high pH meat retained its redness ( $a^*$ ) for longer during cooking due to the higher thermal stability to denaturation of myoglobin in higher pH. Colour

differences observed in raw meat of different *Bos indicus* and intramuscular fat content were largely eliminated by cooking.

### **Interventions**

PEF processing (0.25 kV/cm, 100 Hz, 10  $\mu$ s pulses for 30-60 ms) did not show significant effects on meat quality parameters such as tenderness, colour, cook loss and on the structure (both micro and macro scale) of the eye round beef in this study. Furthermore, no difference in meat quality parameters was found by changing the orientation of muscle fibres towards the electrodes (*i.e.* parallel or perpendicular) during PEF processing.

HPTP (300-650 MPa, 60-89 °C, 5 min) of brine injected samples of eye round significantly ( $P < 0.05$ ) tenderised the meat and reduced cook loss. Tenderness was influenced by processing temperature but not by the pressure applied in this study. Higher processing temperatures resulted in tougher meat and larger cook losses. Within this study, changing the operational conditions (concentrations or type of brine) did not affect the tenderness or cook loss of HPTP samples. The ultrastructure of samples after brine injection and HPTP showed a higher level of disruption and swelling of sarcomeres in comparison to water injected and/or cooked samples, which may likely be the cause for increased tenderness and reduced cook loss.

## Recommendations

Based on the key findings of this study, the following recommendations are advised:

- To limit cook loss and retain juiciness, it is important to avoid longitudinal shrinkage of meat. Therefore, it is crucial to keep core temperatures below 70 °C. The lowest values in PF (the most tender) of cooked meat was achieved when the meat was cooked to a core temperature between 65 °C and 70 °C in a PE bag in a water bath.
- Meat samples with higher pH retain more water in the structure upon cooking which might increase tenderness in some cases. Medium pH (5.71 – 5.93) and high pH (>6.00) meat retains more moisture than low pH meat (5.37 – 5.55) when cooked at high temperatures (above 75 °C). Therefore, medium and high pH meat has greater potential to be marketed as pre-cooked meat products.
- Meat from cattle with high BI content was slightly less tender (by 13% when cooked at 70 °C for 60 min) than that derived from animals with low BI content, despite having the same cook loss. Therefore it is recommended to keep cooking temperature below 70 °C for meat with high BI content, since the cooking temperature had a more influence than the BI content.
- The use of HPTP (60 °C, 550 MPa) combined with brine injection of salt containing (0.2%PPi or 1.0% NaCl) is an effective method to tenderise meat and increase juiciness. This process provides options to the food service industry to manufacture novel meat products, *e.g.* ready-to-eat based meat products.
- We recommend further research into PEF processing as a method of value adding for the meat industry. So far, the results from various studies are divergent and more knowledge is needed in this area of novel processing to deliver practical solutions to the industry.
- The model presented in the report is suitable for simulating the cooking process of meat as a function of cooking conditions (both temperature and time) which minimises cook loss. It is flexible enough to account for other phenomena and extensible enough for other geometries. During cooking of meat, significant structural changes occur. We recommend coupling a mechanical model with the mass and heat model for the prediction of meat tenderness and cook loss. In addition, modelling the cooking process in a way that incorporates the prediction of other food qualities (*i.e.*, sensorial, functional and nutritional) would be important to enable the manipulation and control of food quality to achieve desired attributes.

## 7.0 ACKNOWLEDGEMENTS

Firstly, we would like to acknowledge the role of Robin Warner who was responsible for the initiation and overall planning of the project prior to its commencement.

We would also like to acknowledge the assistance of Janet Stark, Jenny Favaro, Sukhdeep Bhail, Anita Sikes, Joanne Hughes and Michael Kelly for their skill in the execution of the experimental project work. Their technical expertise contributed to the overall success of the project.

Contributions to this work were made by visiting students; these were intern student Phuong-Vy Nguyen (Berlin University of Technology) who studied the changes in connective tissue, B. Sc (Hons) student Deanna Virgillo (RMIT, Melbourne) who investigated the changes resulting from the application of High Pressure Thermal Processing interventions and experiments, and PhD candidate Rahul Arora (RMIT, Melbourne) who contributed to the development to the literature review relating to mathematical modelling. Peter Torley (RMIT, Melbourne) is acknowledged for his support and supervision.

We are grateful to Piotr Swiergon for the swiftness of preparing the PEF equipment for use in this project.

We are grateful to Visiting Scientist Peter Purslow for his extensive meat science expertise during the execution of milestone 2 of this project.

We also thank Joanne Hughes who contributed to the literature review relating to cook loss for the second milestone of this project.

We thank both Jacky Rigby and Debbie Ash who assisted with the financial aspects of the project.

We are grateful to Katrina Spencer, who provided support to contract development and initial engagement with AMPC.

Lastly, we wish to acknowledge the contributions and comments made by the reviewers of this and previous milestone reports; to both Aarti Tobin and Joanne Hughes for reviewing the third milestone report, to Raymond Mawson for the fourth milestone report and Deb Krause for review of this final report.

We also acknowledge the contributions made by Robin Shorthose who reviewed the reports for milestones 4, 8 and 9 as well as this final report. He provided input into the project resulting from the scientific discussions that were held in relation to the project. Robin's extensive meat science expertise proved to be invaluable to the project's success.

## 8.0 ABBREVIATIONS AND GLOSSARY

### Nomenclature

$a^*$	redness	-
$b^*$	yellowness	-
$c$	water concentration	(mol/m <sup>3</sup> )
$C_p$	specific heat capacity at constant pressure	(J/kg·K)
$D$	effective water diffusivity in food	(m <sup>2</sup> /s)
$E_a$	energy activation	(kJ/mol)
$h_c$	heat transfer coefficient	(W/m <sup>2</sup> ·K)
$k$	thermal conductivity	(W/m·K)
$k_c$	mass transfer coefficient	(m/s)
$L^*$	lightness	-
MC	moisture content	(% wet basis)
$M_e$	equilibrium moisture content	(% dry basis)
$n$	direction normal to surface	-
$R$	universal gas constant	(kJ/mol·K)
$RH$	relative humidity	(%)
$T$	food temperature	(K)
$t$	time	(s)

### Subscripts:

$a$	air	-
$w$	water	-
$i$	initial	-
$s$	food surface	-

### Greek letters:

$\lambda$	latent heat of evaporation	(J/kg)
$\rho$	density	(kg/m <sup>3</sup> )

### Latin names of muscles

<i>semimembranosus</i> (SM)	top side
<i>biceps femoris</i> (BF)	outside flat
<i>semitendinosus</i> (ST)	eye round
<i>longissimus dorsi</i> (LD)	striploin
<i>gluteus medius</i> (GM)	rump
<i>pectoralis profundus</i> (PP)	brisket
<i>infraspinatus</i> (IS)	oyster blade

### Abbreviations

3D	three dimensional
AMPC	Australian Meat Processor Corporation
BI	<i>Bos indicus</i>
BT	<i>Bos taurus</i>
CSIRO	Commonwealth Scientific and Industrial Research Organisation
EM	expressible moisture
FC	fat content
FEM	finite element method
FITC	fluorescein isothiocyanate
HPTP	high pressure thermal processing
IMF	intramuscular fat
IY	initial yield
LTE	linear time-invariant
MLA	Meat & Livestock Australia
MSA	Meat Standards Australia
PDEs	partial differential equations
PE	polyethylene
PEF	pulse electric field
PF	peak force
PPi	sodium pyrophosphate
ppm	parts per million
S.E.	standard error
TEM	transmission electron microscope
WB	Warner-Bratzler
WHC	water holding capacity

## 9.0 BIBLIOGRAPHY

- Aroeira, C. N., Torres Filho, R. A., Fontes, P. R., Gomide, L. A., Ramos, A. L., Ladeira, M. M., & Ramos, E. M. (2016). Freezing, thawing and aging effects on beef tenderness from *Bos indicus* and *Bos taurus* cattle. *Meat Science*, *116*, 118-125.
- Arroyo, C., Eslami, S., Brunton, N. P., Arimi, J. M., Noci, F., & Lyng, J. G. (2015). An assessment of the impact of pulsed electric fields processing factors on oxidation, color, texture, and sensory attributes of turkey breast meat. *Poultry Science*, *94*(5), 1088-1095. doi: 10.3382/ps/pev097
- Arroyo, C., Lascorz, D., O'Dowd, L., Noci, F., Arimi, J., & Lyng, J. G. (2015). Effect of pulsed electric field treatments at various stages during conditioning on quality attributes of beef longissimus thoracis et lumborum muscle. *Meat Science*, *99*, 52-59.
- Arthur, P., Hearnshaw, H., Kohun, P., & Barlow, R. (1994). Evaluation of *Bos indicus* and *Bos taurus* straightbreds and crosses. III. Direct and maternal genetic effects on growth traits. *Australian Journal of Agricultural Research*, *45*(4), 807-818.
- ASHRAE. (1989). Thermal properties of foods *ASHRAE Handbook - Fundamentals* (SI ed.). GA: Atlanta: American Society of Heating, Refrigerating and Air Conditioning Engineers.
- ASHRAE. (1995). *Handbook of Fundamentals*. New York: American Association of Heating, Refrigeration and Air Conditioning Engineers, Inc.
- Bekhit Ael, D., Suwandy, V., Carne, A., van de Ven, R., & Hopkins, D. L. (2016). Effect of repeated pulsed electric field treatment on the quality of hot-boned beef loins and topsides. *Meat Sci*, *111*, 139-146.
- Bisceglia, B., Brasiello, A., Pappacena, R., Vietre, R. (2013). *Food cooking process: Numerical simulation of the transport phenomena*. Paper presented at the COMSOL conference, Rotterdam.
- Bouton, P. E., Harris, P. V., Shorthose, W. R., & Baxter, R. I. (1973). A comparison of the effects of aging, conditioning and skeletal restraint on the tenderness of mutton. *Journal of Food Science*, *38*(6), 932-937.
- Bouton, P. E., Harris, P.V. (1972). A comparison of some objective methods used to assess meat tenderness. *Journal of Food Science*(37), 218-221.
- Bouton, P. E. H., P.V.; Shorthose, W.R. (1976). Dimensional Changes in Meat During Cooking. *Journal of Texture Studies* *7*, 179-192.
- Bratzler, L. J. (1932). *Measuring the tenderness of meat by means of a mechanical shear*. M.Sc. Thesis, Kansas State College, Kansas, USA.
- Buckow, R., Schroeder, S., Berres, P., Baumann, P., & Knoerzer, K. (2010). Simulation and evaluation of pilot-scale pulsed electric field (PEF) processing. *Journal of Food Engineering*, *101*, 67-77.
- Buckow, R., Sikes, A., & Tume, R. (2013). Effect of high pressure on physicochemical properties of meat. *Crit Rev Food Sci Nutr*, *53*(7), 770-786.
- Champion, A. E., Purslow, P. P., & Duance, V. C. (1988). Dimensional changes of isolated endomysia on heating. *Meat Science*, *24*(4), 261-273.

- Chiavaro, E., Rinaldi, M., Vittadini, E., Barbanti, D. (2009). Cooking of pork Longissimus dorsi at different temperature and relative humidity values: Effects on selected physico-chemical properties. *Journal of Food Engineering*, 93(2), 158-165.
- Choi, Y., Okos, M.R. . (1987). Effects of temperature and composition on thermal properties of foods. In M. Le Maguer, Jelen, P. (Ed.), *Food Engineering and Process Applications* (Vol. 1, pp. 269-312). New York: Elsevier Applied Science Publishers.
- Domínguez, R., Borrajo, P., Lorenzo, J. M. (2015). The effect of cooking methods on nutritional value of foal meat. *Journal of Food Composition and Analysis*, 43, 61-67.
- Domínguez, R., Gómez, M., Fonseca, S., Lorenzo, J. M. (2014). Influence of thermal treatment on formation of volatile compounds, cooking loss and lipid oxidation in foal meat. *LWT - Food Science and Technology*, 58(2), 439-445.
- Faridnia, F., Ma, Q. L., Bremer, P. J., Burritt, D. J., Hamid, N., & Oey, I. (2015). Effect of freezing as pre-treatment prior to pulsed electric field processing on quality traits of beef muscles. *Innovative Food Science & Emerging Technologies*, 29, 31-40.
- Farkas, D., Hoover, D. (2000). High pressure processing. In special supplement: kinetics of microbial inactivation for alternative food processing technologies. *Journal of Food Science, Special Supplement*(65), 47 - 64.
- Findlay, C. J., & Stanley, D. W. (1984). Differential Scanning Calorimetry of beef muscle - Influence of postmortem conditioning. [Article]. *Journal of Food Science*, 49(6), 1513-1516.
- Gama, L. T., Bressan, M. C., Rodrigues, E. C., Rossato, L. V., Moreira, O. C., Alves, S. P., & Bessa, R. J. (2013). Heterosis for meat quality and fatty acid profiles in crosses among *Bos indicus* and *Bos taurus* finished on pasture or grain. *Meat Sci*, 93(1), 98-104.
- Godsalve, E. W., Davis, E. A., & Gordon, J. (1977). Effect of oven conditions and smaple treatment on water loss of dry cooked bovine muscle. *Journal of Food Science*, 42(5), 1325-1330.
- Gursansky, B., O'Halloran, J. M., Egan, A., & Devine, C. E. (2010). Tenderness enhancement of beef from *Bos indicus* and *Bos taurus* cattle following electrical stimulation. *Meat Sci*, 86(3), 635-641.
- Hamm, R., & Deatherage, F. E. (1960). Changes in hydration and charges of muscle proteins during freeze dehydration of meat. *Journal of Food Science*, 25(5), 573-586.
- Heldman, D. R., Lund, D.B. (2007). *Handbook of Food Engineering*. New York: Marcel Dekker, Inc.
- Highfill, C. M., Esquivel-Font, O., Dikeman, M. E., & Kropf, D. H. (2012). Tenderness profiles of ten muscles from F1 *Bos indicus* x *Bos taurus* and *Bos taurus* cattle cooked as steaks and roasts. *Meat Sci*, 90(4), 881-886.
- Holroyd, R. G., Fordyce, G. (2016). Cost effective strategies for improved fertility in extensive and semi-extensive management conditions in northern Australia, 2016, from [http://www.brahman.com.au/technical\\_information/reproduction/improvedFertility.html](http://www.brahman.com.au/technical_information/reproduction/improvedFertility.html)
- Huang, E., Mittal, G.S. . (1995). Meatball cooking - modeling and simulation. *Journal of Food Engineering*, 24, 87-100.

- Huff-Lonergan, E., & Lonergan, S. M. (2005). Mechanisms of water-holding capacity of meat: The role of postmortem biochemical and structural changes. [Article; Proceedings Paper]. *Meat Science*, *71*(1), 194-204.
- Jung, S., de Lamballerie-Anton, M., & Ghouil, M. (2000). Modifications of ultrastructure and myofibrillar proteins of post-rigor beef treated by high pressure. *Lebensmittel-Wissenschaft Und-Technologie-Food Science and Technology*, *33*(4), 313-319.
- Kondjoyan, A., Kohler, A., Realini, C. E., Portanguen, S., Kowalski, R., Clerjon, S., Debrauwer, L. (2014). Towards models for the prediction of beef meat quality during cooking. *Meat Sci*, *97*(3), 323-331.
- Kondjoyan, A., Ouilic, S., Portanguen, S., & Gros, J. B. (2013). Combined heat transfer and kinetic models to predict cooking loss during heat treatment of beef meat. *Meat Sci*, *95*(2), 336-344.
- Lambe, N. R., McLean, K. A., Gordon, J., Evans, D., Clelland, N., & Bunger, L. (2016). Prediction of intramuscular fat content using CT scanning of packaged lamb cuts and relationships with meat eating quality. *Meat Science*.
- Liang, R. R., Zhu, H., Mao, Y. W., Zhang, Y. M., Zhu, L. X., Cornforth, D., Luo, X. (2016). Tenderness and sensory attributes of the longissimus lumborum muscles with different quality grades from Chinese fattened yellow crossbred steers. *Meat Science*, *112*, 52-57.
- Mao, Y., Hopkins, D. L., Zhang, Y., Li, P., Zhu, L., Dong, P., Luo, X. (2016). Beef quality with different intramuscular fat content and proteomic analysis using isobaric tag for relative and absolute quantitation of differentially expressed proteins. *Meat Science*, *118*, 96-102.
- Meat Standards Australia. (2007). *MSA Standards Manual for Beef Grading*. Meat & Livestock Australia Limited.
- Miller, M. F., Carr, M. A., Ramsey, C. B., Crockett, K. L., & Hoover, L. C. (2001). Consumer thresholds for establishing the value of beef tenderness. *Journal of Animal Science*, *79*(12), 3062-3068.
- Møller, A. J. (1981). Analysis of Warner-Bratzler Shear Pattern with Regard to Myofibrillar and Connective-Tissue Components of Tenderness. *Meat Science*, *5*(4), 247-260.
- Mujumdar, A. S. a. D., S. . (2008). Fundamental principles of drying. In A. S. Mujumdar (Ed.), *Guide to Industrial Drying—Principles, Equipments and New Developments* (pp. 1-21). Mumbai, India: Three S Colors Publications.
- Multiphysics, C. (2007). Chemical Engineering. Stockholm, Sweden.
- O'Dowd, L. P., Arimi, J. M., Noci, F., Cronin, D. A., & Lyng, J. G. (2013). An assessment of the effect of pulsed electrical fields on tenderness and selected quality attributes of post rigor beef muscle. *Meat Sci*, *93*(2), 303-309.
- Obuz, E., Powell, T. H., & Dikeman, M. E. (2002). Simulation of cooking cylindrical beef roasts. *Lebensmittel-Wissenschaft Und-Technologie-Food Science and Technology*, *35*(8), 637-644. doi: 10.1006/fstl.2002.0940
- Okumura, T., Kaoru, S., Toshihiro, N., Satsuki, M., Yasuhisa, M., Hironori, S., Tadashi, K. (2007). Effects of Intramuscular Fat on the Sensory Characteristics of *M. longissimus dorsi* in Japanese Black Steers as Judged by a Trained Analytical Panel *Asian-Aust. J. Anim. Sci*, *20*(4), 577-581.

- Purslow, P. P., Oiseth, S., Hughes, J., & Warner, R. D. (2016). The structural basis of cooking loss in beef: Variations with temperature and ageing. *Food Research International*, *89*, 739-748.
- Rhee, M. S., Wheeler, T. L., Shackelford, S. D., & Koohmaraie, M. (2004). Variation in palatability and biochemical traits within and among eleven beef muscles. [Article]. *Journal of Animal Science*, *82*(2), 534-550.
- Rowe, R. W. D. (1978). Collagen fibrils of the perimysium and endomysium of sheep semitendinosus muscle. *Meat Science*, *2*(4), 275-280.
- Sabarez, H. T. (2012). Computational modeling of the transport phenomena occurring during convective drying of prunes. *Journal of Food Engineering*, *2*(111), 279-288.
- Sabarez, H. T. (2014). Mathematical Modeling of the Coupled Transport Phenomena and Color Development: Finish Drying of Trellis-Dried Sultanas. *Drying Technology*, *32*(5), 578-589.
- Sabarez, H. T. (2015). Modelling of drying processes for food materials. 95-127.
- Sablani, S. S. a. R., M.S. . (2007). Fundamentals of food dehydration. In C. C. Hui YH, Farid MM, Fasina OO, Noomhorm A, Welti-Chenis J. (Ed.), *Food Drying Science and Technology: Microbiology, Chemistry, Applications* (pp. 1-42). Pennsylvania, USA.: DESTech Publications, Inc.
- Shilton, N., Mallikarjunan, P., Sheridan, P. (2002). Modeling of heat transfer and evaporative mass losses during he cooking of beef patties using far-infrared radiation. *Journal of Food Engineering* *55*, 217-222.
- Shorthose, W. R., Harris, P.V. (1991). Effects of growth and composition on meat quality. *Advances in Meat Science*, *7*, 515–549.
- Spurr, A. R. (1969). A Low-Viscosity Epoxy Resin Embedding Medium for Electron Microscopy. *Journal of Ultrastructure Research*, *26*(1-2), 31-&.
- Suwandy, V., Carne, A., van de Ven, R., Bekhit, A. E.-D. A., & Hopkins, D. L. (2015). Effect of Pulsed Electric Field Treatment on the Eating and Keeping Qualities of Cold-Boned Beef Loins: Impact of Initial pH and Fibre Orientation. *Food and Bioprocess Technology*, *8*(6), 1355-1365.
- Suwandy, V., Carne, A., van de Ven, R., Bekhit Ael, D., & Hopkins, D. L. (2015). Effect of pulsed electric field on the proteolysis of cold boned beef M. Longissimus lumborum and M. Semimembranosus. *Meat Science*, *100*, 222-226.
- Thornton, R. F. H., P. M.; Larsen, T. W. . (1981). The relationships between fat, protein and water content of boneless meat. *Food Technology in Australia*, *33*(10), 468.
- Tornberg, E. (2005). Effects of heat on meat proteins - Implications on structure and quality of meat products. *Meat Science*, *70*(3), 493-508.
- van der Sman, R. G. (2007). Moisture transport during cooking of meat: An analysis based on Flory-Rehner theory. *Meat Science*, *76*(4), 730-738.